

**MISE A JOUR DES ETUDES ET  
ASSISTANCE TECHNIQUE POUR LA CONSTRUCTION DU  
BARRAGE DE BISRI  
  
BARRAGE BISRI**



**AVANT PROJET DETAILLE**

**PIECE 3: RAPPORT GEOTECHNIQUE  
3-2: TECHNICAL NOTE ON CPTU ANALYSIS AND  
SETTLEMENT EVALUATION**

February 2015

Updated February 2016



Prof. Antonio Gens, FREng  
Professor of Geotechnical Engineering  
Department of Geotechnical Engineering and Geosciences  
TECHNICAL UNIVERSITY OF CATALUNYA  
Jordi Girona 1-3, Edifici D-2  
Barcelona 08034 SPAIN  
Tel: +34-934016867/7250 Fax: +34-934017251  
e-mail: antonio.gens@upc.edu

---

## **BISRI DAM**

### **TECHNICAL NOTE ON CPTU ANALYSIS AND SETTLEMENT EVALUATION**

#### **1. Introduction and goals**

- 1.1 It is envisaged that the planned Bisri Dam (Lebanon) will be constructed with an inclined clay core supported by gravel/rockfill shoulders. It will have a maximum height of 74 m above natural ground level reaching an elevation of +469 m. Normal water level elevation will be +461 m. The dam will have a crest length of about 720m and a maximum footprint upstream/downstream of 620 m. When completed, Bisri dam will store about 125 Mm<sup>3</sup> of water.
- 1.2 The dam will be founded on a thick alluvial deposit of lacustrine origin that has resulted from a past landslide that blocked the river. Two types of lacustrine deposits can be distinguished:
  - Coarse materials (gravely sand or sandy gravel) that largely occupy the left side of the river valley up to a maximum depth of 30 m.
  - Fine materials occupying most of the rest of the alluvial deposit. They are silty clays interbedded with thin layers of fine sand and/or silt.

In addition, there is old colluvium overlying the bedrock (especially in the right hand side of the river valley) consisting of gravel and coarser materials wrapped in a silty clay matrix. Possible artesian water pressure conditions seem to have been detected on occasions.

Because of the presence of permeable materials in the foundation, a cut-off wall linked to the inclined core will be built to minimize seepage under the dam.

Figure 1.1 shows a typical cross section of the dam.



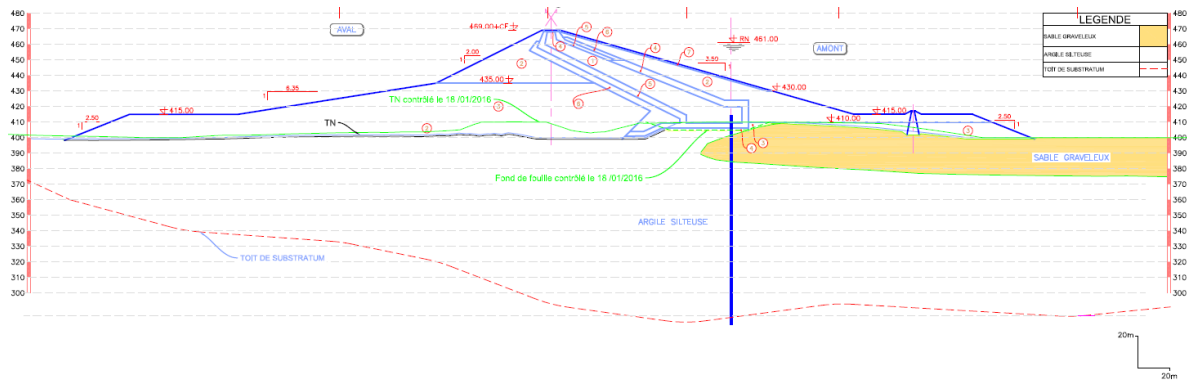


Figure 1.1. Typical cross-section of Bisri dam (pre-existing colluvium is not represented)

1.3 There have been two main site investigations, the first one conducted in 1996/1997 and the second one in 2014 that have provided a significant amount of information regarding ground conditions. However, in order to enhance the information available and clarify some uncertainties, a campaign of 25 cone penetration tests with measurement of pore water pressures (CPTu tests) has been carried out. The CPTu test campaign was performed from October to December 2015. Figure 1.2 shows the plan location of the CPTu tests. The dates and depth of the various CPTu tests are listed in table 1.1

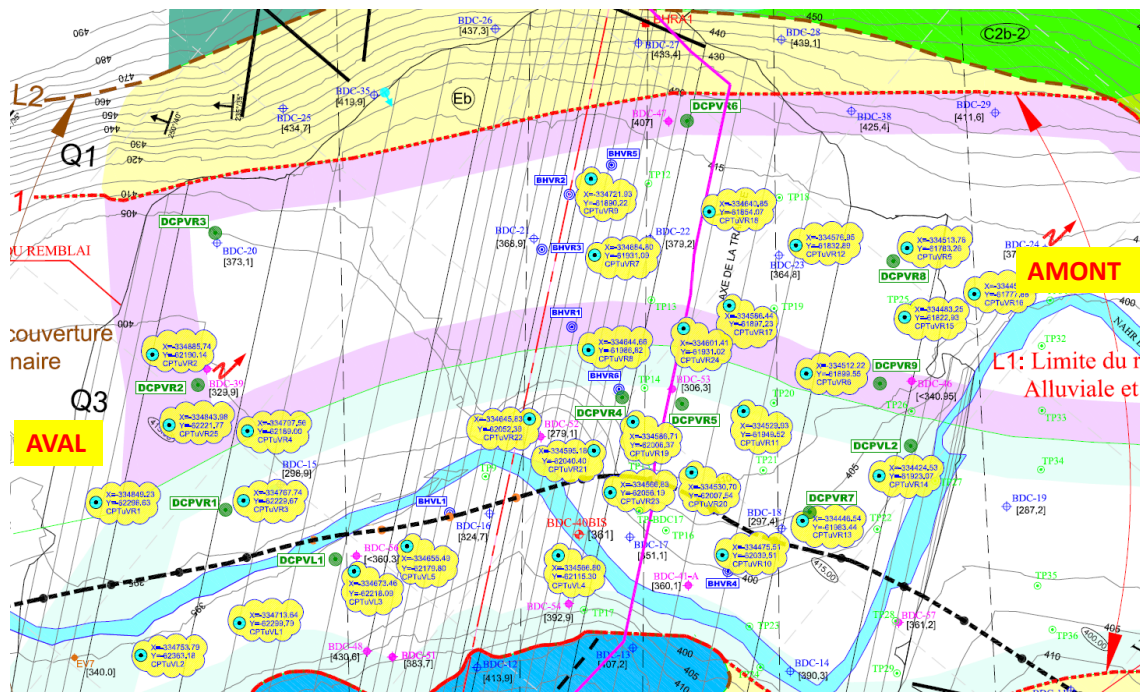


Figure 1.2. Location of the CPTu tests

1.4 In October 2015, the authors of the current report issued a Technical Note<sup>1</sup> containing a number of recommendations concerning the testing procedures to be adopted. Some of the recommendations, concerning notably the recommended advance rate of the cone of 2cm/s, could not be followed precisely in the field.

<sup>1</sup> Bisri dam. Technical note 1. Recommendation on the CPTu tests (UPC-2015)

Table 1.1 Depth and dates of the CPTu tests

CPTU	Depth (m) to reference level	Date
VL1	-26	11/12/2015
VL2	-46	11/12/2015
VL3	-54	10/12/2015
VL4	-30	11/12/2015
VL5	-55	12/12/2015
VR1	-55	9/12/2015
VR2	-62	10/12/2015
VR3	-60	8/12/2015
VR4	-60	8/12/2015
VR5	-41	10/12/2015
VR6	-77	2/11/15
VR7	-42	16/10/2015
VR8	-65	4/12/2015
VR9	-26	16/10/2015
VR10	-51	27/11/2015
VR11	-70	25/11/2015
VR12	-34	9/10/2015
VR14	-56	26/11/2015
VR15	-66	13/10/2015
VR16	-47	8/10/2015
VR17	-43	21/10/2015
VR18	-20	21/10/2015
VR19	-68	7/12/2015
VR20	-70	25/11/2015
VR21	-60	30/11/2015
VR22	-53	1/12/2015
VR23	-60	2/12/2015
VR24	-65	5/12/2015
VR25	-58	9/12/2015
VRRL13	-65	4/12/2015

- 1.5 This report contains a number of tasks performed based on the information provided by the CPTu tests performed. Specifically, the following items are addressed:
- a) Estimation of some key parameters based on CPTu data
  - b) Numerical analysis of the construction of the dam

## 2. Estimation of parameters from CPTu data

2.1 In this section the key features and parameters required in the analyses will be evaluated using the data obtained in the CPTu campaign. They are:

- Identification of coarse permeable layers (denoted as sand) and of fine-grained low permeability layers (denoted as clay)
- Compression index,  $C_c$ , of the clay; this parameter controls the volume change of the fine-grained layers and, therefore, the magnitude of most of the settlements.
- Undrained shear strength,  $c_u$ , of the clay. This parameter controls the stability at all stages of the analysis. It increases due to pore pressure dissipation and consolidation.
- Permeability and coefficient of consolidation of the clay; they control the rate of dissipation of pore pressures and consolidation times
- Stiffness of the coarse permeable material. It will control the contribution of granular layers to settlement.

2.2 The results of the CPTu tests are collected in Appendix 1. They are plotted in terms of undrained shear strength, compression index, pore pressure measured and Soil Index Behaviour. The tests have been grouped together on the bases of proximity to the cross- and longitudinal sections used later for analyses (see section 3). In order to estimate parameters and indices the most commonly used correlations have been used as indicated below.

2.3 As pointed out before, due to operational difficulties it has not been always possible to maintain the standard rate of penetration of 2 cm/s. This should be taken into account when using the results of the CPTu tests. Figure 2.1 shows a summary of the penetration rates used in the different tests and depths.

2.4 The distinction between coarse and fine-grained materials has been based mainly on the combination of pore pressure measurements and Soil Index Behaviour,  $I_c$ . Values of  $I_c$  below 3 tend to identify sand-like behaviour and values of  $I_c$  above 3 are associated with clay-like behaviour (Jefferies and Davies, 1993; Robertson 1998, 2009). A more direct identification can be based on the fact that pore pressure are generated during penetration in low permeability fine-grained soils whereas no increment of pore pressures are observed when penetrating coarser permeable materials.

2.5 There are sound correlations concerning compression index,  $C_c$ , and plasticity index (Wood and Wroth, 1978; Belokas & Kavvadas, 2006). According to the laboratory reports, the plasticity index of the clay-like material lies in the range of 25-30%. In that case those correlations provide values in the range of 0.32 to 0.42. On the other hand, and somewhat less reliable, it is also possible to use the CPTu tests to estimate  $C_c$  using the correlation of Robertson (2009) based on the cone penetration resistance and the value of  $I_c$ . The values of  $C_c$  computed in this way are shown in the plots of Appendix 1. It can be observed that rather high values are obtained ranging from 0.3 to 1. It is unlikely that such high values are correct, they would be incompatible with other information available. Consequently a value of



0.42 is adopted for the analyses, at the higher end of the range of values considered more reliable. The settlements of the clay layers will be largely proportional to  $C_c$ , so evaluating the effect of using a different value is quite straight forward.

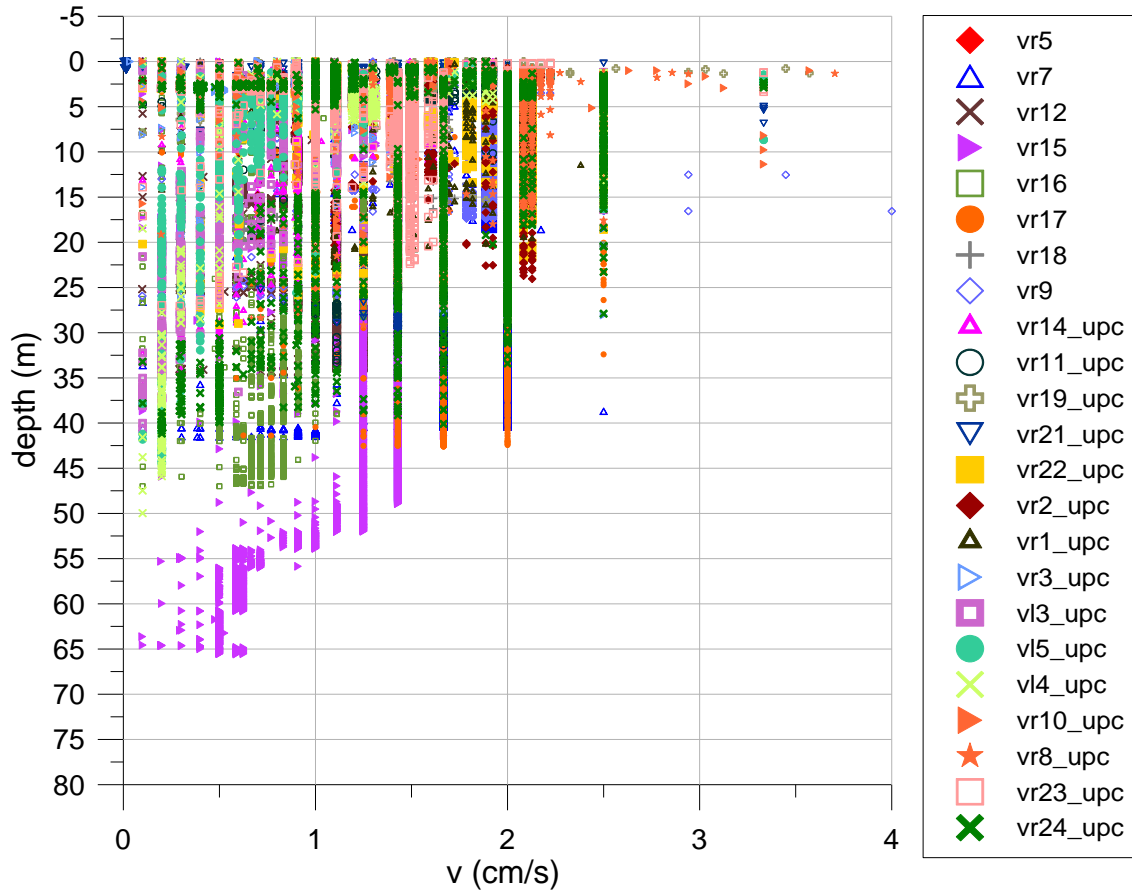


Figure 2.1 Penetration rates used in the different tests and at different depths.

2.6 The fine-grained materials are likely to be at or near a normally consolidated state. In that case, it should be expected that there is an approximately constant relationship between  $c_u$  and the consolidation vertical effective stress,  $\sigma'_v$ . This is borne out by the  $c_u$  values obtained from the CPTu tests using the usual value of  $N_k=15$  (Appendix 1). All the distributions with depth of undrained shear strength have been collected in Figure 5.2. The lower values correspond to the clay-like materials and the thick dashed line represents the relationship  $c_u/\sigma'_v=0.3$ . There are a number of results that plot below this line but they invariably correspond to CPTu tests performed at slower rates of penetration. Therefore it is believed that the value of 0.3 corresponds to a prudent but realistic value of the undrained shear strength.

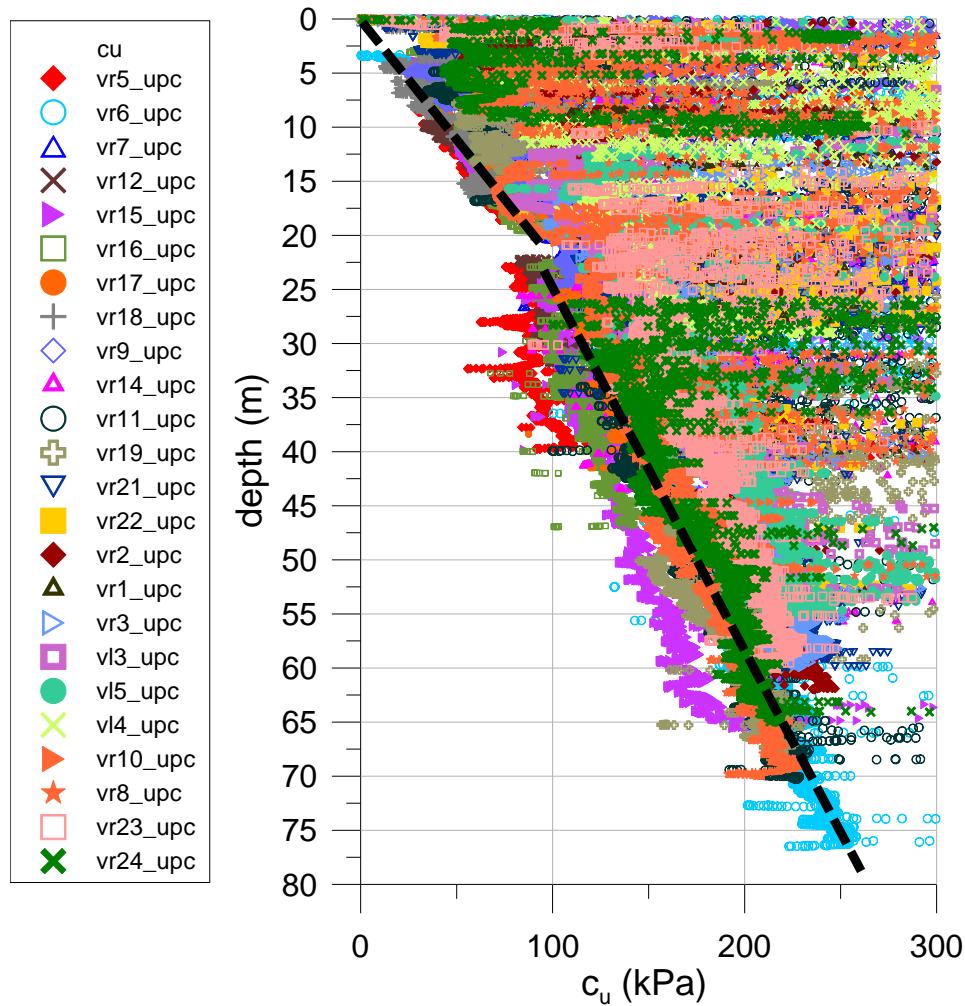


Figure 2.2 Computed undrained shear strength distributions with depth from CPTu tests.

2.7 Again with limited reliability, it is possible to estimate horizontal permeability,  $k_h$ , and horizontal coefficient of consolidation,  $C_h$ , values based on the penetration data from CPTu tests (Robertson 2010), see Figure 2.3. Alternatively, the horizontal coefficient of consolidation can also be estimated from correlations; the results are shown in Figure 2.4.

2.8 However, it is more direct to obtain the horizontal coefficient of consolidation from the dissipation tests that were performed at various points of the foundation during the CPTu tests. The results obtained using the classical method of Teh and Houlsby (1991) are collected in Figure 2.5. A value of  $6 \cdot 10^{-7} \text{ m}^2/\text{s}$  has been finally selected. This value is assumed constant and the permeability will have to vary to account for the variation of stiffness as the soil compresses. A reference initial value of horizontal permeability of  $3.9 \cdot 10^{-10} \text{ m/s}$  is thereby obtained. It can be seen (Figure 2.3) that this value is in the correct range of values estimated independently with the CPTu tests. The same can be said of the adopted horizontal coefficient of consolidation (Figure 2.4). For the vertical permeability and coefficient of consolidation, values 10 times smaller have been adopted.

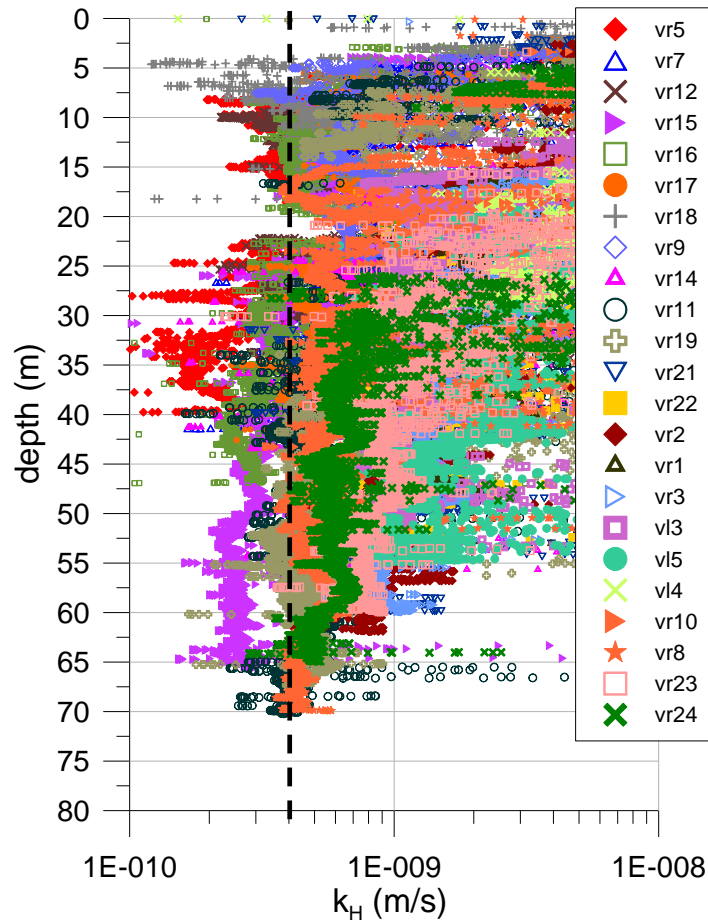


Figure 2.3 Estimated horizontal permeability distributions with depth from CPTu tests.

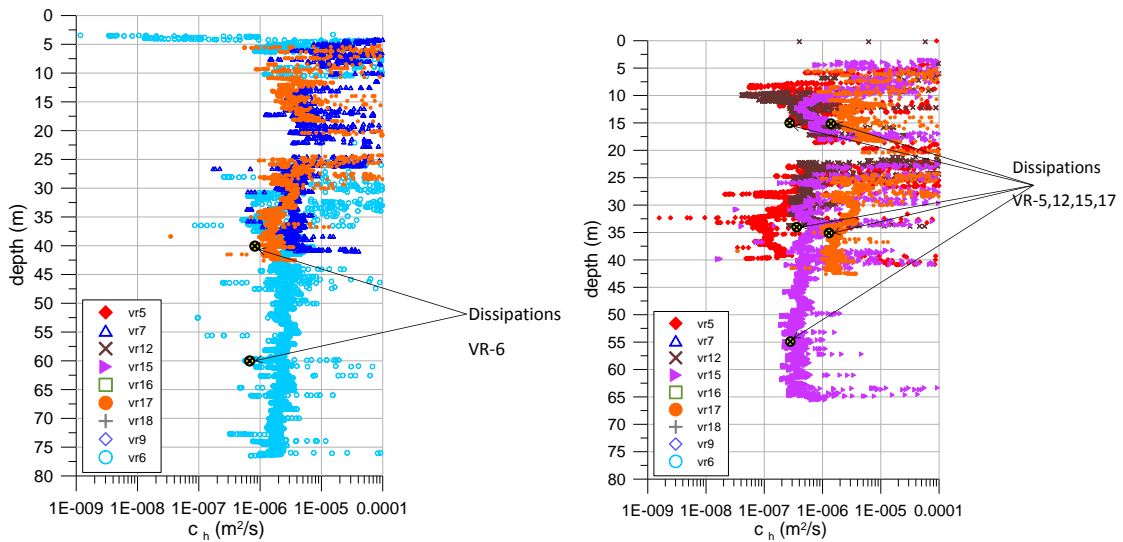


Figure 2.4 Estimated horizontal coefficient of consolidation distributions with depth from CPTu tests.

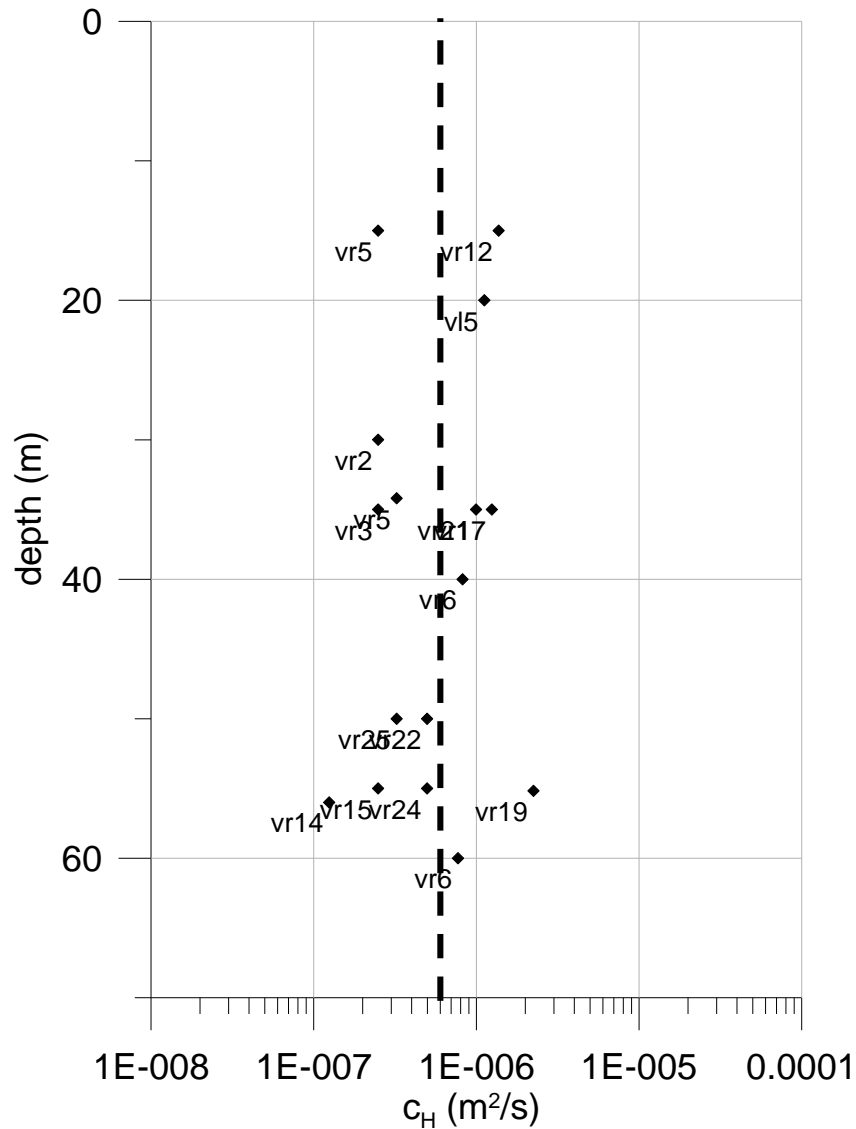


Figure 2.5 Horizontal coefficient of consolidation determined from dissipation tests.

2.9 It would be expected that the stiffness parameter (Young's modulus) of the coarser soils would increase with depth. This is indeed confirmed by the results of CPTU tests (Figure 2.6). The correlation proposed by Robertson (2012) of young uncemented sands has been used for this purpose. In the same Figure 2.6, the variation of elastic modulus with depth selected for the analyses is shown. Again, it can be considered a prudent but realistic estimate.



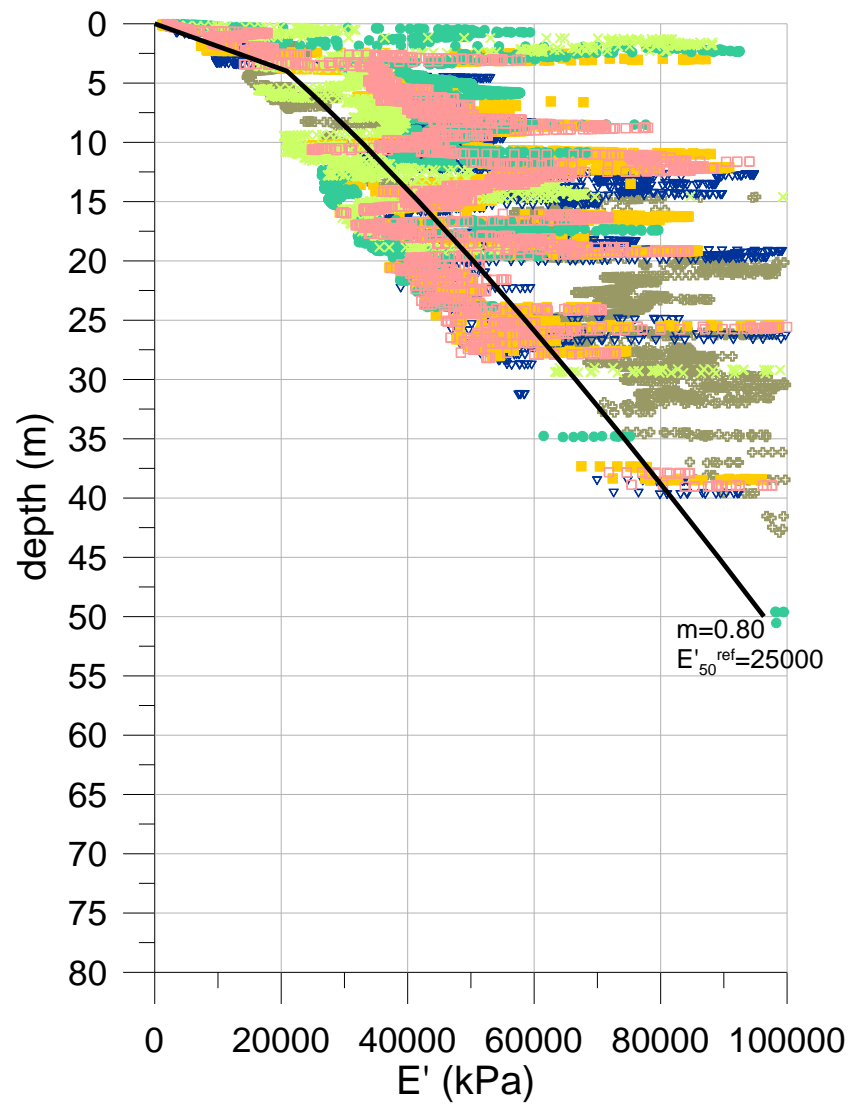


Figure 2.6 Estimated variation of Young's modulus with depth...

### 3. Numerical analyses of dam construction. General features

3.1 Five different dam sections have been analysed using the software Plaxis 2D (version 2015). Three cross-section C-1, C-2 and C-3 and two longitudinal sections, Section A along the dam axis (crest) and Section C following the cut-off footprint, have been studied (see Figure 3.1).

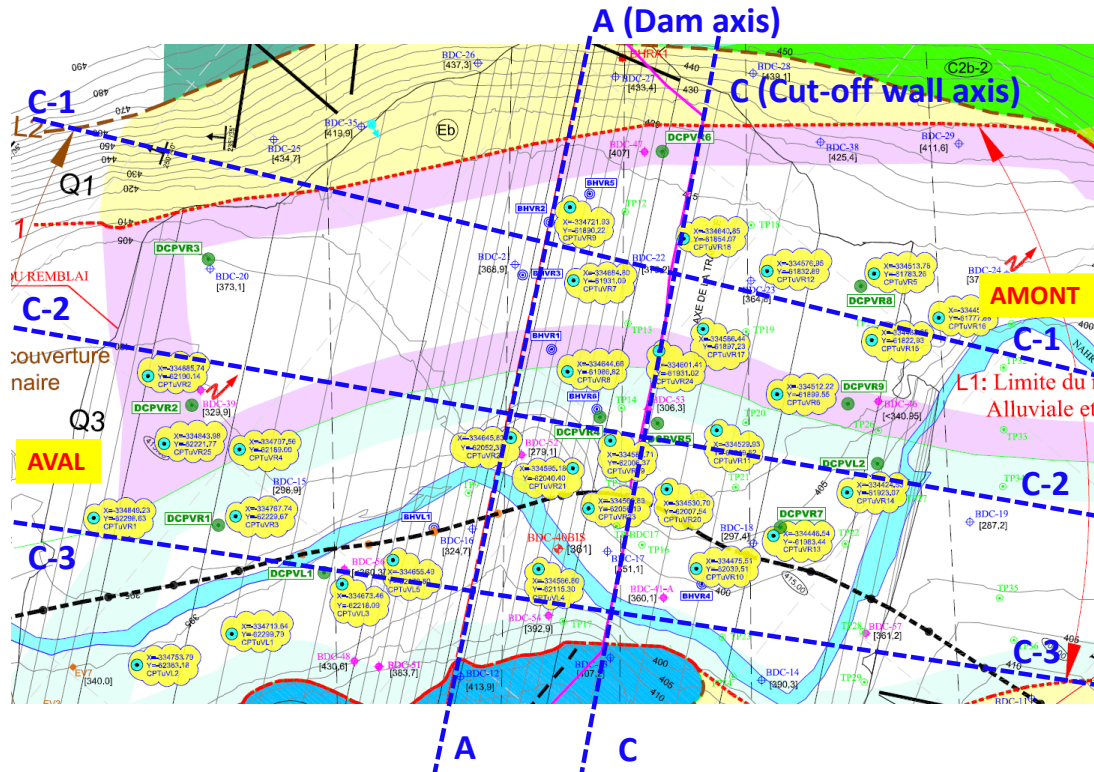


Figure 3.1. Location of the section for analysis

3.2 Six different materials have been considered in the analyses: Filter/alluvium, Core, Rockfill, Bedrock, Sand and Clay. The foundation material has been divided into Sand (coarse materials of high permeability) and Clay (fine-grained materials of low permeability), based on the results of the CPTu tests. Figures 3.2 to 3.6 show the geometry of the different sections together with distribution of materials considered in the analyses. Colluvium material covering the bedrock is not represented.

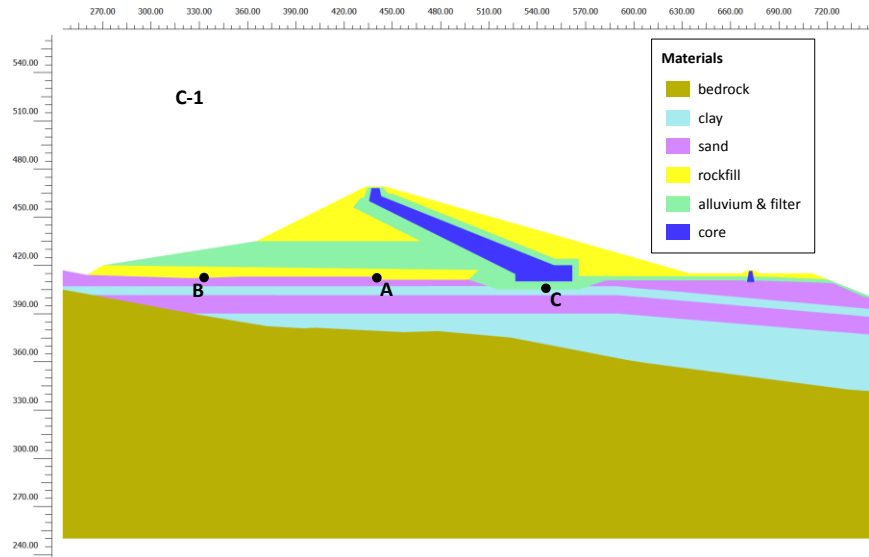


Figure 3.2. Geometry of cross-section C1

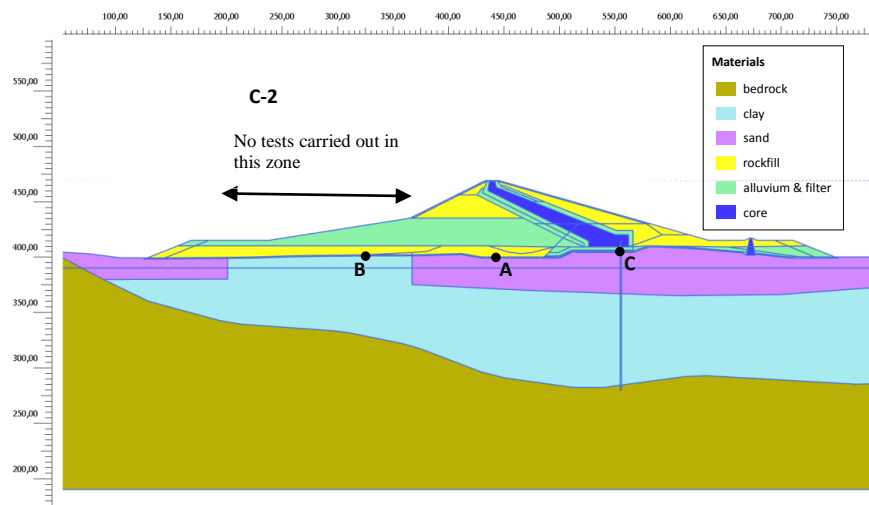


Figure 3.3. Geometry of cross-section C2

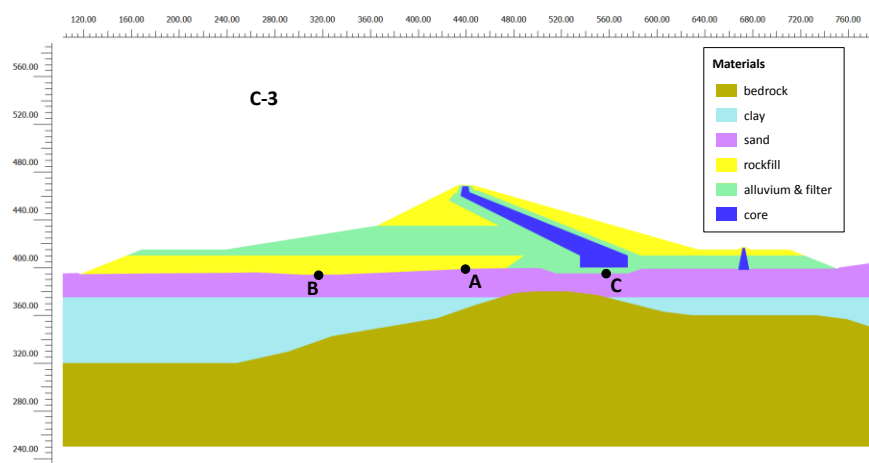


Figure 3.4. Geometry of cross-section C3

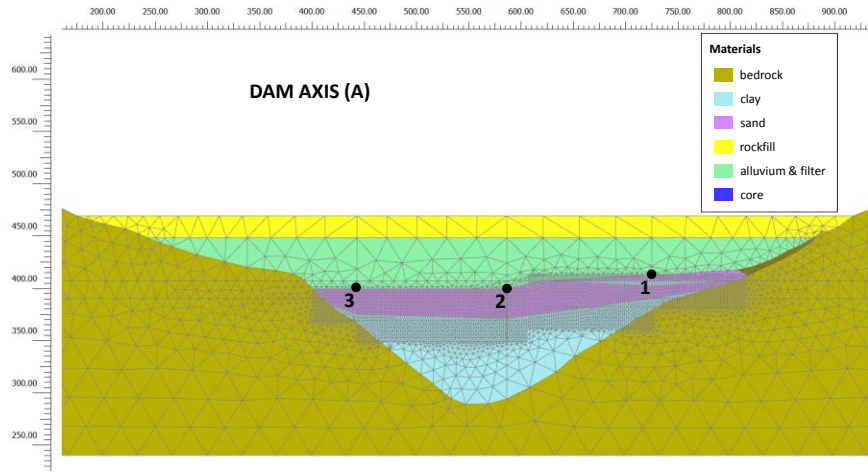


Figure 3.5. Geometry of longitudinal section A (dam axis)

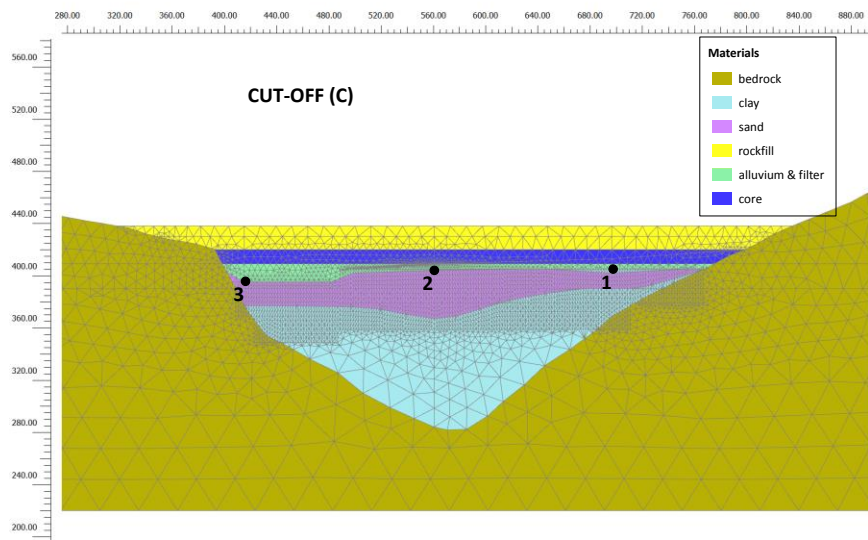


Figure 3.6. Geometry of longitudinal section C (cut-off wall)

3.3 The constitutive models and soil type adopted for the analyses are shown in Table 3.1. It should be noted that the specification drained/undrained only applies to the instantaneous construction stages, in the consolidation stages the specified permeability applies.

Table 3.1: Constitutive models and soil types

Material	Constitutive model	Soil Type
Filter/alluvium	Mohr-Coulomb	Drained
Core	Mohr-Coulomb	Undrained
Rockfill	Mohr-Coulomb	Drained
Bedrock	Mohr-Coulomb	Drained
Sand	Hardening Soil	Drained
Clay	Soft Soil	Undrained



3.4 The most sophisticated constitutive models have been adopted for the foundation Sand and Clay, the deformation and strength of which are the focus of this report. The Soft Soil model has been used for the foundation Clay because its behaviour will be dominated by volume changes upon loading whereas the hardening Soil model is more appropriated for coarse granular materials where deformation due to deviatoric stresses are more significant.

3.5 The parameters used in the analyses are specified in Tables 3.2 to 3.5. Some comments:

- As indicated, most of the parameters of Filter/alluvium, Core and Rockfill have been selected based on previous work on the design of Bisri dam.
- A high permeability has been used for all the drained materials (Filter/alluvium, Rockfill, Bedrock and Foundation Sand), the precise value is not important as long as it is very much higher than those in the core and in the foundation clay.
- A very high stiffness has been selected for the bedrock so that it does not contribute to the settlements calculated. The other parameters have no influence on the results.
- The stiffness values of the foundation Sand is based on the results of the CPTu tests (section 2). The value of  $m=0.8$  ensures an adequate increase of stiffness with depth. The friction angle of  $28^\circ$  is probably a lower bound to the real one but it has been chosen to account for the potential presence of some proportion of fines.
- The parameters of the Soft soil model for the foundation Clay have been chosen to obtain the desired value of  $c_u/\sigma'_v=0.3$ . The estimated value of  $C_c=0.42$  is also directly adopted.
- The permeability of the clay has been chosen in such a way that the estimated value of  $6 \cdot 10^{-7} \text{ m}^2/\text{s}$  for the horizontal coefficient of consolidation is obtained. The  $C_k$  parameter of 0.42 controls the variation of permeability with void ratio ensuring that the horizontal coefficient of consolidation remains constant throughout. The vertical permeability is one order of magnitude lower.
- The  $K_0$  values used in the specification of initial stresses have been obtained assuming normally consolidated conditions and Jaky's formula  $K_0=1-\sin\phi'$

Table 3.2 Parameters for Filter/Alluvium and Core

Identification	Unit	Filter/Aluvium	Core
Material model		Mohr-Coulomb	Mohr-Coulomb
Drainage type		Drained	Undrained
$\gamma_{\text{unsat}}$	kN/m <sup>3</sup>	22 <sup>(2)</sup>	20 <sup>(2)</sup>
$\gamma_{\text{sat}}$	kN/m <sup>3</sup>	22 <sup>(2)</sup>	20 <sup>(2)</sup>
E	kN/m <sup>2</sup>	3.0E+05 <sup>(1)</sup>	2.0E+04 <sup>(1)</sup>
$\nu$ (nu)		0.25	0.25
$c_{\text{ref}}$	kN/m <sup>2</sup>	1	10 <sup>(2)</sup>
$\phi$ (phi)	°	38 <sup>(2)</sup>	25 <sup>(2)</sup>
$\psi$ (psi)	°	0	0
$k_x$	m/day	0.864	8.64E-05
$k_y$	m/day	0.864	8.64E-05

<sup>(1)</sup> Billaux D. & Catalano E.(2015)

<sup>(2)</sup> Chraibi et al. (2013)

Table 3.3 Parameters for Rockfill and Bedrock

Identification	Unit	Rockfill	Bedrock
Material model		Mohr-Coulomb	Mohr-Coulomb
Drainage type		Drained	Drained
$\gamma_{\text{unsat}}$	kN/m <sup>3</sup>	22 <sup>(2)</sup>	23
$\gamma_{\text{sat}}$	kN/m <sup>3</sup>	22 <sup>(2)</sup>	23
E	kN/m <sup>2</sup>	8.0E+04 <sup>(1)</sup>	5.00E+06
$\nu$ (nu)		0.25	0.25
$c_{\text{ref}}$	kN/m <sup>2</sup>	1	10
$\phi$ (phi)	°	45 <sup>(2)</sup>	40
$\psi$ (psi)	°	0	0
$k_x$	m/day	0.864	1.00E-03
$k_y$	m/day	0.864	1.00E-03

<sup>(1)</sup> Billaux D. & Catalano E.(2015)

<sup>(2)</sup> Chraibi et al. (2013)

Table 3.4 Parameters of foundation Sand

Identification		Sand
Material model		Hardening soil
Drainage type		Drained
$\gamma_{\text{unsat}}$	kN/m <sup>3</sup>	20
$\gamma_{\text{sat}}$	kN/m <sup>3</sup>	20
$e_{\text{init}}$		1
$E_{50}^{\text{ref}}$	kN/m <sup>2</sup>	2.50E+04
$E_{\text{oed}}^{\text{ref}}$	kN/m <sup>2</sup>	2.00E+04
$E_{\text{ur}}^{\text{ref}}$	kN/m <sup>2</sup>	1.10E+05
power (m)		0.8
$c_{\text{ref}}$	kN/m <sup>2</sup>	1
$\phi$ (phi)	°	28
$\psi$ (psi)	°	0
$v_{\text{ur}}$		0.2
$p_{\text{ref}}$	kN/m <sup>2</sup>	100
$K_0^{\text{nc}}$		0.5305
$k_x$	m/day	0.864
$k_y$	m/day	0.864

Table 3.5 Parameters of foundation Clay

Identification		Clay
Material model		Soft soil
Drainage type		Undrained (A)
$\gamma_{\text{unsat}}$	kN/m <sup>3</sup>	20
$\gamma_{\text{sat}}$	kN/m <sup>3</sup>	20
$C_c$		0.42
$C_s$		0.0525
$e_{\text{init}}$		1
$c_{\text{ref}}$	kN/m <sup>2</sup>	1
$\phi$ (phi)	°	25 ( $c_u=0.30\sigma'_v$ )
$k_x$	m/day	3.4E-05 ( $\approx 3.9\text{E-}10$ m/s)
$k_y$	m/day	3.4E-06 ( $\approx 3.9\text{E-}11$ m/s)
$c_k$		0.42

#### 4. Numerical analysis of cross-section C-2

4.1 The analysis of section C-2 will be considered as a reference Base Case and it is presented in detail; the analyses of the other sections will be described more summarily to avoid repetitions. The effect of using preloading and/or vertical drains will also be examined. The geometry and material considered are depicted in Figure 4.1. Points A, B and C will be used to represent the evolution of settlements, point A is under the axis of the wall, point B is in the downstream part of the dam and point C corresponds to the location of the cut-off wall. Note that the vertical line at the cut-off location is for representation purposes only, the wall has not been included in the model.

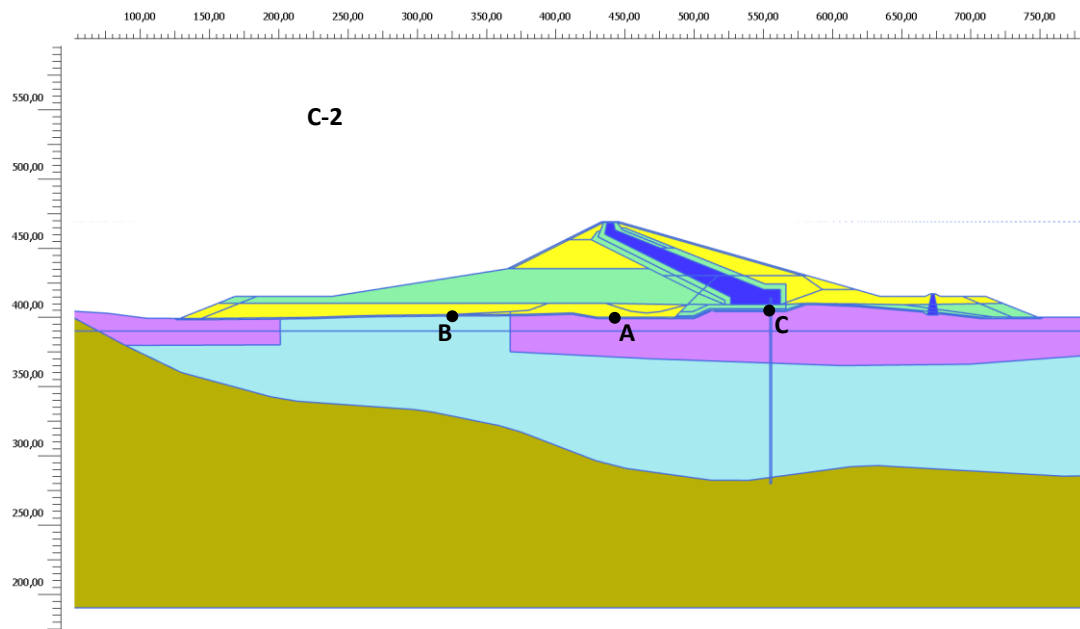


Figure 4.1. Geometry and materials used in the analyses of section C-2.

4.2 The analysis tries to follow as closely as possible the envisaged sequence of dam construction. Table 4.1 presents the various phases considered in the analyses and Figure 4.2 shows the geometry considered in each of them.



Table 4.1 Phases of analyses for Base Case (no preload)

	Description	Duration	Comments
Phase 0	Initial stress state	-	Applied using the Ko procedure
Phase 1	Initial topography	-	The end of this Phase constitutes the initial state for construction. Ignore undrained behaviour. Displacements set to zero.
Phase 2	Excavation for dam construction	-	If considered, the vertical drains are also installed during this phase. Ignore undrained behaviour.
Phase 3	1st construction stage	360 days	
Phase 4	Consolidation	390 days	The cut-off wall is assumed to be constructed in this Phase
Phase 5	2nd construction stage	390 days	End of construction
Phase 6	Consolidation	360 days	1 year after end of construction
Phase 7	Consolidation	360 days	2 years after end of construction
Phase 8	Consolidation	1800 days	5 years after end of construction
Phase 9	Consolidation	3600 days	10 years after end of construction
Phase 10	Consolidation 90%	Variable	The analysis is terminated on reaching a 90% degree of consolidation

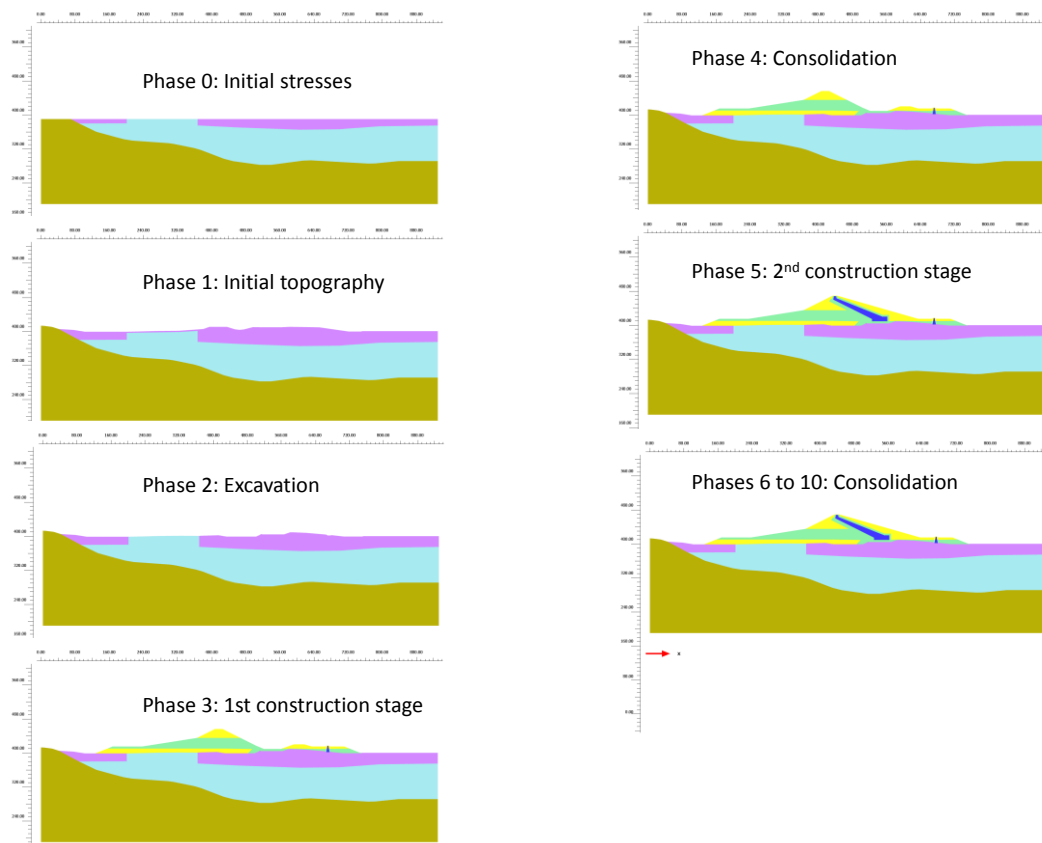


Figure 4.2. Phases of the analyses. Base Case (no preload)

4.3 Because of the low permeability of some of the materials in the foundation, dam construction sets up significant excess pore water pressures, the dissipation of which will give rise to consolidation settlements that are the most significant proportion of total settlements. For illustration purposes, the contours of excess pore pressures at important stages of the analyses are shown in Figure 4.3. It can be observed that the excess pore water pressures have practically vanished when reaching the 90% degree of consolidation stage. The (magnified) deformed mesh at the end of the analysis is shown in Figure 4.4.

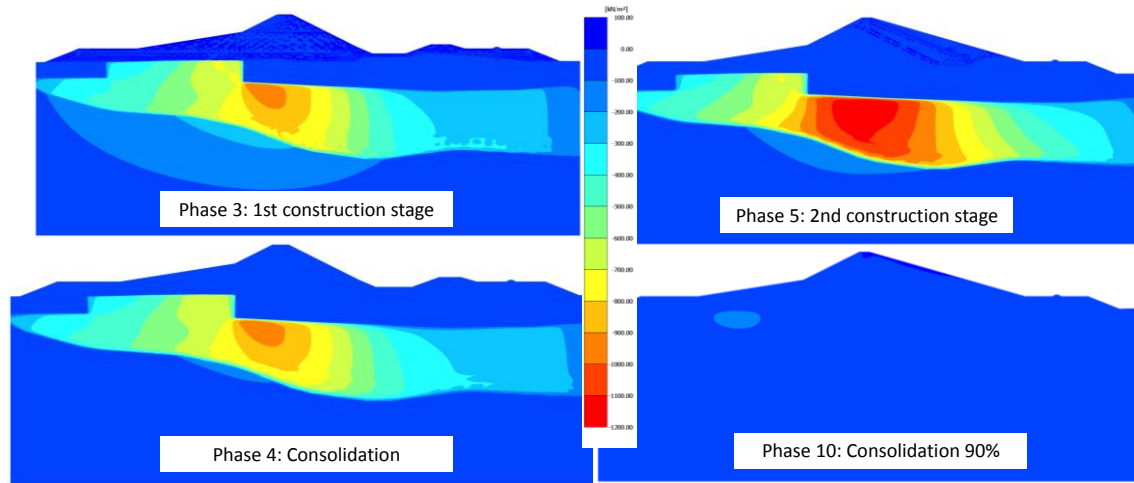


Figure 4.3. Excess pore water pressure at various phases of the analysis. Base Case (no preload)

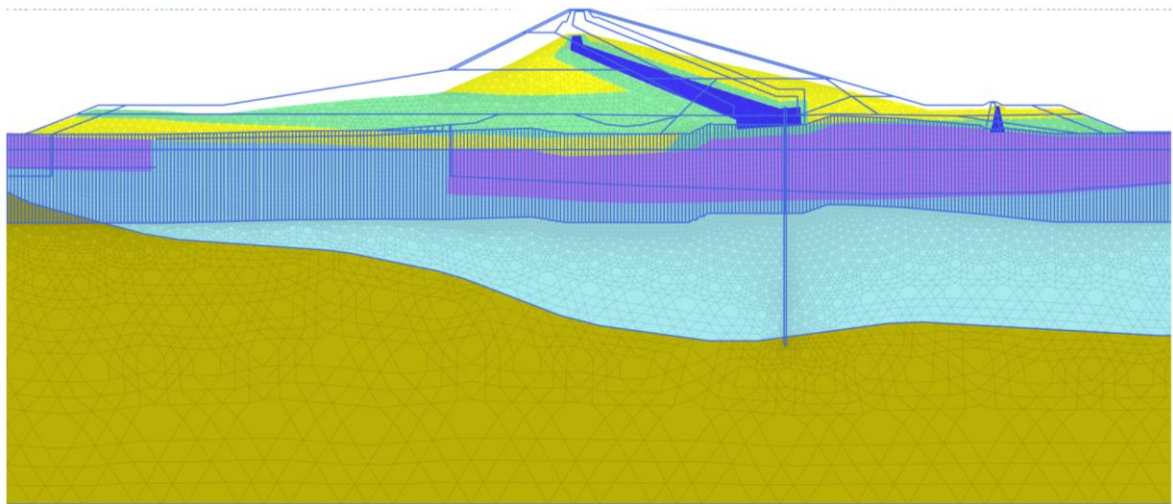


Figure 4.4. Deformed mesh (magnified) at the end of the analysis. Base Case (no preload)

4.4 The main goal of this work, however, is to estimate the settlements of the ground. Figures 4.5 to 4.7 present the settlements of the ground surface at three different stages of the analyses. In the same plots, the vertical distributions of settlements at points A, B and C are also depicted. It can be observed that very large settlements are obtained; by far the greatest contribution are the consolidation settlements of the clay soil. The final distribution of settlements follows roughly the profile of the dam. The numerical values of settlements at all phases of the analysis are listed in

Table 4.2. The settlements that will affect the cut-off wall are those occurring at point C between Phase 3 (highlighted in yellow) and Phase 10 (highlighted in grey).

4.5 The evolution of settlements with time for points A, B and C are plotted in Figures 4.8 to 4.10. It can be observed that the consolidation during construction is very limited, most of the consolidation settlements occur after construction and they continue for extremely long periods of time. Indeed, the time to reach 90% degree of consolidation is in excess of 1000 years. The computed consolidation times are very unrealistic; they are so long because in the 2D plane strain analysis no 3D effects can be considered. Also, it is extremely unlikely that the clay layer will be perfectly homogenous, there are bound to exist distributed coarser permeable layers that will help drainage and reduce consolidation times when considering the ground as a whole.

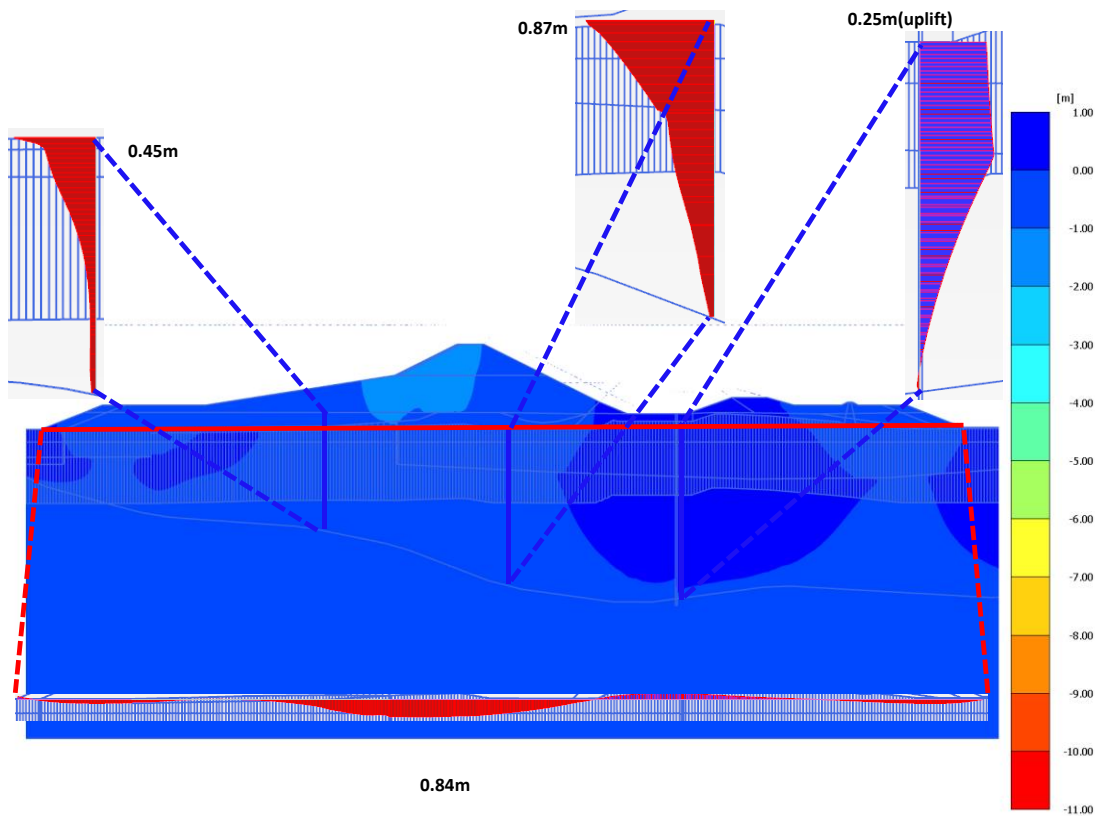


Figure 4.5. Distribution of settlements after the 1st construction stage (Phase 3). Base Case (no preload)

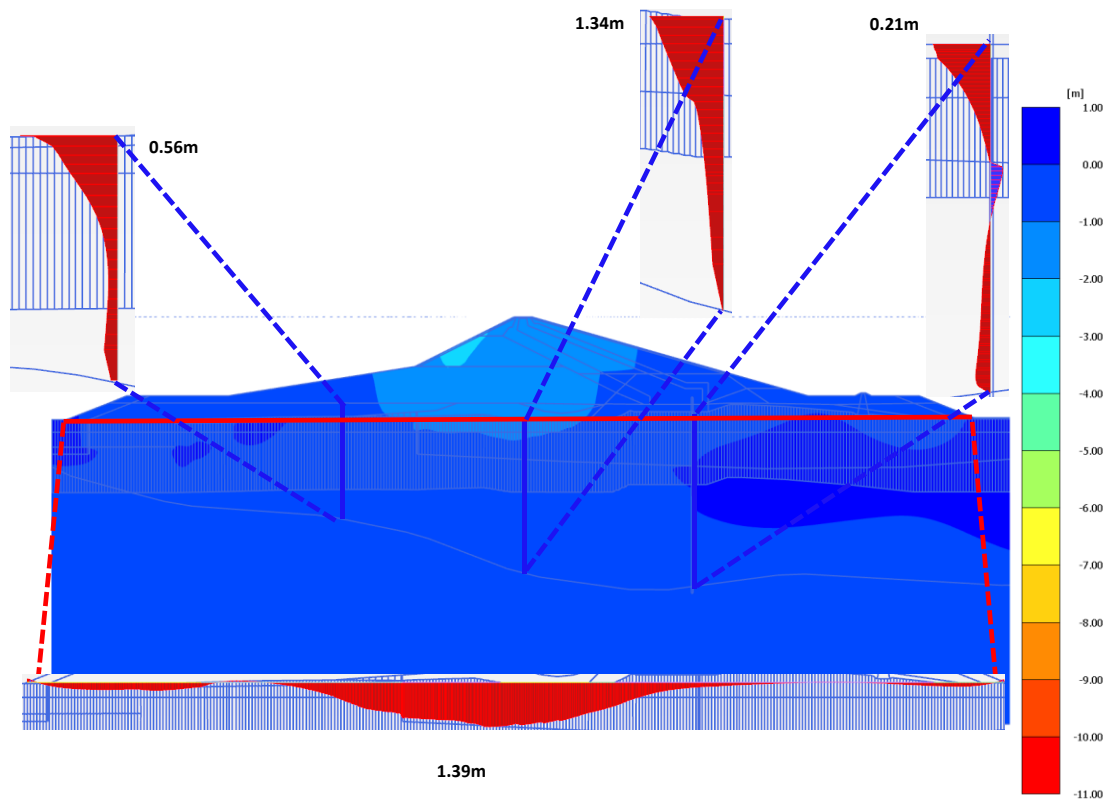


Figure 4.6. Distribution of settlements after the 2nd construction stage (Phase 5). Base Case (no preload)

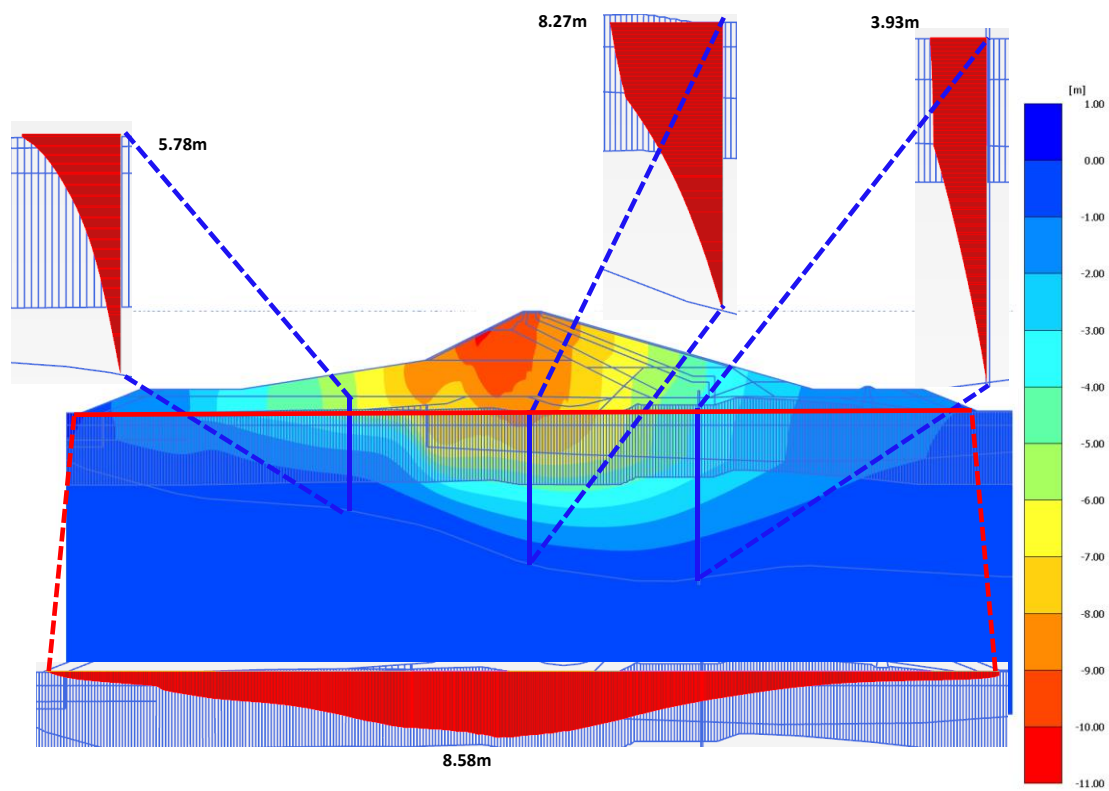


Figure 4.7. Distribution of settlements at 90% degree of consolidation (Phase 10). Base Case (no preload)

Table 4.2 Computed total settlements (m) at points A, B and C at different phases of the analyses. Settlements of point C between Phases 3 and 10 affect the cut-off wall.

C2	No preload		
	A	B	C
Phase 0: Initial state	-	-	-
Phase 1: Initial topography	-	-	-
Phase 2: Excavation	-0.21	0	-0.12
Phase 3: 1 <sup>st</sup> construction stage	0.62	0.41	0.22
Phase 4: Consolidation	0.74	0.51	0.2
Phase 5: 2 <sup>nd</sup> construction stage	1.28	0.46	0.19
Phase 6: Consolidation (1 year)	1.44	0.51	0.27
Phase 7: Consolidation (2 year)	1.49	0.53	0.29
Phase 8: Consolidation (5 year)	1.72	0.63	0.39
Phase 9: Consolidation (10 year)	2.08	0.82	0.55
Phase 10: Consolidation (U 90%)	8.25	5.88	3.91
Years to reach U 90%	1282		

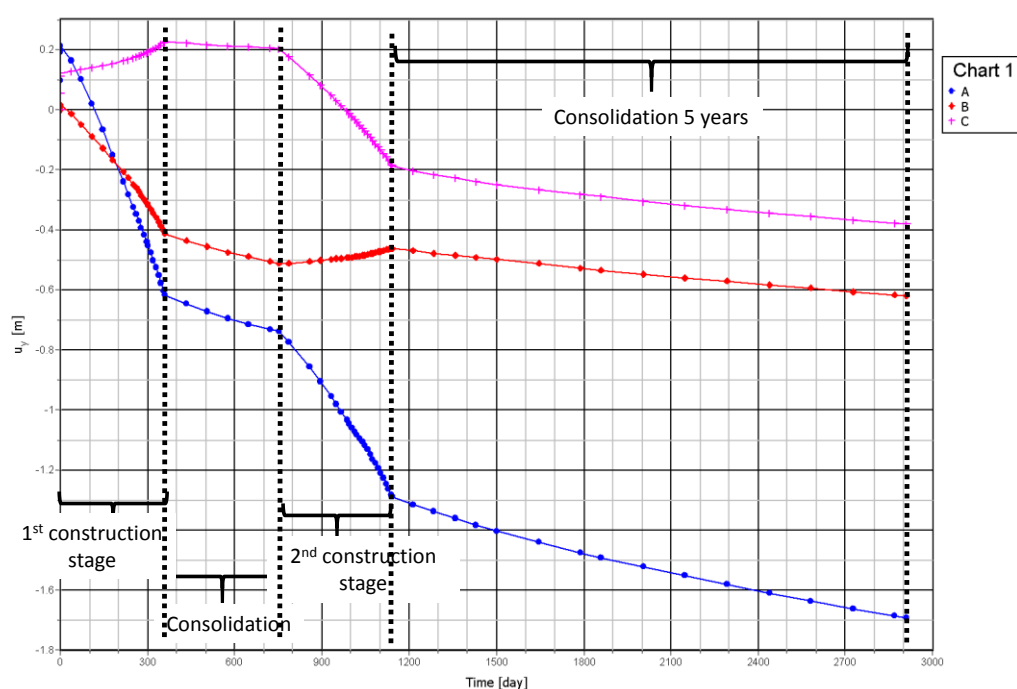


Figure 4.8. Evolution of settlements with time (up to 5 years) for points A, B and C. Base Case (no preload)

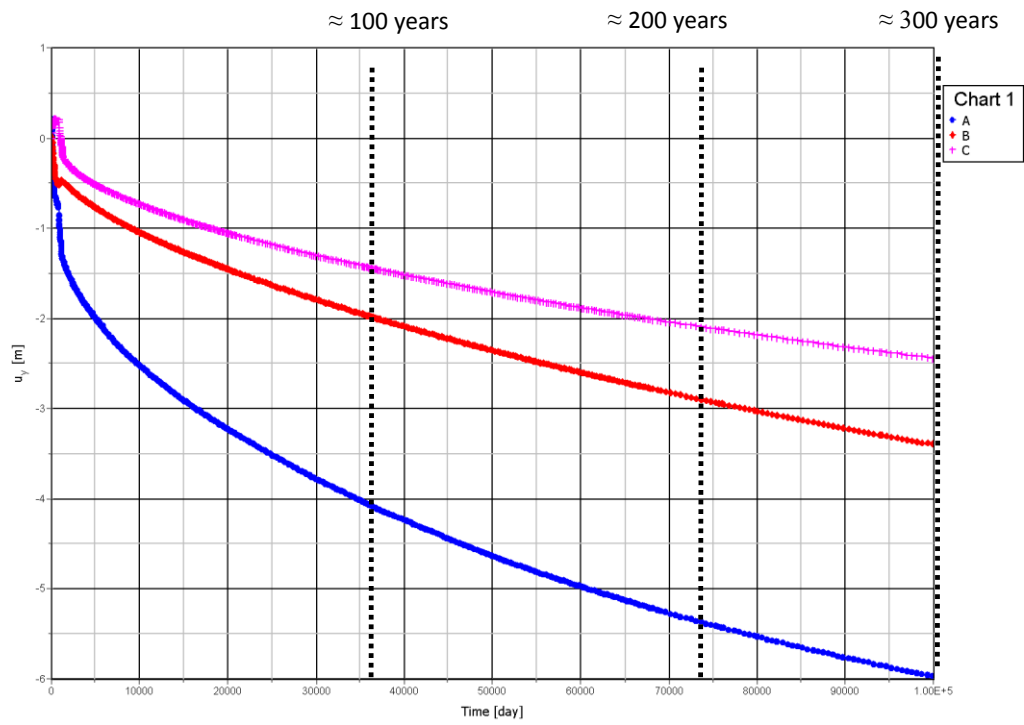


Figure 4.9. Evolution of settlements with time (up to 300 years) for points A, B and C. Base Case (no preload)

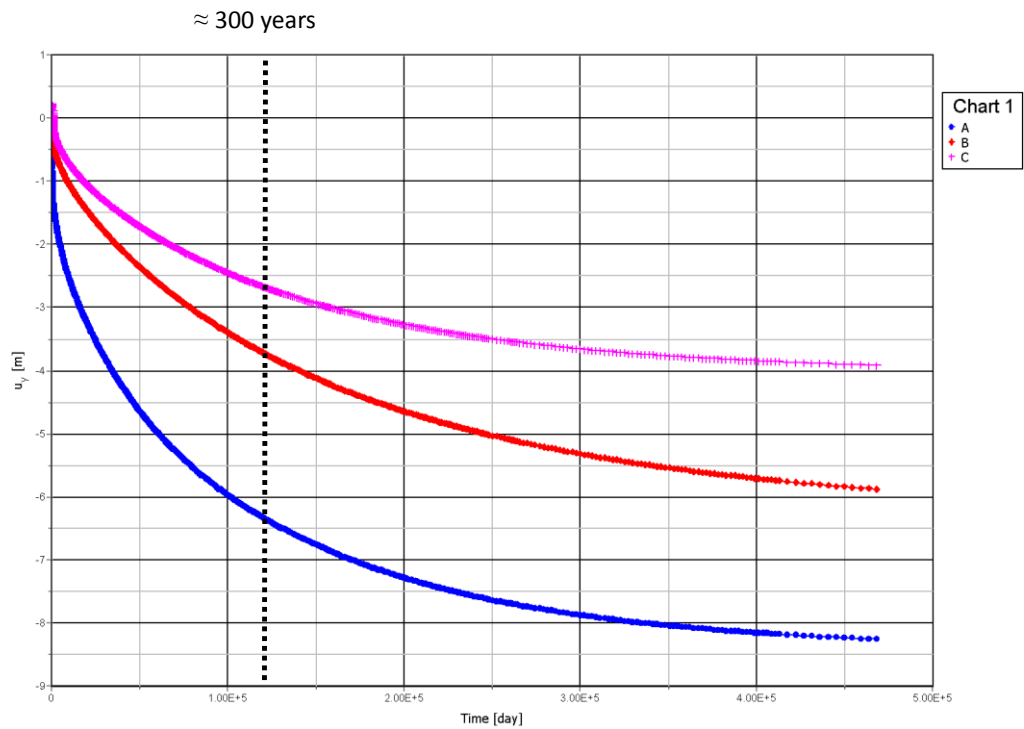


Figure 4.10. Evolution of settlements with time (up to 90% degree of consolidation) for points A, B and C. Base Case (no preload)



4.6 The effect of installing prefabricated vertical drains in the foundation has also been examined. Two drain lengths have been considered: 30 m and 50 m, the latter probably being at the limit of what is reasonably feasible in practice (Figures 4.11 and 4.12). A 1.2 m spacing has been adopted. The installation of the drains is performed during Phase 2. It can be observed (e.g. Figure 4.11) that in some parts of the foundation, the permeable material is about or more than 30 m thick at the surface. In that zone, vertical drains will have no discernible effect.

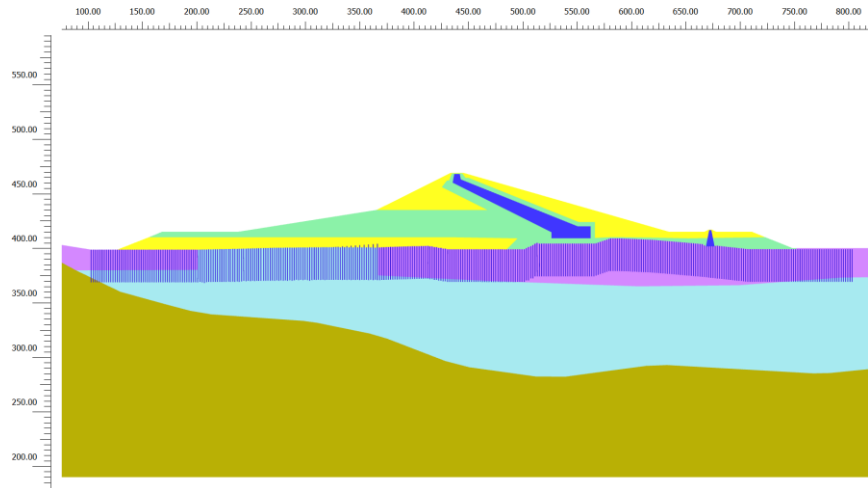


Figure 4.11. Geometry of the cross-section C-2 with 30 m long vertical drains. Base Case (no preload)

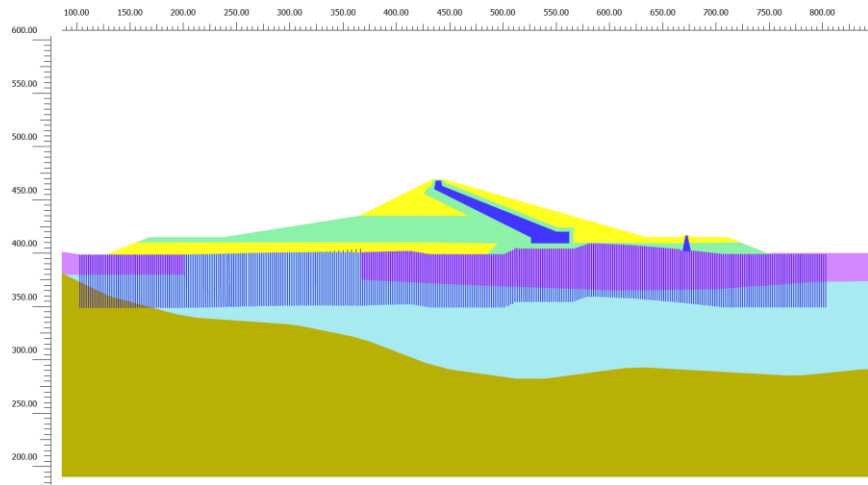


Figure 4.12. Geometry of the cross-section C-2 with 50 m long vertical drains. Base Case (no preload)

4.7 Naturally, the effect of installing vertical drains is to accelerate consolidation in the foundation areas where they are present. This can be readily observed by plotting the excess pore water pressures at key stages of the analyses (Figure 4.13). It can be noted that the excess pore water pressures outside the vertical drain zones is only marginally affected.

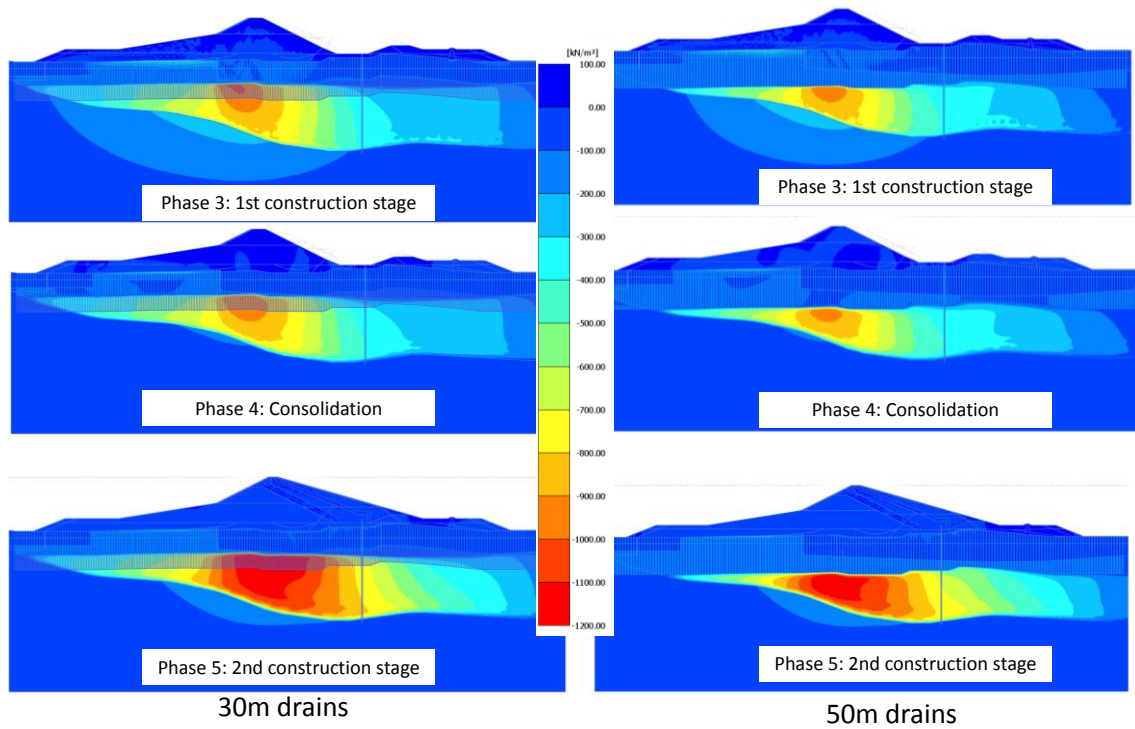


Figure 4.13. Excess pore water pressure at various phases of the analysis with 30m and 50m long vertical drains. Base Case (no preload)

4.8 The evolution of settlements is naturally affected by the presence of vertical drains, compare Figures 4.14 and 4.15 (with drains) with Figure 4.8 (no drains). The shorter term development of settlements most affected by the presence of vertical drains is that of point B that corresponds to a zone where it has been estimated that there are no high permeability layers. The effect is more muted at point A (under the axis of the dam) although some effect can be seen especially with the 50 m long drains. Finally, at point C that corresponds to the cut-off wall, the effect of the 30 m long drains is very small because of the presence of a thick permeable layer in the upper part of the ground profile. The effect of the 50 m long drains is more noticeable although still not large. The computed settlements at all stages of the analyses are collected in Table 4.3.

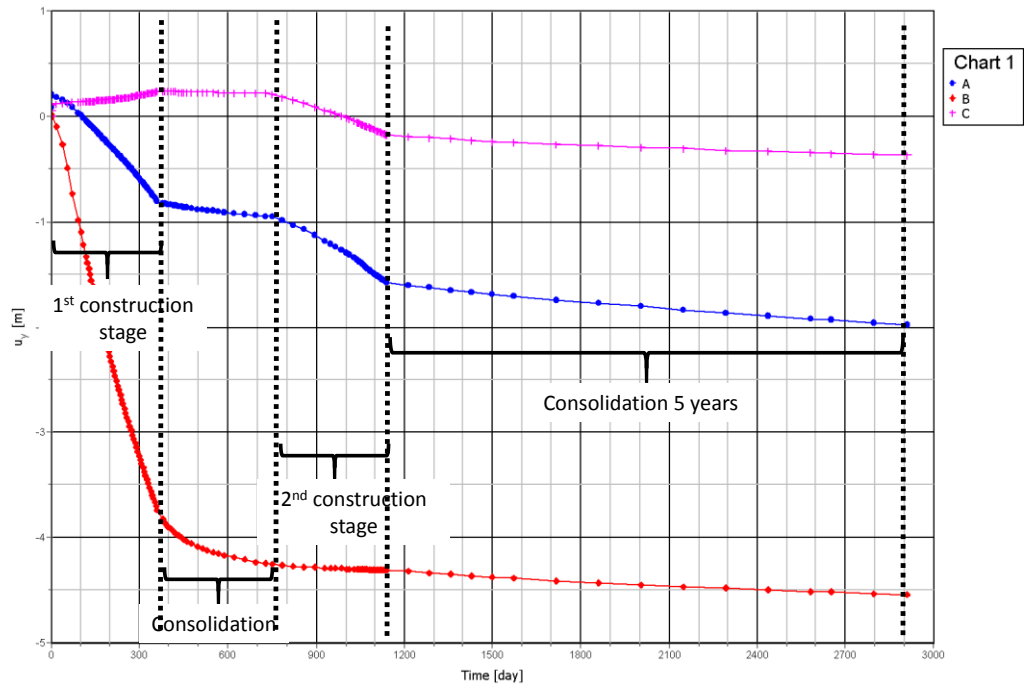


Figure 4.14. Evolution of settlements with time (up to 5 years) for points A, B and C with 30m long drains. Base Case (no preload)

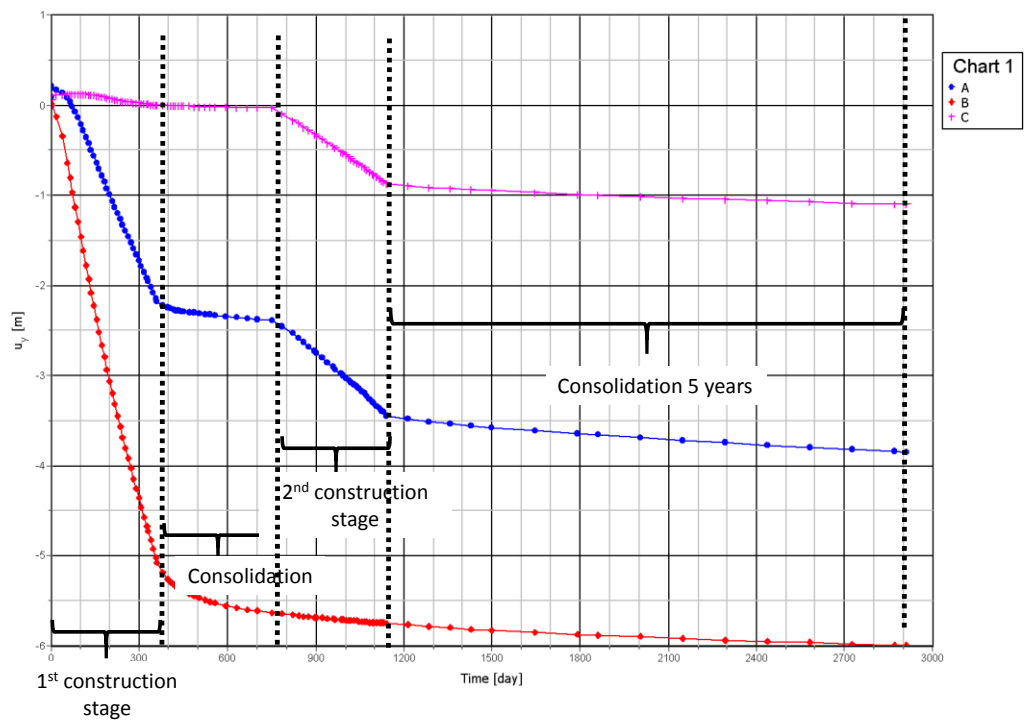


Figure 4.15. Evolution of settlements with time (up to 5 years) for points A, B and C with 50m long drains. Base Case (no preload)

Table 4.3 Computed total settlements (m) at points A, B and C at different phases of the analyses (with and without vertical drains). Settlements of point C between Phases 3 and 10 affect the cut-off wall. Base Case (no preload)

C2	No preload			No prel. 30m drain			No prel. 50m drain		
	A	B	C	A	B	C	A	B	C
Phase 0: Initial state	-	-	-	-	-	-	-	-	-
Phase 1: Initial topography	-	-	-	-	-	-	-	-	-
Phase 2: Excavation	-0.21	0	-0.12	-0.21	0	0.12	0.21	0	-0.11
Phase 3: 1 <sup>st</sup> construction stage	0.62	0.41	0.22	0.79	3.7	-0.22	2.18	5.07	0.01
Phase 4: Consolidation	0.74	0.51	0.2	0.81	4.26	-0.19	2.44	5.64	0.09
Phase 5: 2 <sup>nd</sup> construction stage	1.28	0.46	0.19	1.54	4.3	0.15	3.44	5.75	0.87
Phase 6: Consolidation (1 year)	1.44	0.51	0.27	1.7	4.39	0.24	3.61	5.85	0.97
Phase 7: Consolidation (2 year)	1.49	0.53	0.29	1.77	4.43	0.28	3.66	5.88	0.99
Phase 8: Consolidation (5 year)	1.72	0.63	0.39	2	4.55	0.37	3.87	6.01	1.11
Phase 9: Consolidation (10 year)	2.08	0.82	0.55	2.39	4.74	0.54	4.2	6.19	1.29
Phase 10: Consolidation (U 90%)	8.25	5.88	3.91	7.85	6.96	3.92	7.27	7.24	3.77
Years to reach U 90%	1282			860			523		

4.9 The factors of safety of the dam at various key stages of the analysis have been computed using the Plaxis strength reduction method. The fine grained materials have been considered to behaviour undrained at failure. The critical failure mechanisms as well the associated factor of safety values are presented in Figures 4.16 and 4.17. Table 4.4 shows all the values of factor of safety obtained for this case.

4.10 A number of points can be observed:

- During construction, the critical failure mechanism involves the foundation.
- At the end of consolidation, the failure occurs though the core
- Provision of vertical drains increases the factor of safety because of the enhanced pore pressure dissipation in the foundation (fine-grained layers).
- With the 50 m long drains, there are no critical failure mechanisms affecting the foundation. During the first construction stage, a shoulder failure is obtained.
- As expected, the final factor of safety is basically the same independently of the use or not of vertical drains.

Table 4.4 Factors of safety at various stages of the analysis. Base Case (no preload).

FoS	C-2		
	No drain	30m drain	50m drain
Phase 3: 1 <sup>st</sup> construction stage	1.39 (1)	1.47 (1)	1.71*
Phase 5: 2 <sup>nd</sup> construction stage	1.36 (1)	1.51 (1)	1.76 (2)
Phase 10: Consolidation (90%)	1.84 (1)	1.85 (2)	1.86 (2)

(1) Failure through the foundation (2) Failure through the core \* Shoulder failure

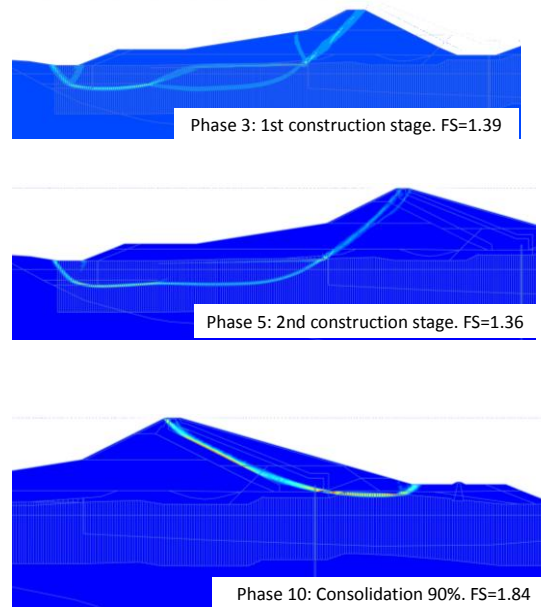


Figure 4.16. Failure mechanisms at various stages of the analysis. No drains. Base Case (no preload)

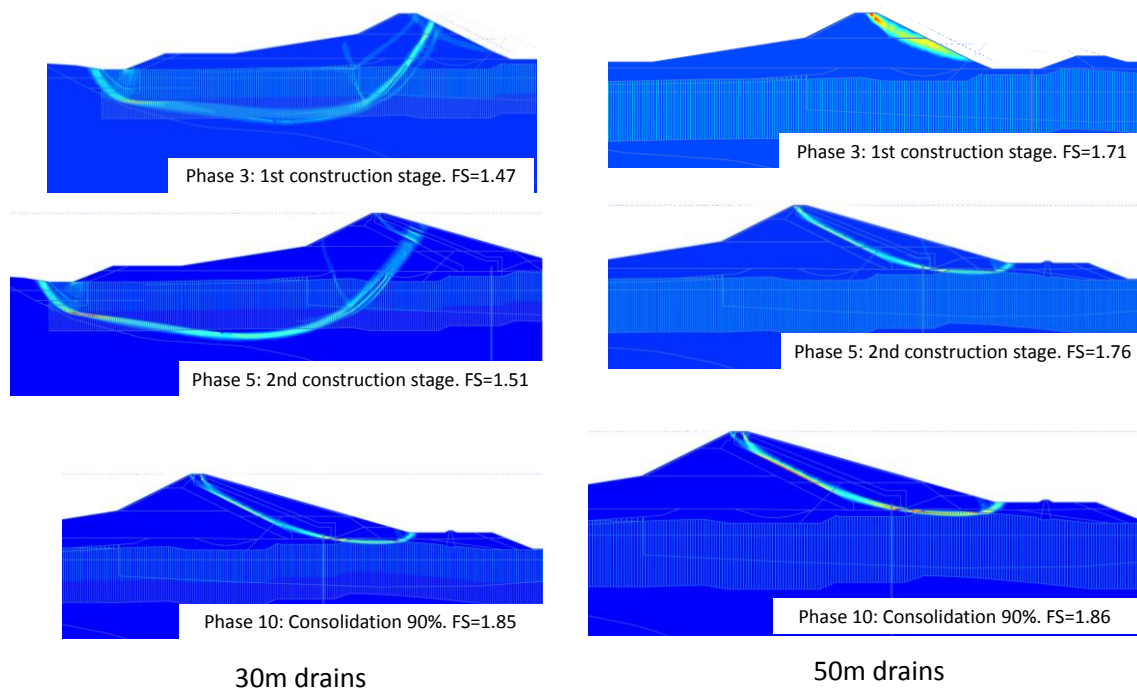


Figure 4.17. Failure mechanisms at various stages of the analysis. 30m and 50 m long drains. Base Case (no preload)

- 4.11 An alternative incorporating the application of a 20 m high preload in the zone of the cut-off wall has been examined. This has required the splitting of Phase 3 in four new phases (3a to 3d) to include the construction and removal of the preload. Table 4.5 presents the various phases considered in the analyses and Figure 4.18 shows the geometry considered in each of them.

Table 4.4 Phases of analyses for Base Case with preload

	<b>Description</b>	<b>Duration</b>	<b>Comments</b>
Phase 0	Initial stress state	-	Applied using the Ko procedure
Phase 1	Initial topography	-	The end of this Phase constitutes the initial state for construction. Ignore undrained behaviour. Displacements set to zero.
Phase 2	Excavation for dam construction	-	If considered, the vertical drains are also installed during this phase. Ignore undrained behaviour.
Phase 3a	1st construction stage (first part)	60 days	Preliminary construction before applying the preloads
Phase 3b	Preload construction	30 days	
Phase 3c	1st construction stage (2nd part)	300 days	
Phase 3d	Preload removal	30 days	
Phase 4	Consolidation	390 days	The cut-off wall is assumed to be constructed in this Phase
Phase 5	2nd construction stage	390 days	End of construction
Phase 6	Consolidation	360 days	1 year after end of construction
Phase 7	Consolidation	360 days	2 years after end of construction
Phase 8	Consolidation	1080 days	5 years after end of construction
Phase 9	Consolidation	1800 days	10 years after end of construction
Phase 10	Consolidation 90%	Variable	The analysis is terminated on reaching a 90% degree of consolidation

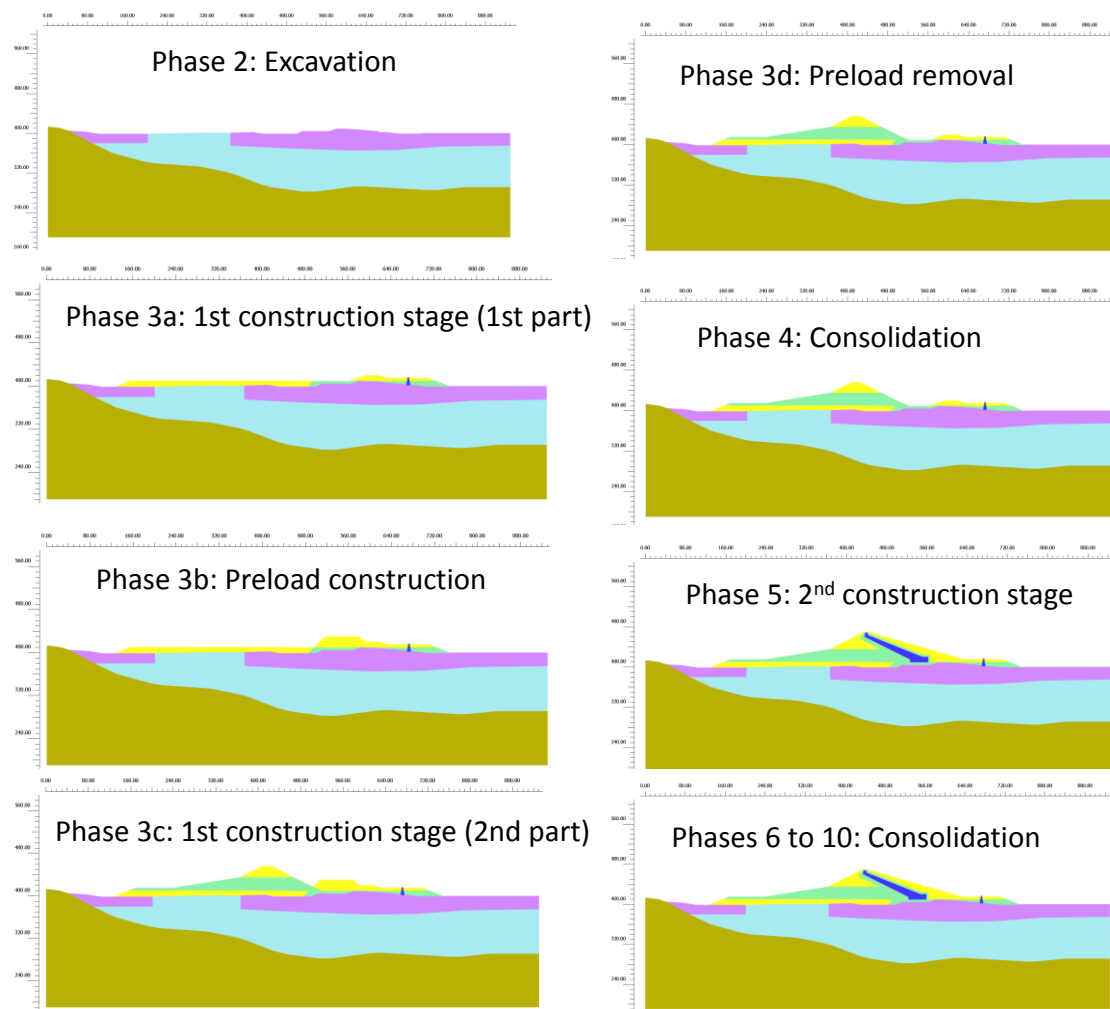


Figure 4.18. Phases of the analyses. Base Case (preload)

- 4.12 As Figures 4.19 to 4.21 demonstrate, the effect of a preload is marginal at best in this case. The reason is that the upper part of the soil profile, where the stresses applied by the preload are higher, is occupied by granular permeable materials and the soil improvement achieved is thereby limited. Also the low permeability of the fine grained layers implies that the settlements achieved by the preload are very limited during the time of application (about 330 days). Only in the case of 50 m long drains, the preload achieves a settlement of about 0.85 m occurring before the cut-off wall construction. It is still a modest improvement considering the computed total settlement of 4.3 m. The settlements computed for points A, B and C at all stages of the analyses for the preload case are collected in Table 4.5.
- 4.13 The results of the factor of safety analyses are presented in Table 4.6. They are basically the same in terms of both factors of safety values and the type of failure mechanism.

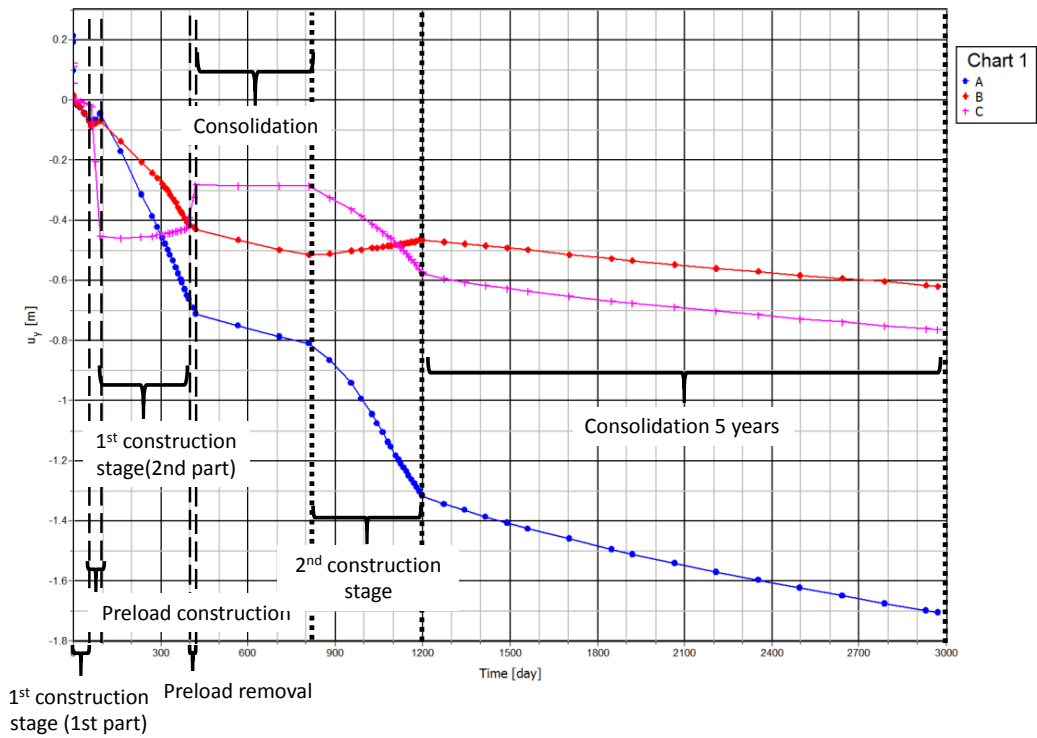


Figure 4.19. Evolution of settlements with time (up to 5 years) for points A, B and C. Base Case (preload)

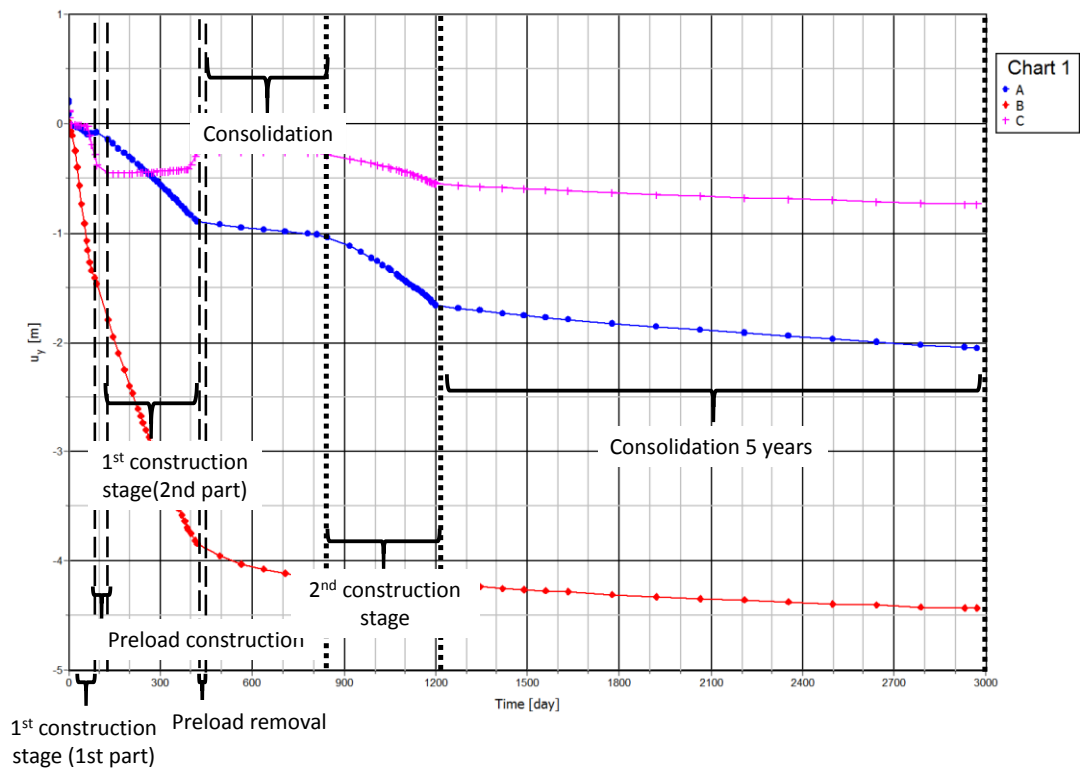


Figure 4.20. Evolution of settlements with time (up to 5 years) for points A, B and C with 30m long drains. Base Case (preload)



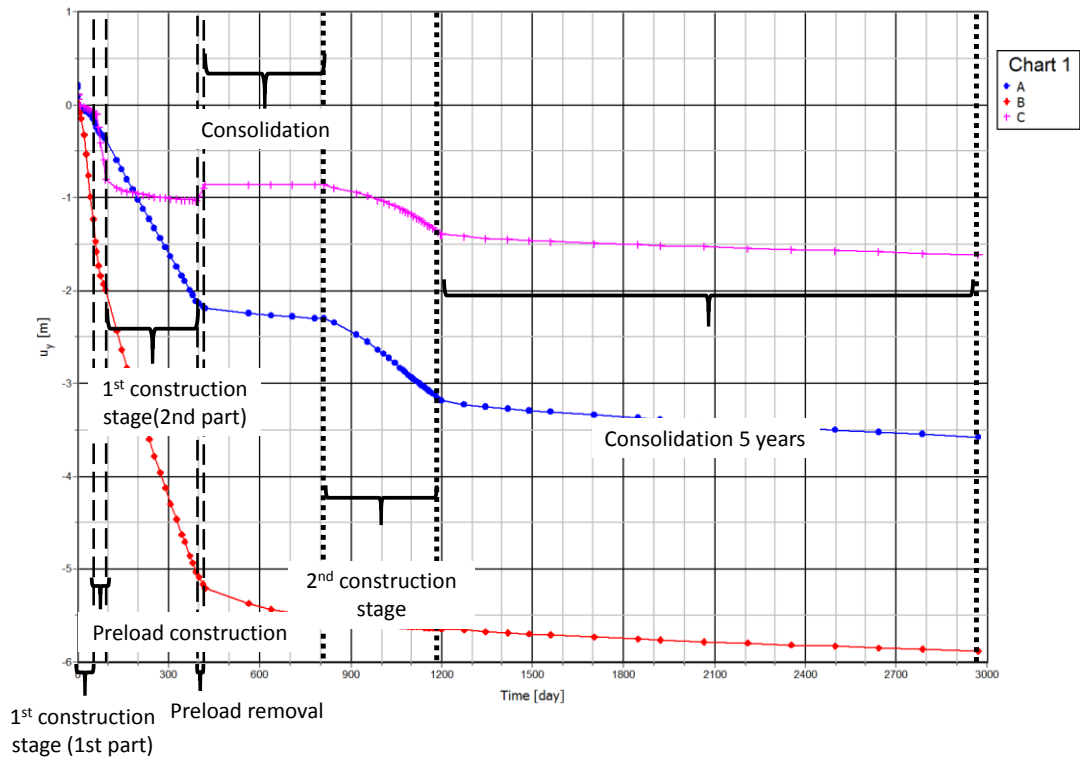


Figure 4.21. Evolution of settlements with time (up to 5 years) for points A, B and C with 30m long drains. Base Case (preload)

Table 4.5 Computed total settlements (m) at points A, B and C at different phases of the analyses (with and without vertical drains). Settlements of point C between Phases 3d and 10 affect the cut-off wall. Base Case (preload)

C2	Preload			Preload 30m drain			Preload 50m drain		
	A	B	C	A	B	C	A	B	C
Phase 0: Initial state	-	-	-	-	-	-	-	-	-
Phase 1: Initial topography	-	-	-	-	-	-	-	-	-
Phase 2: Excavation	-	-	-	-	-	-	-	-	-
Phase 3a: 1 <sup>st</sup> construction stage (1)	0.08	0.09	0.02	0.09	1.15	0.02	0.24	1.58	0.11
Phase 3b: Preload construction	0.17	0.14	0.46	0.15	1.79	0.45	0.59	2.43	0.89
Phase 3c: 1 <sup>st</sup> construction stage (2)	0.65	0.41	0.48	0.82	3.7	0.41	2.12	5.03	1.03
Phase 3d: Preload removal	0.75	0.47	0.29	0.92	3.95	0.26	2.24	5.37	0.85
Phase 4: Consolidation	0.81	0.52	0.29	1	4.16	0.26	2.3	5.52	0.86
Phase 5: 2 <sup>nd</sup> construction stage	1.35	0.47	0.59	1.62	4.22	0.56	3.22	5.66	1.42
Phase 6: Consolidation (1 year)	1.43	0.5	0.64	1.71	4.27	0.6	3.31	5.71	1.47
Phase 7: Consolidation (2 year)	1.51	0.55	0.69	1.82	4.34	0.66	3.41	5.78	1.53
Phase 8: Consolidation (5 year)	1.73	0.62	0.77	1.99	4.43	0.73	3.57	5.88	1.61
Phase 9: Consolidation (10 year)	2.08	0.81	0.93	2.38	4.63	0.91	3.92	6.07	1.8
Phase 10: Consolidation (U 90%)	8.3	5.9	4.32	7.85	6.85	4.32	6.98	7.11	4.31
Years to reach U 90%	1288			877			543		

Table 4.6 Factors of safety at various stages of the analysis. Base Case (preload).

FoS	C-2		
	No drain	30m drain	50m drain
Phase 3c: 1 <sup>st</sup> construction stage	1.39 (1)	1.69*	1.69*
Phase 5: 2 <sup>nd</sup> construction stage	1.38 (1)	1.51 (1)	1.71 (2)
Phase 10: Consolidation (U 90%)	1.84(2)	1.91 (2)	1.88 (2)

(1) Failure through the foundation (2) Failure through the core \* Shoulder failure

4.14 Because there is always a significant uncertainty concerning the actual values of permeability (and therefore of degree of consolidation), an additional set of analyses have been performed using a permeability 10 times higher for the foundation clay material. The results in terms of settlements for the different phases of analyses are shown in Table 4.7. It can be observed that no significant differences arise in the settlements that occur during construction. As expected, the final settlements are also the same as in the Base Case. The only difference is that now the time to reach the 90% degree of consolidation is one order of magnitude shorter.

Table 4.7 Computed total settlements (m) at points A, B and C at different phases of the analyses (with and without vertical drains). Settlements of point C between Phases 3d and 10 affect the cut-off wall. Preload case with clay permeability 10 times higher.

C2 (k x10)	Preload			Preload 30m drain			Preload 50m drain		
	A	B	C	A	B	C	A	B	C
Phase 0: Initial state	-	-	-	-	-	-	-	-	-
Phase 1: Initial topography	-	-	-	-	-	-	-	-	-
Phase 2: Excavation	-	-	-	-	-	-	-	-	-
Phase 3a: 1 <sup>st</sup> construction stage (1)	0.09	0.14	0.03	0.11	1.96	0.03	0.32	2.52	0.15
Phase 3b: Preload construction	0.09	0.14	0.5	0.13	2.2	0.49	0.54	2.82	0.94
Phase 3c: 1 <sup>st</sup> construction stage (2)	0.83	0.56	0.55	0.99	4.29	0.54	2.34	5.69	1.18
Phase 3d: Preload removal	0.94	0.63	0.41	1.13	4.42	0.39	2.43	5.83	1.01
Phase 4: Consolidation	1.21	0.9	0.42	1.42	4.7	0.41	2.68	6.09	1.06
Phase 5: 2 <sup>nd</sup> construction stage	1.96	1	0.83	2.18	4.8	0.83	3.76	6.26	1.74
Phase 6: Consolidation (1 year)	2.28	1.13	0.99	2.52	4.92	1	4.04	6.38	1.9
Phase 7: Consolidation (2 year)	2.57	1.28	1.13	2.82	5.04	1.49	4.29	6.49	2.07
Phase 8: Consolidation (5 year)	3.18	1.62	1.42	3.46	5.29	1.46	4.77	6.7	2.4
Phase 9: Consolidation (10 year)	4.39	2.39	2.01	4.68	5.8	2.08	5.58	6.98	3.03
Phase 10: Consolidation (U 90%)	8.1	5.92	4.27	7.7	6.94	4.29	6.88	7.21	4.32
Years to reach U 90%	137			96			63		

## 5. Numerical analysis of cross-sections C-1 and C-3

5.1 Two additional cross sections have been analysed, C-1 and C-3. Their locations are presented in Figure 3.1. The analyses have been performed without vertical drains and with 30m long and 50 m long vertical drains.

5.2 In Section C-1, the same cases as for cross-section C-2 have been considered: no preload and a 20 m high preload. The corresponding geometries are shown in Figure 5-1. The calculation phases are also the same as for cross-section C-2.

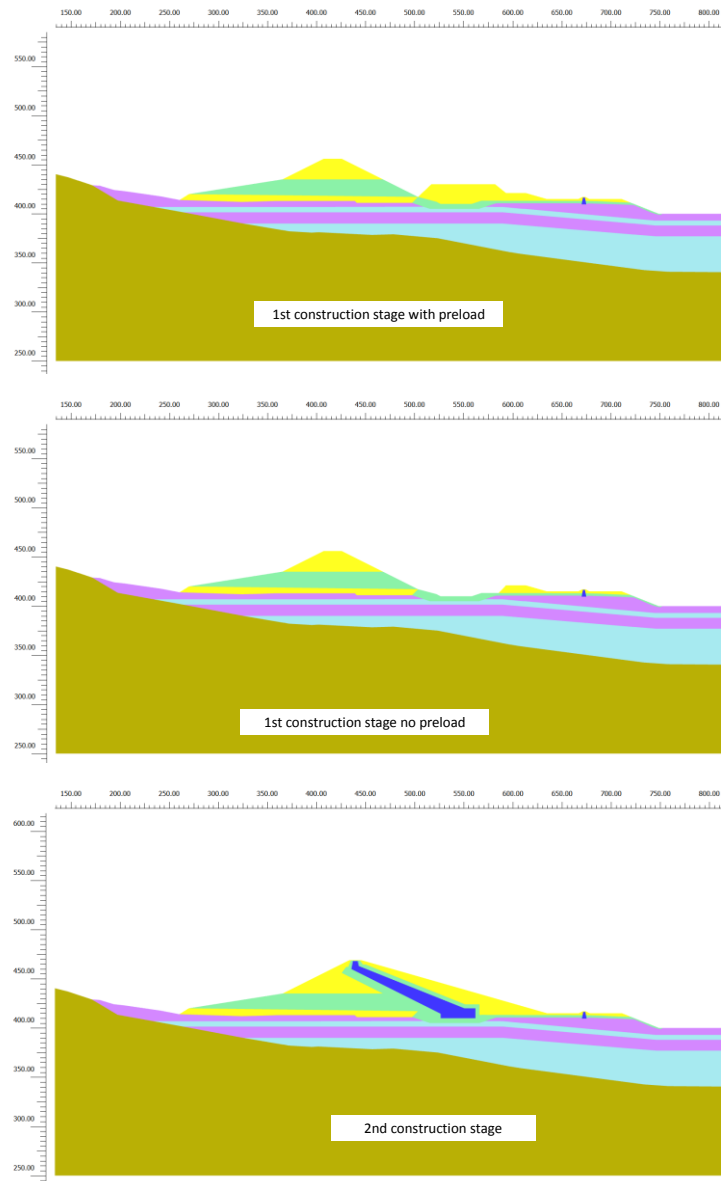


Figure 5.1. Construction stages for Section C-1

5.3 The results of the analyses in terms of settlements of points A, B and C (Figure 3.2) are collected in Tables 5.1 and 5.2. In this case, the benefits of the preload to reduce the settlements affecting the cut-off wall are evident. This is due to the fact that in this case most of the soil profile is constituted by low permeability clay materials. The fact that the total thickness of soft ground is smaller also contributes to the higher effectiveness of the preload.

Table 5.1 Computed total settlements (m) at points A, B and C at different phases of the analyses (with and without vertical drains). Settlements of point C between Phases 3 and 10 affect the cut-off wall. Cross-section C-1 (no preload).

C1	No preload			No prel. 30m drain			No prel. 50m drain		
	A	B	C	A	B	C	A	B	C
Phase 0: Initial state	-	-	-	-	-	-	-	-	-
Phase 1: Initial topography	-	-	-	-	-	-	-	-	-
Phase 2: Excavation	-	-	-	0	0	-0.16	0	0	-0.16
Phase 3: 1 <sup>st</sup> construction stage	-	-	-	2.07	0.8	0.02	2.23	0.79	0.08
Phase 4: Consolidation	-	-	-	2.31	0.86	0.06	2.337	0.86	0.11
Phase 5: 2 <sup>nd</sup> construction stage	-	-	-	2.82	0.86	1.33	2.9	0.86	1.61
Phase 6: Consolidation (1 year)	-	-	-	2.9	0.86	1.47	2.93	0.86	1.7
Phase 7: Consolidation (2 year)	-	-	-	2.91	0.86	1.5	2.94	0.86	1.71
Phase 8: Consolidation (5 year)	-	-	-	2.93	0.86	1.56	2.94	0.86	1.72
Phase 9: Consolidation (10 year)	-	-	-	2.93	0.86	1.65	2.94	0.86	1.72
Phase 10: Consolidation (U 90%)	-	-	-	2.93	0.86	1.81	2.94	0.86	1.72
Years to reach U 90%				70			19		

Table 5.2 Computed total settlements (m) at points A, B and C at different phases of the analyses (with and without vertical drains). Settlements of point C between Phases 3d and 10 affect the cut-off wall. Cross-section C-1 (preload).

C1	Preload			Preload 30m drain			Preload 50m drain		
	A	B	C	A	B	C	A	B	C
Phase 0: Initial state	-	-	-	-	-	-	-	-	-
Phase 1: Initial topography	-	-	-	-	-	-	-	-	-
Phase 2: Excavation	-	-	-	-	-	-0.15	-	-	-0.15
Phase 3a: 1 <sup>st</sup> construction stage (1)	0.08	0.1	0.02	0.39	0.34	0.24	0.43	0.34	0.3
Phase 3b: Preload construction	0.11	0.11	0.27	0.45	0.38	0.86	0.5	0.38	1.05
Phase 3c: 1 <sup>st</sup> construction stage (2)	0.67	0.23	0.39	1.84	0.91	1.41	1.93	0.91	1.64
Phase 3d: Preload removal	-	-	-	1.88	0.92	1.31	1.97	0.92	1.51
Phase 4: Consolidation	-	-	-	2.05	0.93	1.29	2.1	0.93	1.52
Phase 5: 2 <sup>nd</sup> construction stage	-	-	-	2.53	0.93	1.82	2.57	0.93	2.11
Phase 6: Consolidation (1 year)	-	-	-	2.61	0.93	1.94	2.62	0.93	2.19
Phase 7: Consolidation (2 year)	-	-	-	2.62	0.93	1.97	2.62	0.93	2.19
Phase 8: Consolidation (5 year)	-	-	-	2.63	0.93	2.03	2.62	0.93	2.2
Phase 9: Consolidation (10 year)	-	-	-	2.64	0.93	2.1	2.62	0.93	2.2
Phase 10: Consolidation (U 90%)	-	-	-	2.65	0.93	2.24	2.62	0.93	2.2
Years to reach U 90%	-			704			21		

5.4 Due to the location of cross-section C-3, no preload has been considered. The geometries of the two stages of construction are shown in Figure 5.2. Again, the calculation phases are the same as for cross-section C-2. The results of the analyses in terms of settlements of points A, B and C (Figure 3.4) are shown in Table 5.3. In this case, the settlements affecting the cut-off wall are quite small because the limited thickness of alluvial ground is largely constituted by permeable coarse materials.

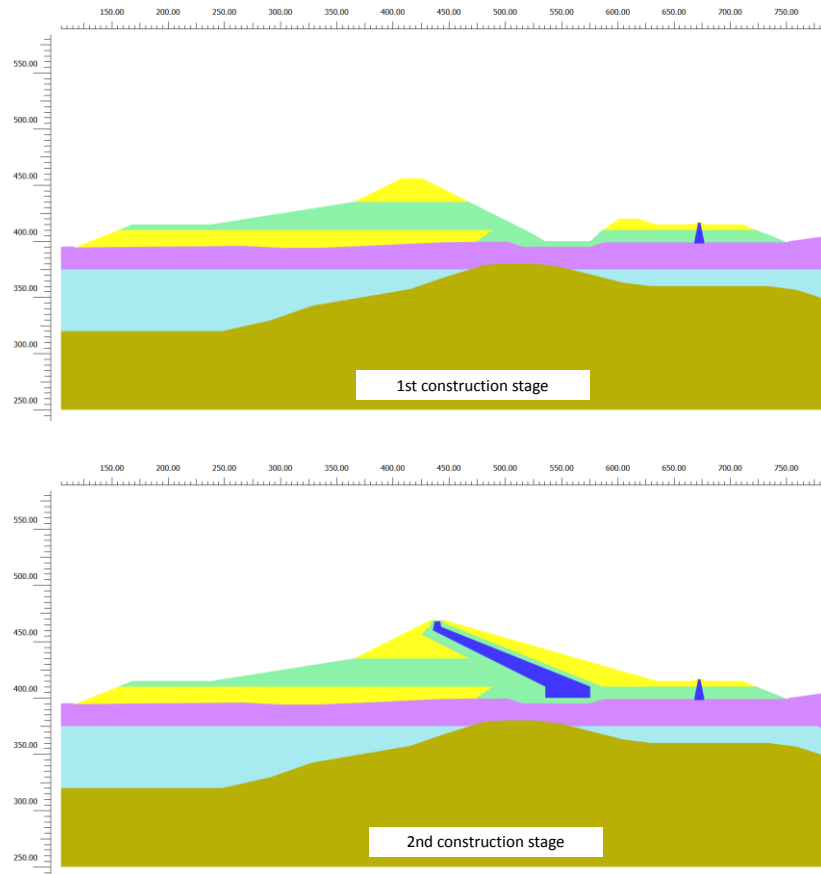


Figure 5.2. Construction stages for Section C-3

5.5 It is interesting to note that without vertical drains cross-sections C-1 and C-3 experienced failure during the construction stages. Provision of vertical drains managed to avoid failure because of the increase of undrained shear strength associated with a faster dissipation of pore pressures. The computed Factors of Safety (using the Plaxis strength reduction technique) are shown in Tables 5.4 and 5.5.

Table 5.3 Computed total settlements (m) at points A, B and C at different phases of the analyses (with and without vertical drains). Settlements of point C between Phases 3 and 10 affect the cut-off wall. Cross-section C-3 (no preload).

C3	No preload			No prel. 30m drain			No prel. 50m drain		
	A	B	C	A	B	C	A	B	C
Phase 0: Initial state	-	-	-	-	-	-	-	-	-
Phase 1: Initial topography	-	-	-	-	-	-	-	-	-
Phase 2: Excavation	0	0	0	0	0	-0.02	0	0	0
Phase 3: 1 <sup>st</sup> construction stage	0.73	0.54	0	1.44	1.68	0.01	2.01	3.37	0.02
Phase 4: Consolidation	0.88	0.66	0.02	1.62	1.86	0.02	2	3.51	0.02
Phase 5: 2 <sup>nd</sup> construction stage	-	-	-	2.16	1.96	0.21	2.27	3.61	0.2
Phase 6: Consolidation (1 year)	-	-	-	2.36	2.03	0.22	2.3	3.65	0.21
Phase 7: Consolidation (2 year)	-	-	-	2.45	2.07	0.22	2.31	3.67	0.21
Phase 8: Consolidation (5 year)	-	-	-	2.66	2.2	0.23	2.34	3.74	0.21
Phase 9: Consolidation (10 year)	-	-	-	2.85	2.36	0.24	2.38	3.82	0.21
Phase 10: Consolidation (U 90%)	-	-	-	3.48	4.07	0.25	2.41	4.21	0.21
Years to reach U 90%				336			134		

Table 5.4 Factors of safety at various stages of the analysis. Cross-sections C-1 and C-3 (no preload)

FoS	C-1			C-3		
	No drain	30m drain	50m drain	No drain	30m drain	50m drain
Phase 3: 1 <sup>st</sup> construction stage	<1	1.45*	1.45*	1.27	1.43 (1)	1.54*
Phase 5: 2 <sup>nd</sup> construction stage		1.55*	1.55*	<1	1.18 (1)	1.78 (1)
Phase 10: Consolidation (U 90%)		1.60*	1.60*		1.81 (2)	1.81 (2)

(1) Failure through the foundation (2) Failure through the core \* Shoulder failure

Table 5.5 Factors of safety at various stages of the analysis. Cross-sections C-1 (preload)

FoS	C-1		
	No drain	30m drain	50m drain
Phase 3c: 1 <sup>st</sup> construction stage	1.03 (1)	1.51*	1.51*
Phase 5: 2 <sup>nd</sup> construction stage	<1	1.55 (2)	1.54(2)
Phase 10: Consolidation (U 90%)		1.59 (2)	1.58 (2)

(1) Failure through the foundation (2) Failure through the core \* Shoulder failure

5.6 Some representative mechanisms of failure for cross-section C-1 are shown in Figure 5.3. Without drains, the first construction stage is not stable. If preload is applied, the dam is just about stable but it fails when the preload is removed. In

contrast, the installation of drains allows all the construction to proceed with an adequate factor of safety even without drains or preload.

- 5.7 Failure mechanisms for cross-section C-3 are presented in Figure 5.4. Without drains, the first construction stage can be completed but it fails during the second construction stage. Again, provision of vertical drains to dissipate pore pressures more rapidly allow the second construction stage to be achieved. It can be note that the factor of safety increases with the longer drains as the critical failure surface has to go deeper into the ground. It should be noted that the critical failure surface passes near the bedrock, where slope wash deposit should improve the locally the strength of the deposit and increase the safety factor.
- 5.8 Although the analysis have been made with vertical drains spanning the whole width of the dam section, if drains are installed to increase the factor of safety only, they would only be required in the zone affected by the failure mechanism.

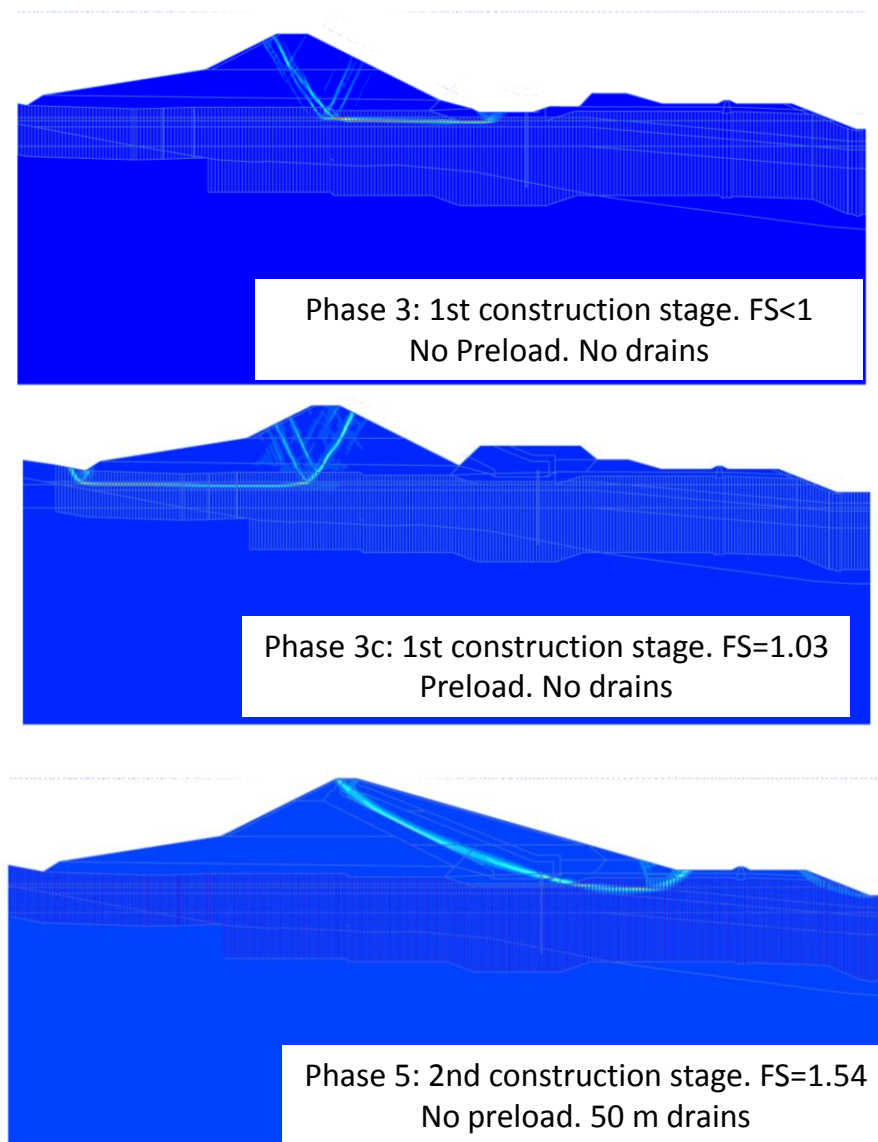


Figure 5.3. Failure mechanisms for cross-section C-1



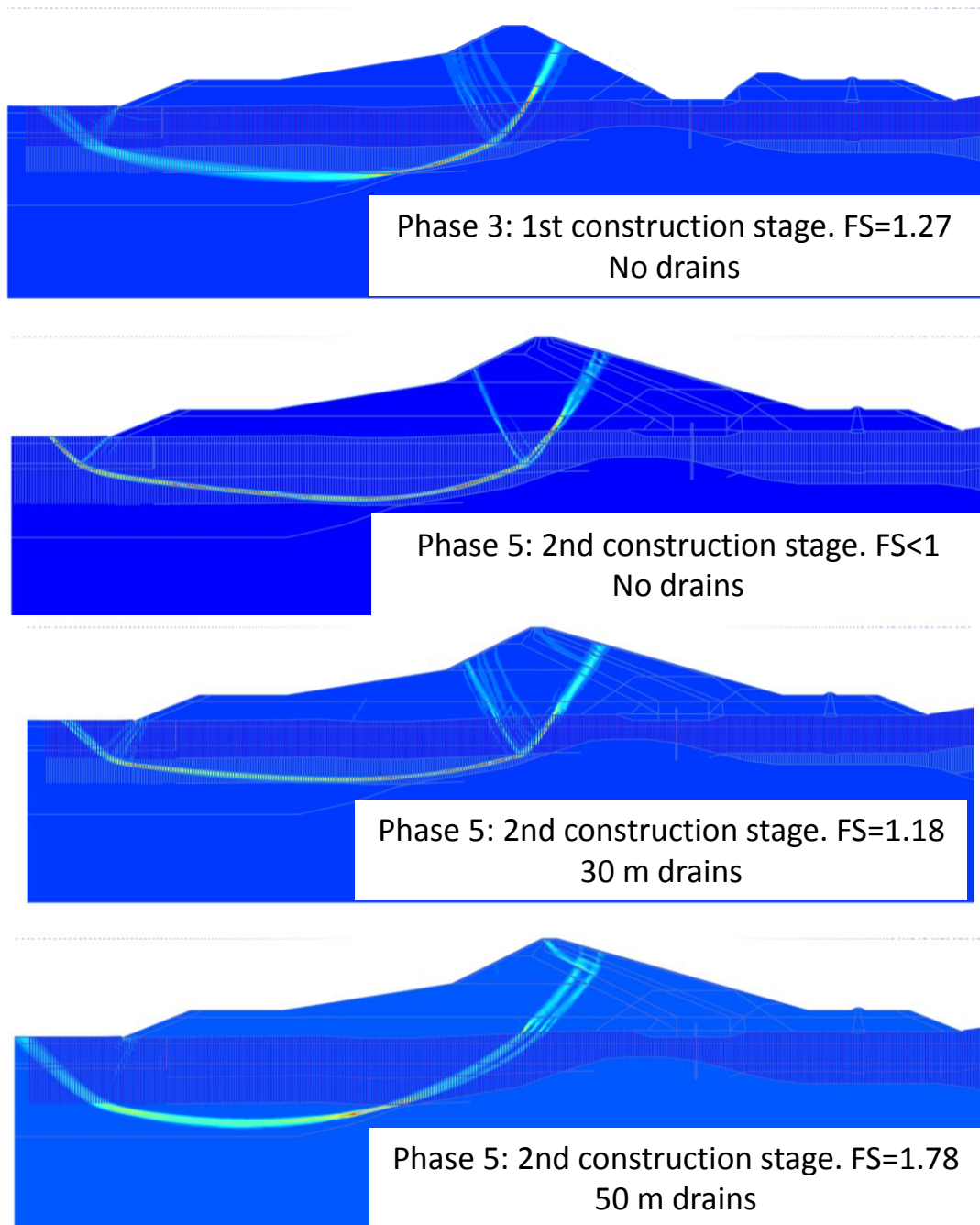


Figure 5.4. Failure mechanisms for cross-section C-3

## 6. Numerical analysis of longitudinal sections

6.1 To complete the picture of the behaviour of the dam during construction, two longitudinal sections have been analysed: section A (along the axis of the dam) and section C (along the cut-off footprint). The plan locations of the sections are shown in Figure 3.1 and the geometries and material distribution in Figures 3.5 and 3.6 where the locations of cross-sections 1, 2 and 3 are indicated.

6.2 The phases of analyses have been the same as for the analyses of the cross sections. The load attributed to each phase corresponds to the materials and height of the dam along a vertical line at the section considered. Naturally, the loading has now some quite unrealistic features as it is implicitly assumed that the entire valley is filled to the same height but it is the only way to examine the potential effects of the variation of ground profile along the dam in a 2D computation. The potential use of the preload has only been considered in the case of section C (cut-off). Obviously in the case of longitudinal sections, it does not make sense to compute factors of safety.

6.3 For longitudinal section A, the distributions of settlements at the end of construction and at 90% consolidation for the case of no drains are plotted in Figures 6.1 and 6.2. It can be seen that most of the settlements occur after the end of construction and their distribution is strongly dependent on the bedrock profile. This is consistent with the variation of excess pore water pressures depicted in Figure 6.3.

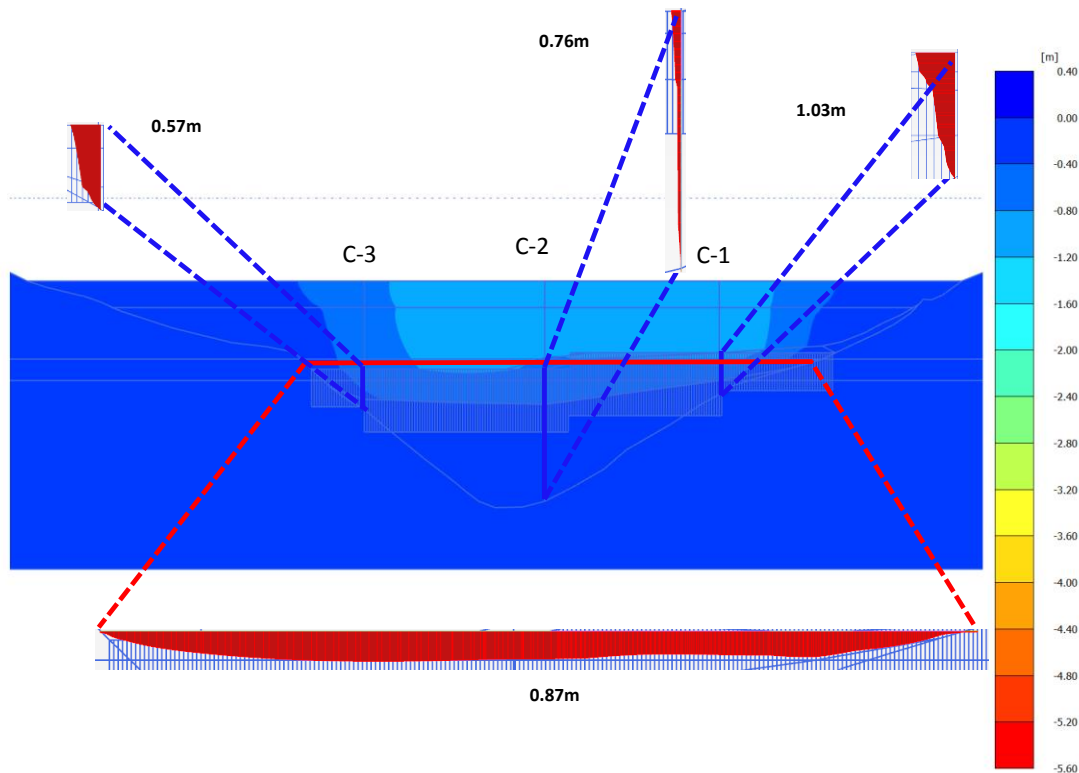


Figure 6.1. Distribution of settlements after the 2nd construction stage (Phase 5). Longitudinal Section A (dam axis). No drains

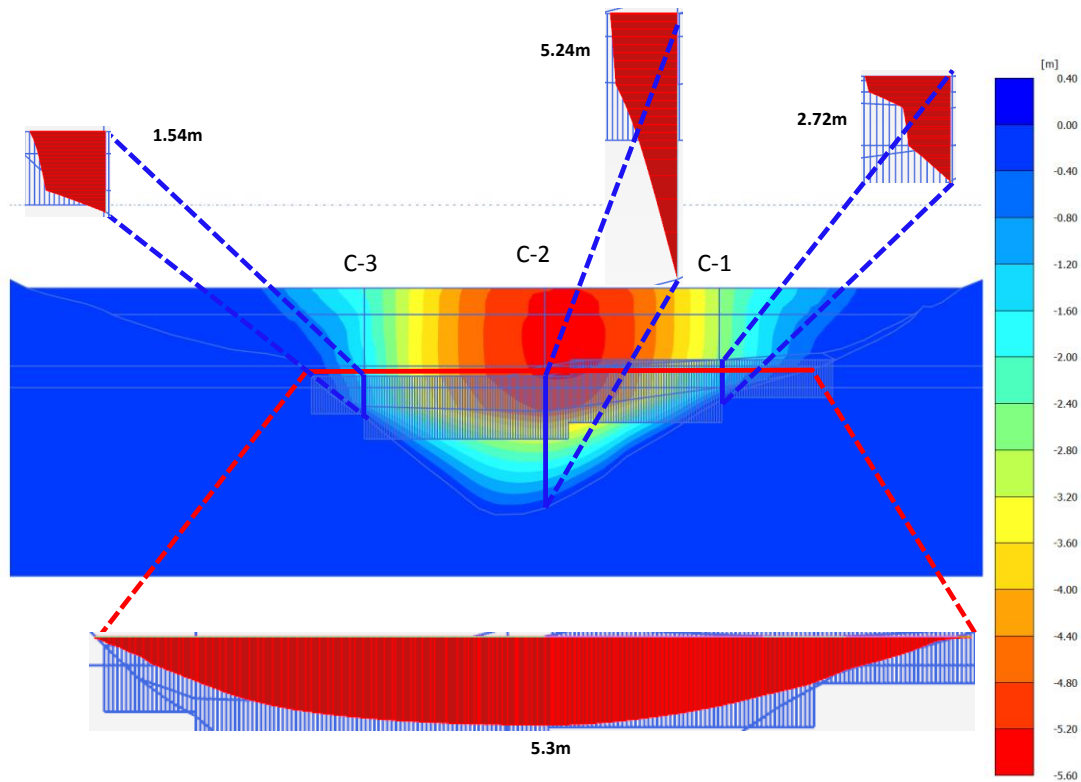


Figure 6.2. Distribution of settlements at 90% degree of consolidation (Phase 10). Longitudinal Section A (dam axis). No drains

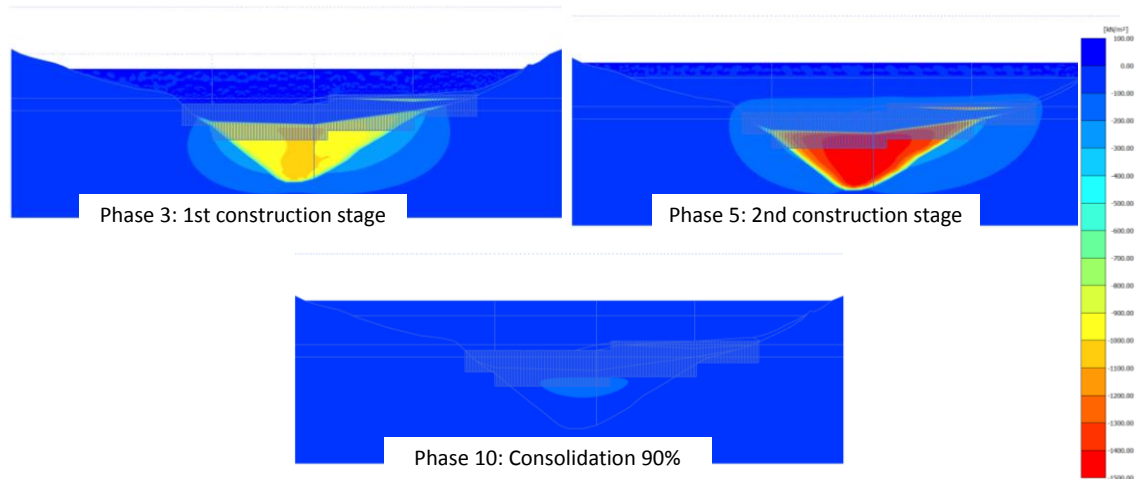


Figure 6.3. Excess pore water pressure at various phases of the analysis. Longitudinal section A (dam axis). No drains

6.4 The numerical values of the settlements for all phases of the calculation are listed in Table 6.1. It can be seen that only the 50 m long drains have a significant effect on the settlements that occur during construction. More relevant is the fact that for the locations of cross-sections C-2 (especially) and C-3, the computed settlements in the longitudinal section are notably lower than those computed for the cross-sections in spite of the apparent overestimation of loading intensity. This observation strongly suggests that the 3D effects not considered in the analyses may be significant.

Table 6.1 Computed total settlements (m) at at locations C-1, C-2 and C-3 at different phases of the analyses (with and without vertical drains). Settlements of point C between Phases 3d and 10 affect the cut-off wall. Longitudinal section A (dam axis).

Dam Axis	No preload			No prel. 30m drain			No prel. 50m drain		
	C-1	C-2	C-3	C-1	C-2	C-3	C-1	C-2	C-3
Phase 0: Initial state	-	-	-	-	-	-	-	-	-
Phase 1: Initial topography	-	-	-	-	-	-	-	-	-
Phase 2: Excavation	-	-0.12	-	0	-0.12	0	0	-0.12	0
Phase 3: 1 <sup>st</sup> construction stage	0.57	0.37	0.36	1.29	0.56	0.58	1.77	2.09	0.98
Phase 4: Consolidation	0.78	0.55	0.46	1.46	0.75	0.67	1.92	2.34	1.06
Phase 5: 2 <sup>nd</sup> construction stage	1.03	0.76	0.57	1.83	1.07	0.85	2.37	3.1	1.33
Phase 6: Consolidation (1 year)	1.2	0.92	0.64	1.91	1.23	0.9	2.45	3.27	1.38
Phase 7: Consolidation (2 year)	1.3	1.01	0.68	1.95	1.32	0.92	2.47	3.35	1.38
Phase 8: Consolidation (5 year)	1.53	1.28	0.77	2.06	1.59	0.99	2.55	3.58	1.43
Phase 9: Consolidation (10 year)	1.75	1.59	0.86	2.17	1.89	1.07	2.62	3.83	1.47
Phase 10: Consolidation (U 90%)	2.7	5.24	1.5	2.81	5.17	1.52	2.86	5.37	1.65
Years to reach U 90%	397			345			161		

6.5 For longitudinal section C (cut-off), the distributions of settlements at the end of construction and at 90% consolidation for the case of no drains are plotted in Figures 6.4 and 6.5. Again, most of the settlements occur after the end of construction and their distribution is strongly dependent on the bedrock profile. The contours of excess pore water pressures for various phases are plotted in Figure 6.6.

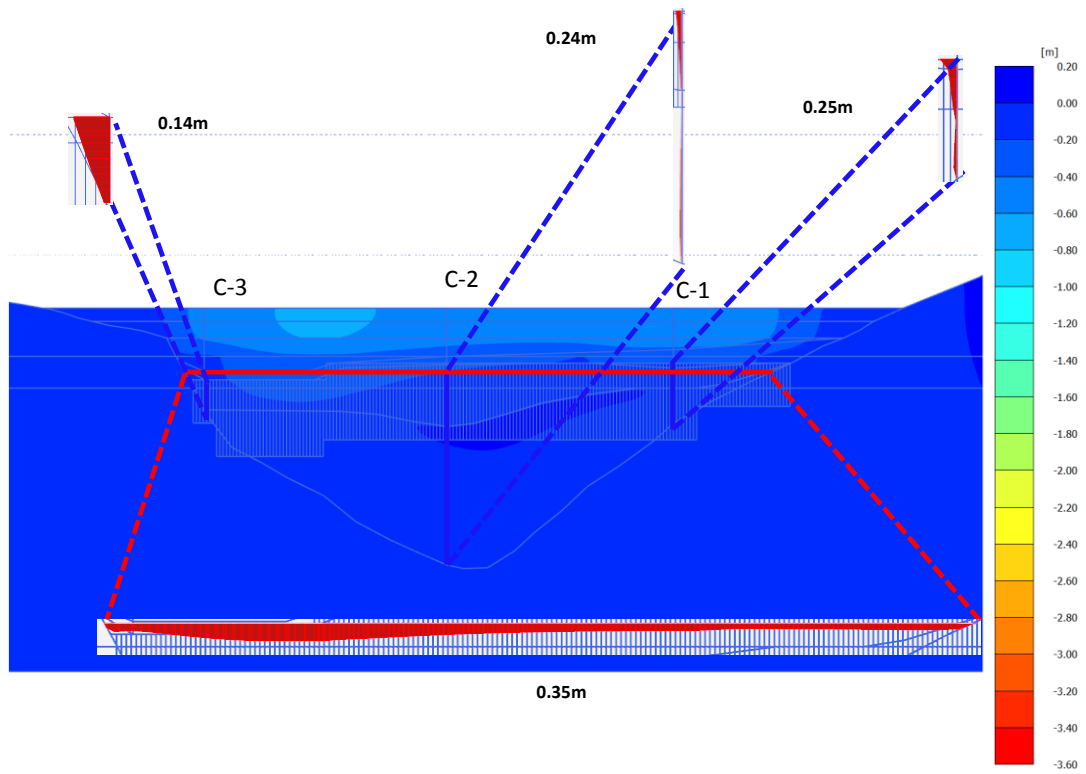


Figure 6.4. Distribution of settlements after the 2nd construction stage (Phase 5). Longitudinal Section C (cut-off). No drains

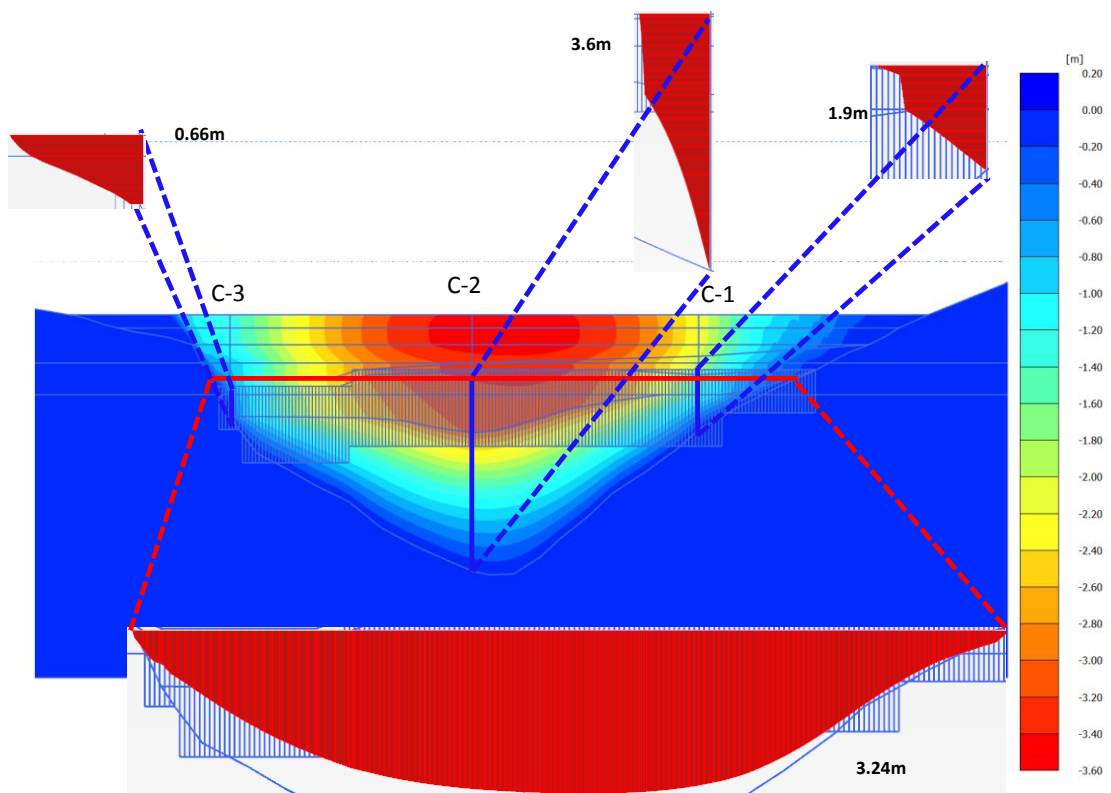


Figure 6.5. Distribution of settlements at 90% degree of consolidation (Phase 10). Longitudinal Section C (cut-off). No drains

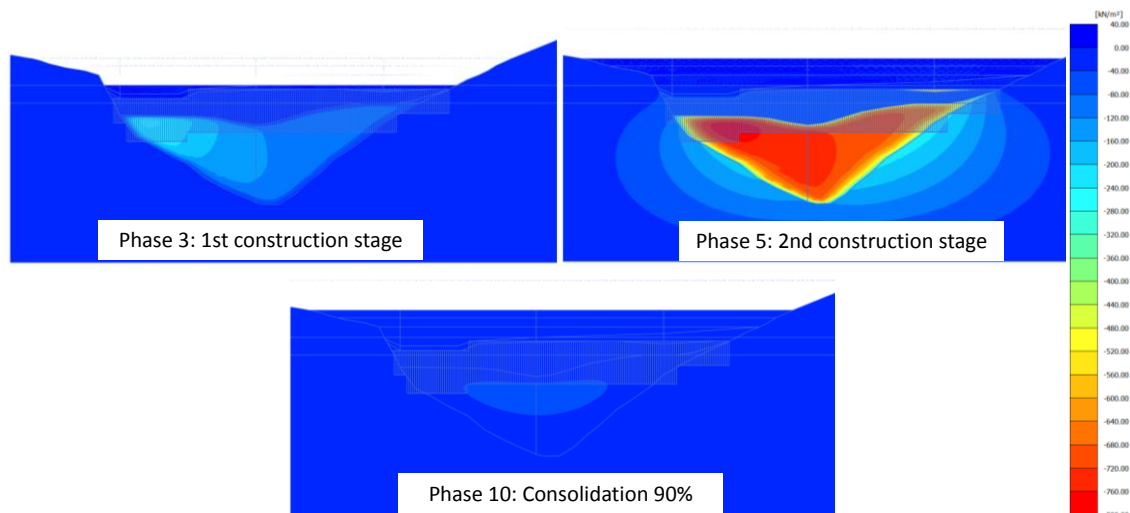


Figure 6.6. Excess pore water pressure at various phases of the analysis. Longitudinal section C (cut-off). No drains

6.6 The values of the settlements for all phases of the calculation with no preload are listed in Table 6.1. Again, it can be seen that only the 50 m long drains have a significant effect on the settlements that occur during construction. In this case, 3D effects appear to be less important as the differences between the longitudinal section settlements and the cross-sections settlements at the same points are more comparable.

Table 6.2 Computed total settlements (m) at locations C-1, C-2 and C-3 at different phases of the analyses (with and without vertical drains). Settlements of point C between Phases 3d and 10 affect the cut-off wall. Longitudinal section C (cut-off). No preload.

Cut-off wall	No preload			Standard 30m drain			Standard 50m drain		
	C-1	C-2	C-3	C-1	C-2	C-3	C-1	C-2	C-3
Phase 0: Initial state	-	-	-	-	-	-	-	-	-
Phase 1: Initial topography	-	-	-	-	-	-	-	-	-
Phase 2: Excavation	-0.18	-0.14	-0.05	-0.17	-0.14	-0.05	-0.18	-0.14	-0.05
Phase 3: 1 <sup>st</sup> construction stage	-0.14	-0.11	0	-0.1	-0.11	0.01	-0.08	-0.05	0.03
Phase 4: Consolidation	-0.11	-0.09	0	-0.07	-0.07	0.02	-0.05	0.02	0.04
Phase 5: 2 <sup>nd</sup> construction stage	0.25	0.24	0.15	1.01	0.28	0.31	1.48	1.17	0.52
Phase 6: Consolidation (1 year)	0.41	0.34	0.19	1.12	0.4	0.34	1.58	1.31	0.56
Phase 7: Consolidation (2 year)	0.49	0.4	0.21	1.16	0.46	0.35	1.6	1.38	0.57
Phase 8: Consolidation (5 year)	0.68	0.55	0.26	1.24	0.64	0.39	1.67	1.54	0.6
Phase 9: Consolidation (10 year)	0.85	0.73	0.31	1.33	0.83	0.43	1.73	1.73	0.63
Phase 10: Consolidation (U 90%)	1.89	3.26	0.65	1.97	3.2	0.73	2.04	3.21	0.8
Years to reach U 90%	447			392			229		

6.7 Finally, the computed settlement values for longitudinal section C considering a 20m high preload are presented in Table 6.3. Preload effects are generally noticeable for the 50 m long drains; the effects of the 30 m long drains are more concentrated in the area of cross Section C-1.

Table 6.3 Computed total settlements (m) at locations C-1, C-2 and C-3 at different phases of the analyses (with and without vertical drains). Settlements of point C between Phases 3d and 10 affect the cut-off wall. Longitudinal section C (cut-off). Preload.

Cut-off wall	Preload			Preload 30m drain			Preload 50m drain		
	C-1	C-2	C-3	C-1	C-2	C-3	C-1	C-2	C-3
Phase 0: Initial state	-	-	-	-	-	-	-	-	-
Phase 1: Initial topography	-	-	-	-	-	-	-	-	-
Phase 2: Excavation	-0.17	-0.14	-0.05	-0.17	-0.14	-0.05	-0.17	-0.13	-0.05
Phase 3a: 1 <sup>st</sup> construction stage (1)	-0.12	-0.06	0.01	-0.04	-0.05	0.04	0	0.1	0.08
Phase 3b: Preload construction	-0.06	0.02	0.03	0.45	0.11	0.17	0.74	0.66	0.32
Phase 3c: 1 <sup>st</sup> construction stage (2)	0.15	0.16	0.10	0.76	0.21	0.22	1.13	0.94	0.43
Phase 3d: Preload removal	0.13	0.13	0.10	0.69	0.17	0.21	1.04	0.86	0.42
Phase 4: Consolidation	0.1	0.11	0.09	0.66	0.17	0.2	1.01	0.84	0.41
Phase 5: 2 <sup>nd</sup> construction stage	0.31	0.29	0.16	1.1	0.34	0.31	1.57	1.23	0.54
Phase 6: Consolidation (1 year)	0.45	0.38	0.19	1.2	0.44	0.35	1.66	1.36	0.57
Phase 7: Consolidation (2 year)	0.53	0.43	0.21	1.24	0.5	0.36	1.69	1.42	0.58
Phase 8: Consolidation (5 year)	0.71	0.58	0.27	1.32	0.66	0.4	1.75	1.58	0.61
Phase 9: Consolidation (10 year)	0.84	0.75	0.32	1.41	0.85	0.44	1.8	1.75	0.63
Phase 10: Consolidation (U 90%)	1.9	3.24	0.53	2.05	3.19	0.71	2.12	3.22	0.85
Years to reach U 90%	427			395			238		

## 7. Concluding remarks

- 7.1 A large series of 2D numerical analyses have been performed using three cross-sections (C-1, C-2 and C-3) and two longitudinal sections: A (along dam axis) and C (along cut-off wall). The effects of installing drains 30 m and 50 m long have been evaluated as well the influence of having a preload in some selected sections (C-1, C-2 and longitudinal C)..
- 7.2 The key parameters for the analyses have been selected carefully taking into account the evidence and data available. In this context, the results from the CPTu tests have played a key role towards a more reliable and founded estimation of parameters.
- 7.3 A number of concluding remarks can be made concerning the results of the analyses:
- The results obtained are very much controlled by the thickness of the soft ground above the bedrock (relatively well known) and the more uncertain distribution of the soil profile between coarse permeable material (modelled as Sand) and fine-grained low permeability material (modelled as Clay).
  - The distinction between the two types of materials has been based on the results of the CPTu tests that provide a quite good way of discriminating between the two. However, it should be borne in mind when examining the results of the numerical analyses that the distribution between coarse and fine-grained materials is probably spatially quite complex and difficult to determine precisely notwithstanding the quite numerous, but necessarily limited, number of CPTu tests. Also, there is an area where it has not been possible to perform CPTu tests; a clay-dominated profile has been conservatively assumed there.
  - The low values of permeability derived from the CPTu tests inevitably lead to extremely long consolidation times in any foundation zone without presence of vertical drains. The values of permeability adopted are low but not unprecedented. However, it is unlikely that such long times will actually occur in the field due to 3D effects and the likely presence of more pervious sublayers that have not been accounted for in the analysis. Therefore, the computed consolidation times should be regarded as upper bounds. If this issue becomes critical, it may be worthwhile to consider the possibility of constructing one or more suitably instrumented trial embankments.
  - The numerical results clearly show the benefits of installing vertical drains regarding the acceleration of pore pressure dissipation, but the effect does not noticeably go beyond the depth of installation. Naturally, vertical drains are unnecessary in the coarse high permeability layers.
  - The beneficial effect of applying a preload on subsequent settlements is very much dependent on the nature of the materials present, especially close to the ground surface. Thus, in cross-section C-2, the effects are minimal because the upper 30 m in the cut-off area is coarse permeable material; more significant effects are identified in cross-section C-1 where the ground profile is different. In any case, preloading requires vertical drains to be effective.



- Perhaps surprisingly, the settlements computed in the longitudinal sections are in various locations quite smaller than the equivalent values in the transversal (upstream/downstream) cross-sections in spite of the unrealistic load distribution applied. This suggests that 3D effects may be quite significant, especially taking into account the strong variation of bedrock depth.
- By computing settlements at every stage of the construction, it is possible to determine the settlements that will potentially affect the cut-off wall, a major design concern. It should be noted, however, that those settlements do not correspond directly to the settlements that the wall will undergo, the actual wall movements will result from the interaction between the wall and the ground.
- Factors of safety (using the Plaxis strength reduction technique) have been computed at different stages and in different sections; the values obtained are mostly adequate. However, failure during construction has been obtained in cross Sections C-1 and C-3 in the cases with no vertical drains. Installation of vertical drains readily makes the dam stable at all stages. In the case that vertical drains are adopted for stabilization purposes only, they are only required on the foundation zone involved in the failure.

Barcelona, 26th February 2015



Daniel Tarragó  
Civil Engineer



Antonio Gens  
Professor of Geotechnical Engineering

## References

- Belokas, G. & Kavvadas, M. (2011). An Intrinsic Compressibility Framework for Clayey Soils. *Geotechnical and Geological Engineering*. DOI 10.1007/s10706-011-9422-0
- Billaux D. & Catalano E. (2015). "Numerical stability analysis and and subsidence evaluation of the Bisri dam in Lebanon under seismic loading." ITASCA CONSULTANTS, S.A.S
- Chraibi A.F., Aayadi T., E. Haddad (2013). "Note de calculs de stabilité statique et pseudo-statique - Barrage Bisri Revue des études d'avant projet ». NOVEC CDG Developpement
- Jefferies, M.G., and Davies, M.P., (1993). "Use of CPTU to estimate equivalent SPT N60." *Geotechnical Testing Journal*, ASTM, **16**(4): 458-468.
- Robertson, P.K., (1998). "Risk-based site investigation." *Geotechnical News*: 45- 47, September 1998.
- Robertson, P.K., (2009). "Interpretation of cone penetration tests – a unified approach." *Canadian Geotechnical Journal*, 46:1337-1355.
- Robertson, P.K. (2012). "Guide to Cone Penetration Testing." *Gregg Drilling and Testing*
- Teh, C.I., and Houlsby, G.T. (1991). "An analytical study of the cone penetration test in clay." *Geotechnique*, 41 (1): 17-34.
- Wroth, C.P. and Wood D. M. (1978) . The correlation of index properties with some basic engineering properties of soils. *Canadian Geotechnical Journal*, 15(2): 137-145,

## Appendix 1. Results of the CPTu tests

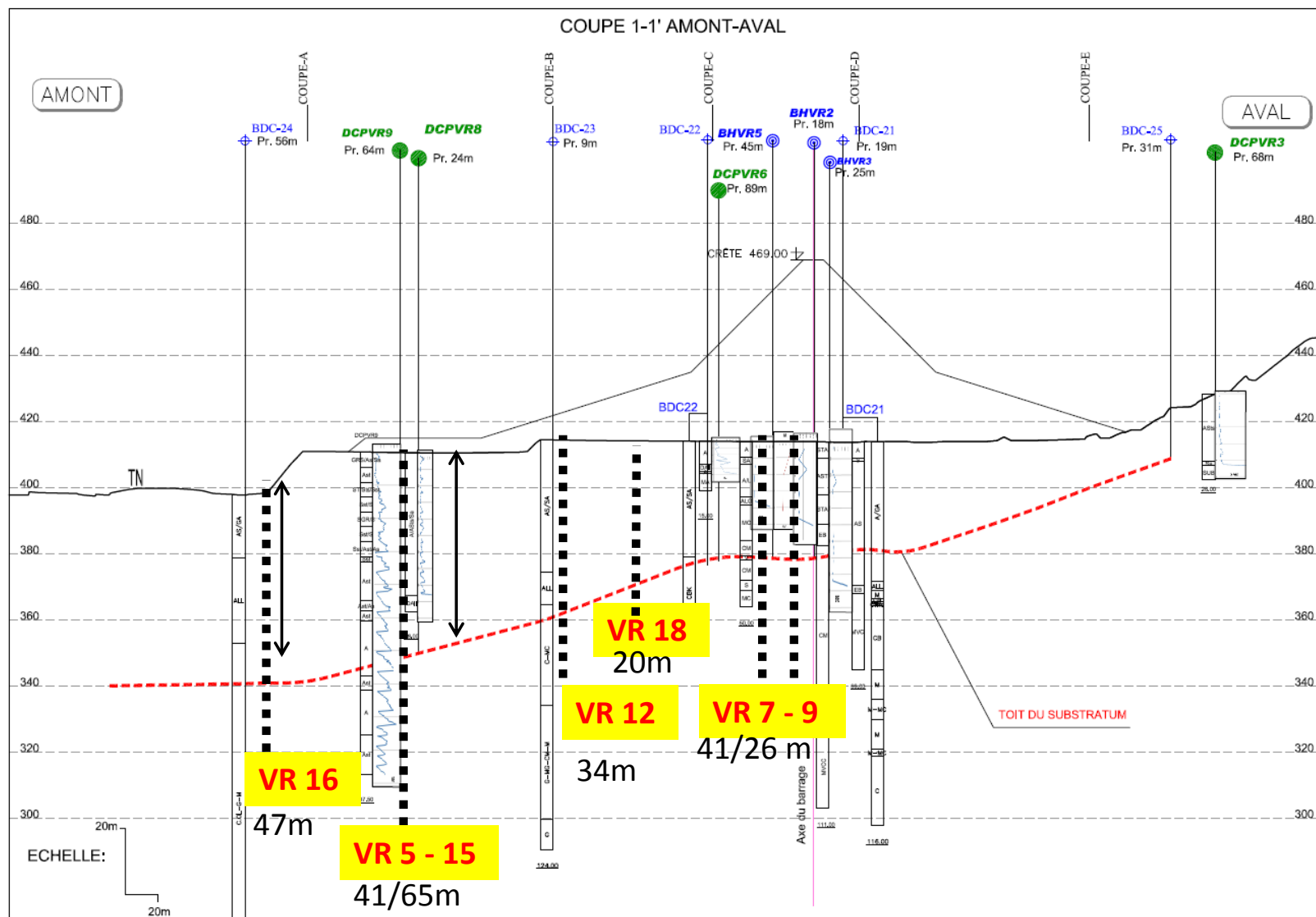


Figure A1.1. CPTu tests near cross-section C-1

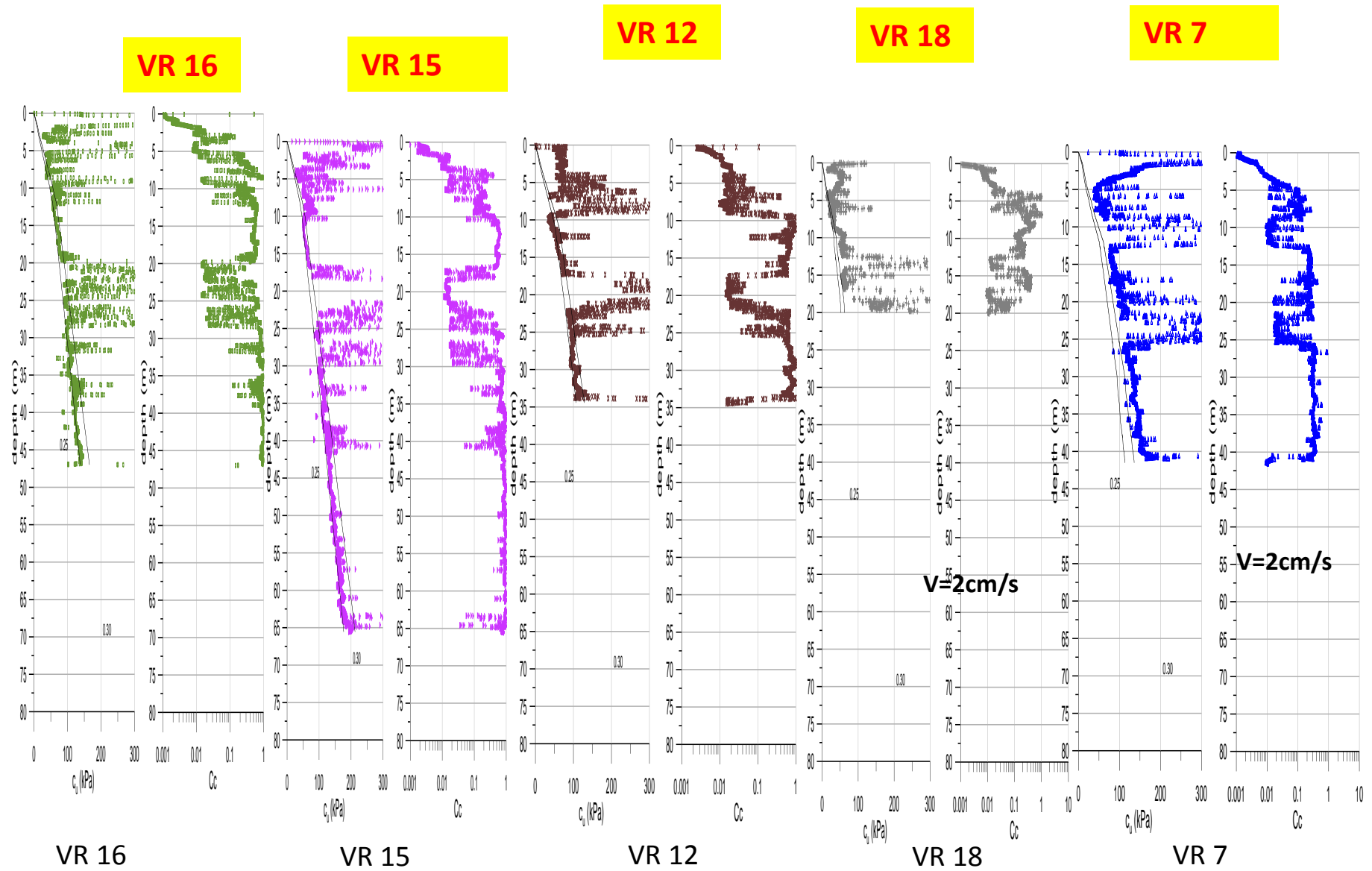


Figure A1.2. CPTu tests near cross-section C-1. Estimation of undrained shear strength,  $c_u$ , and compression index,  $C_c$ .

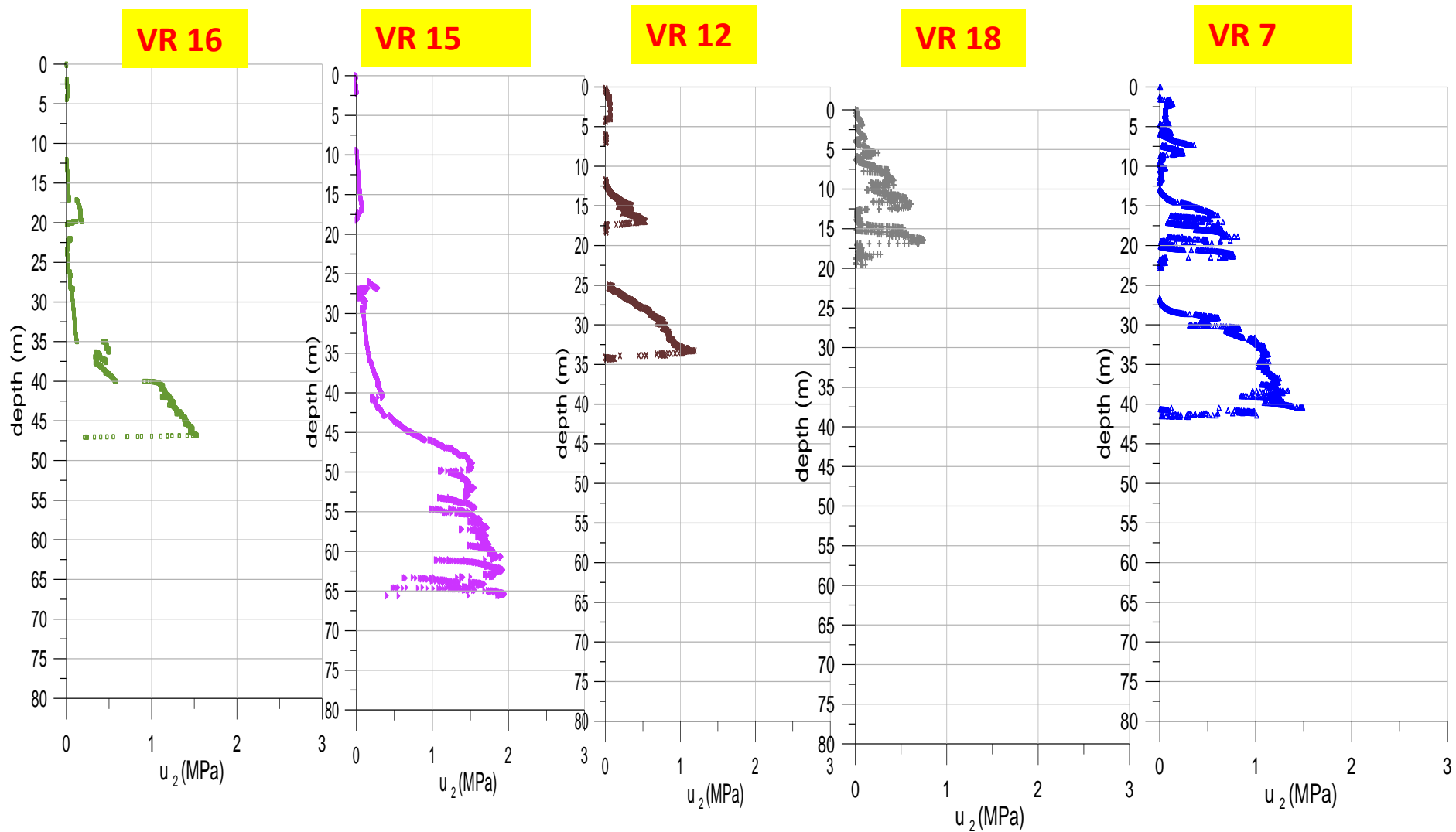


Figure A1.3. CPTu tests near cross-section C-1. Measurement of pore pressure

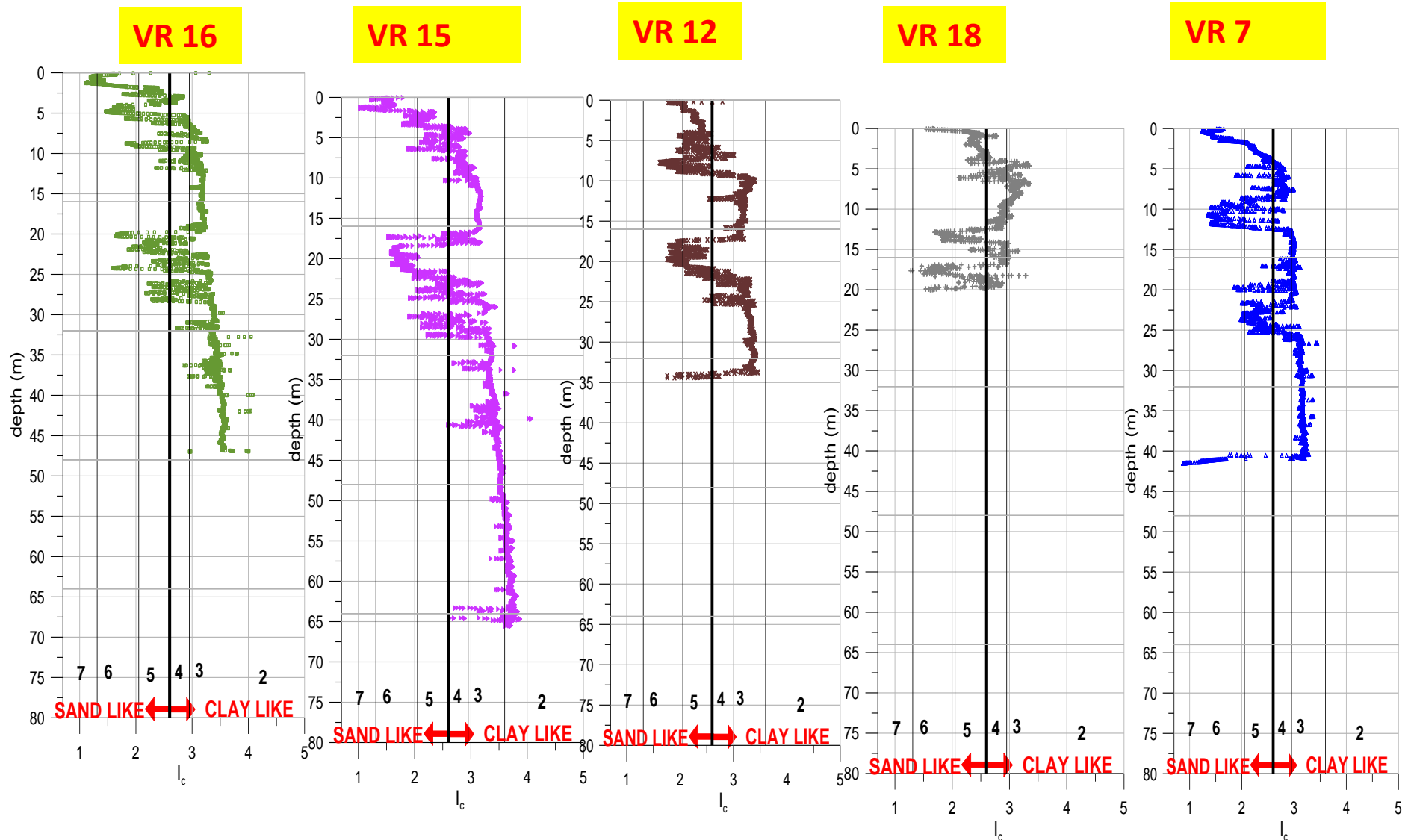


Figure A1.4. CPTu tests near cross-section C-1. Estimation of Soil Index Behaviour ( $I_c$ )

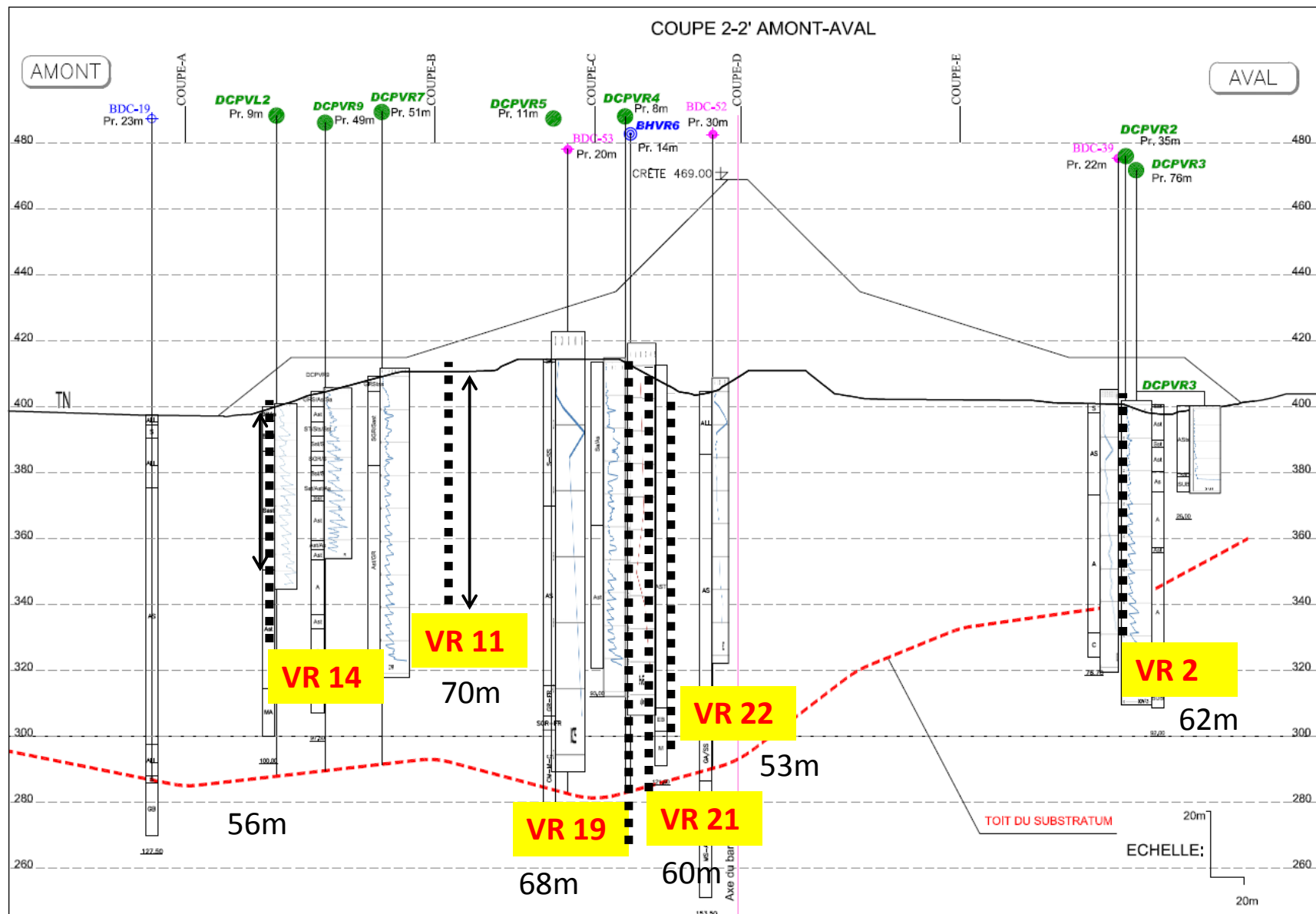


Figure A1.5. CPTu tests near cross-section C-2

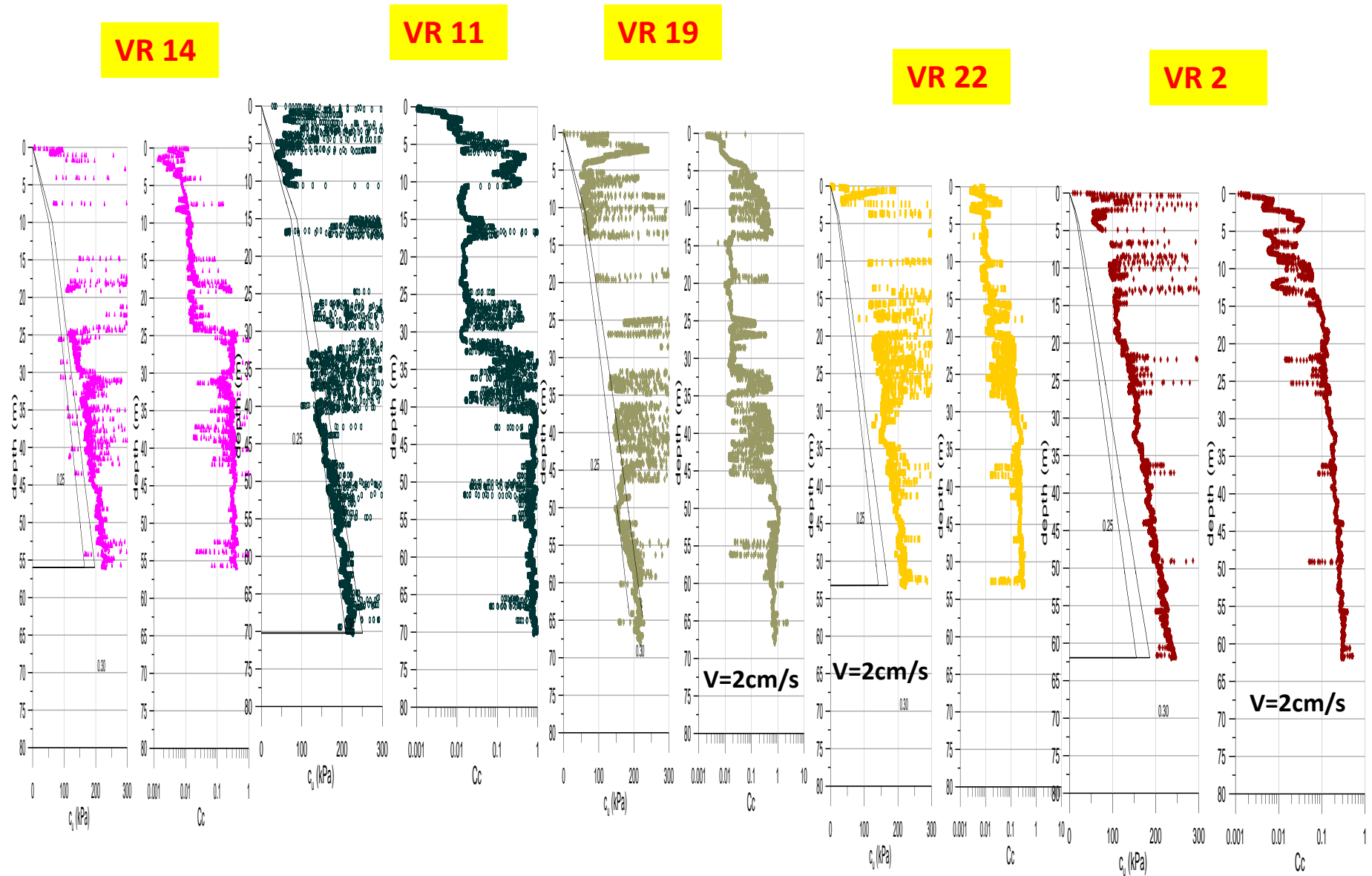


Figure A1.6. CPTu tests near cross-section C-2. Estimation of undrained shear strength,  $c_u$ , and compression index,  $C_c$ .



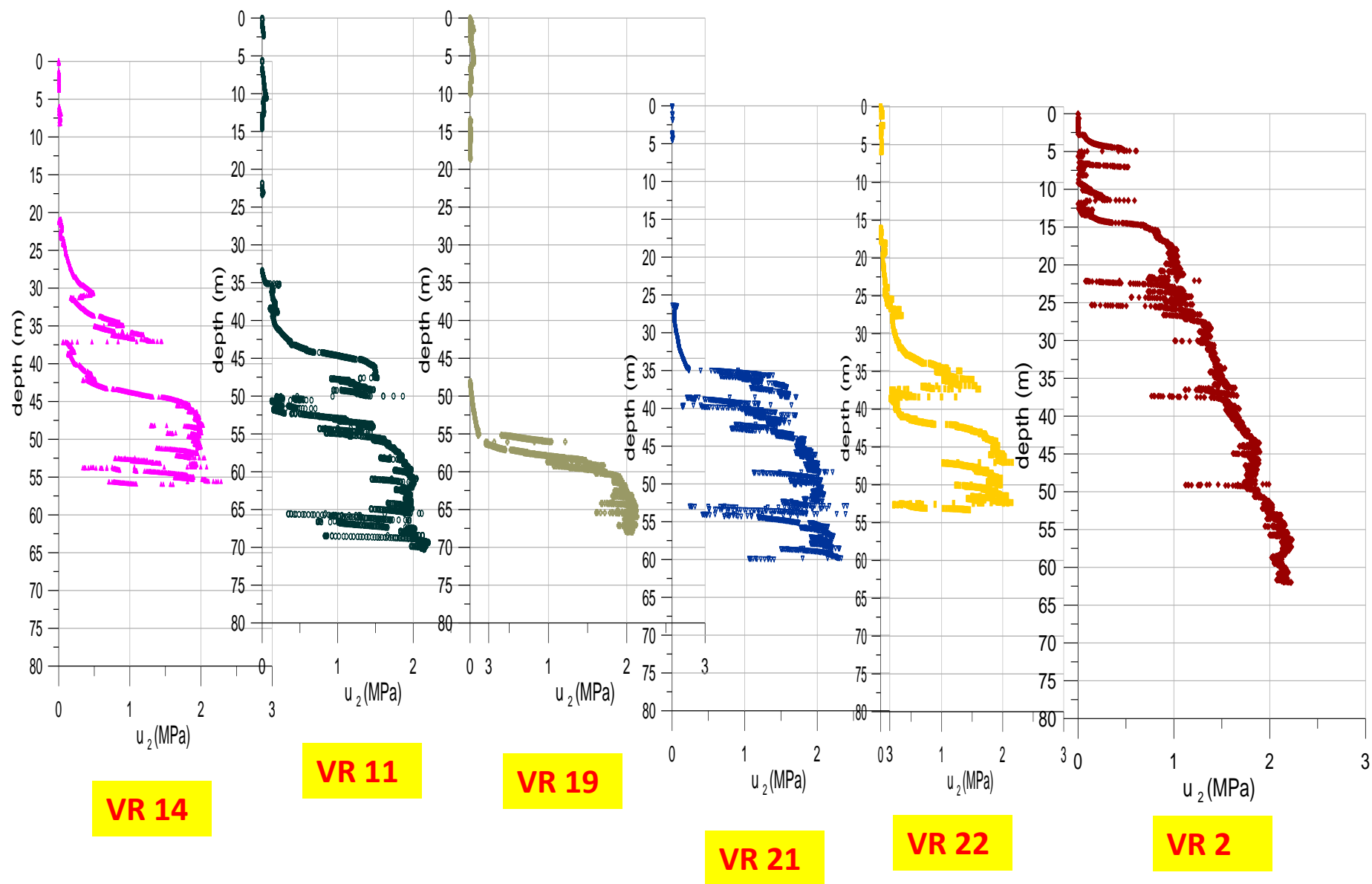


Figure A1.7. CPTu tests near cross-section C-2. Measurement of pore pressure

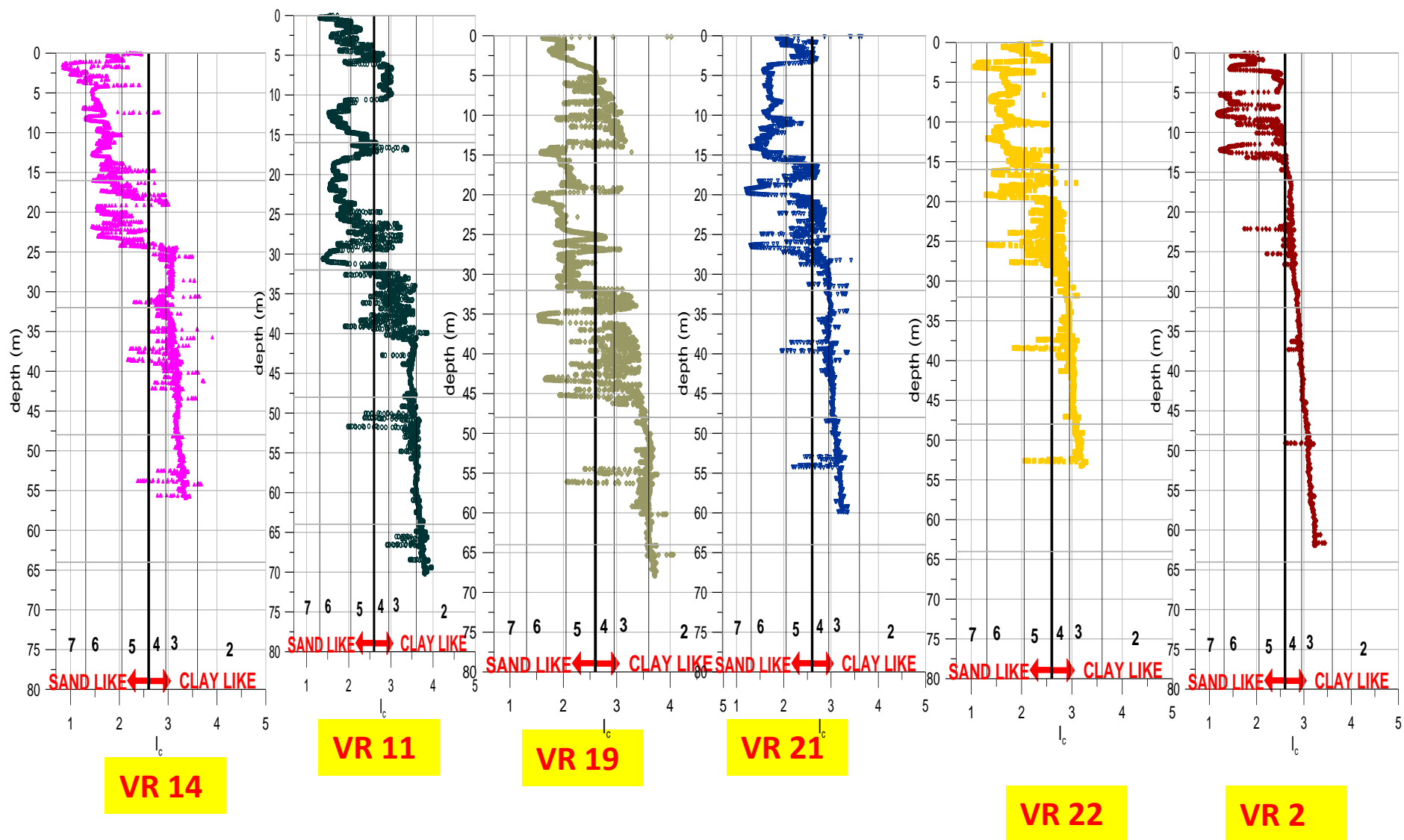


Figure A1.8. CPTu tests near cross-section C-2. Estimation of Soil Index Behaviour ( $I_c$ )

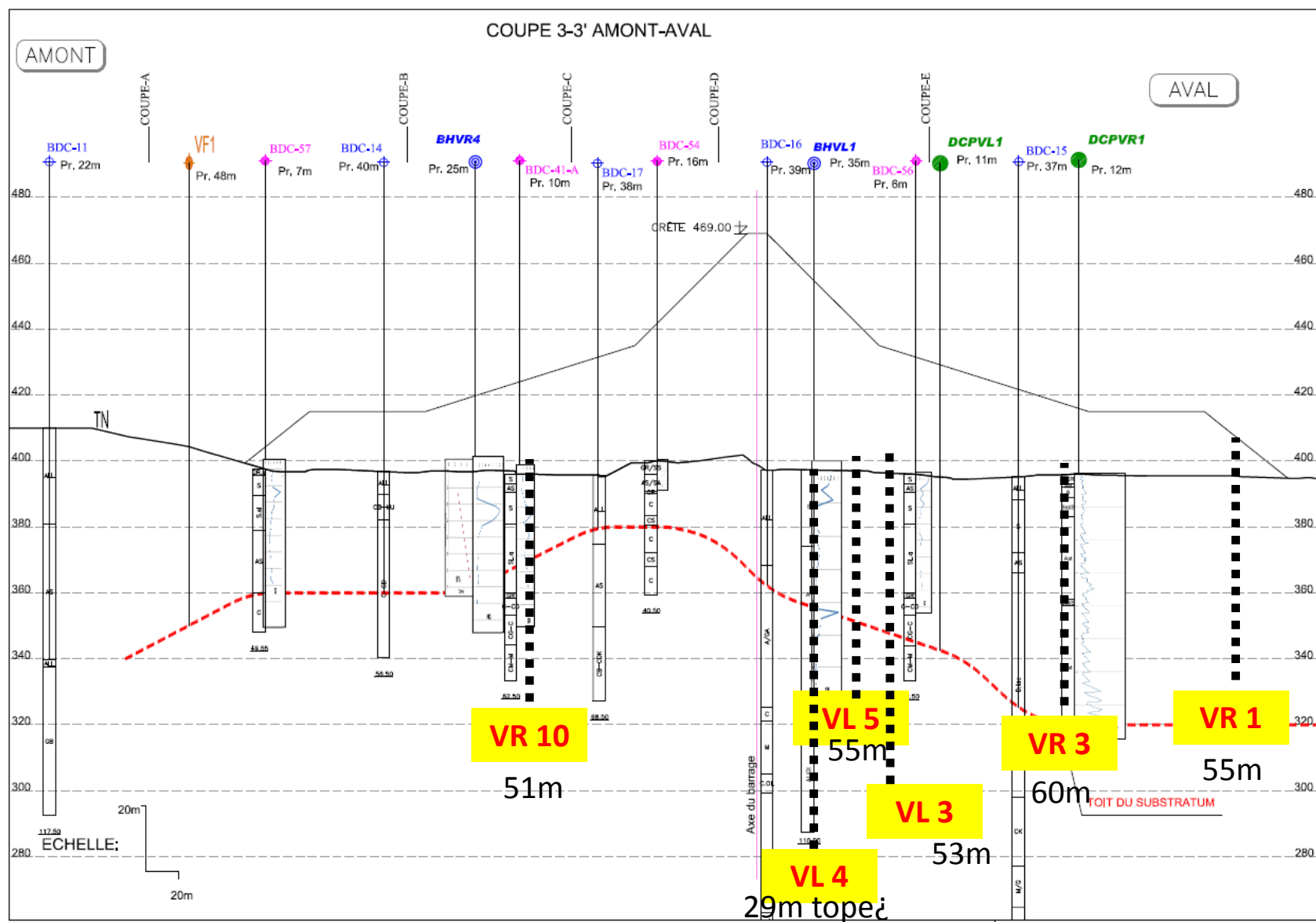


Figure A1.9. CPTu tests near cross-section C-3

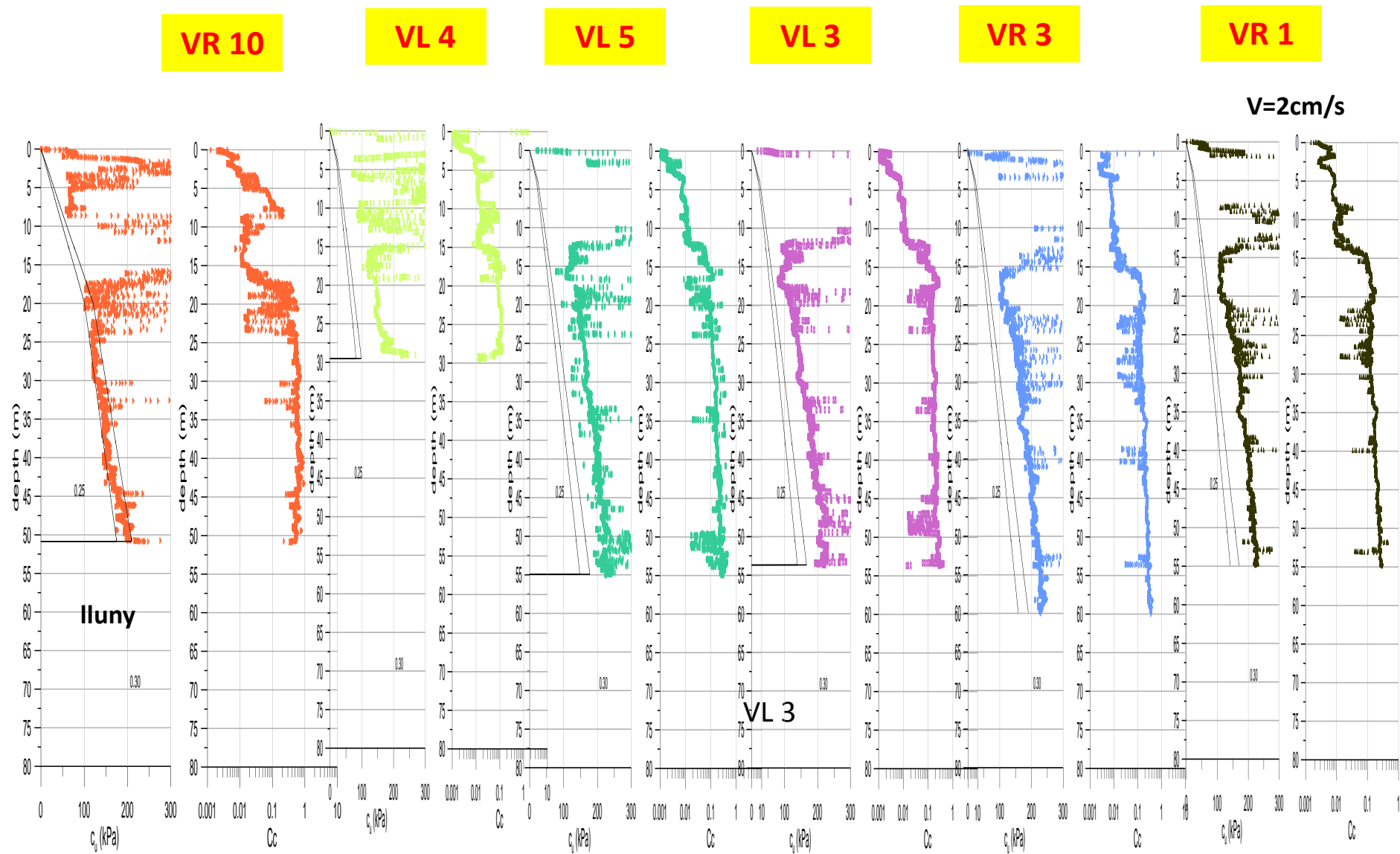


Figure A1.10. CPTu tests near cross-section C-3. Estimation of undrained shear strength,  $c_u$ , and compression index,  $C_c$ .

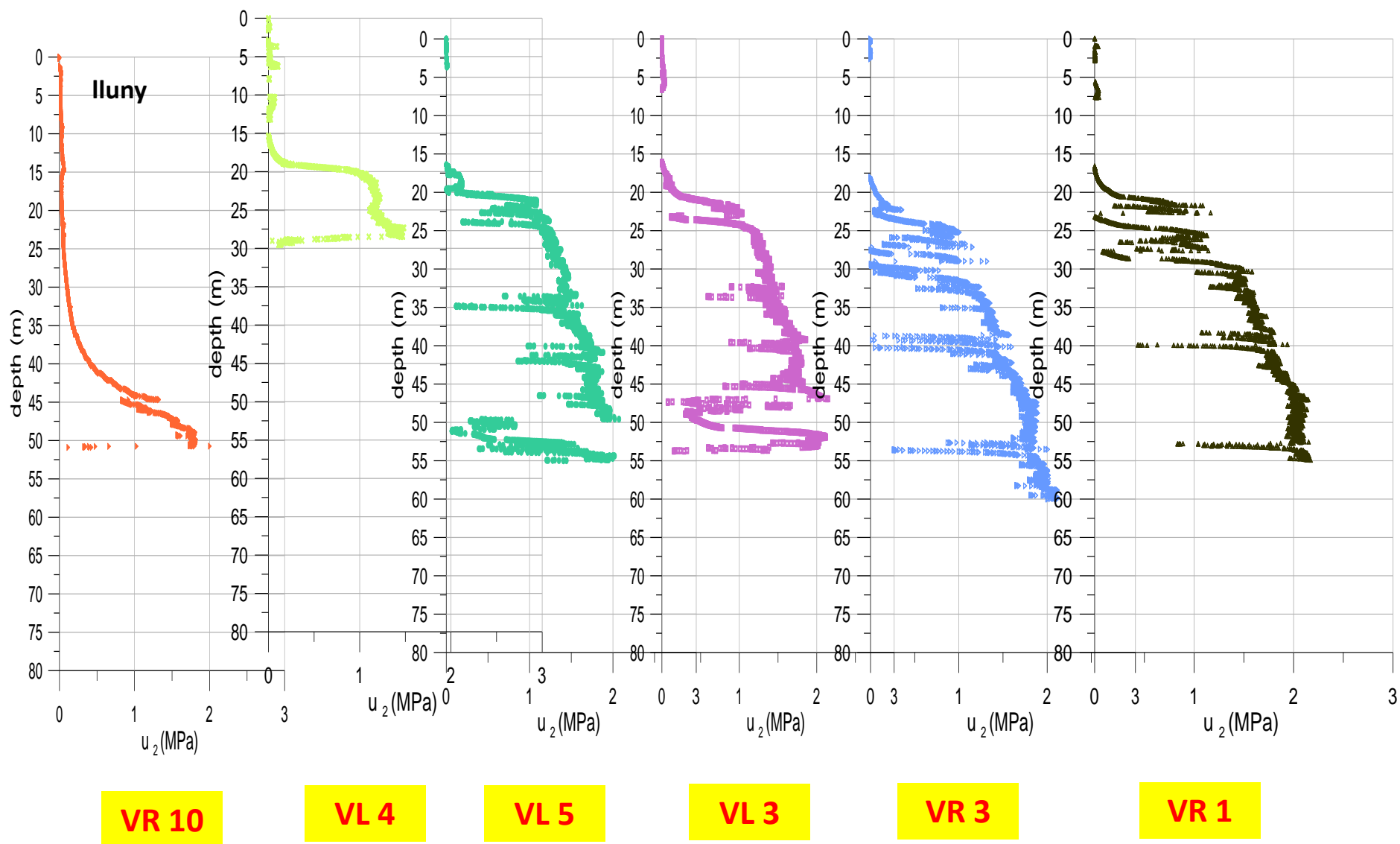


Figure A1.11. CPTu tests near cross-section C-3. Measurement of pore pressure

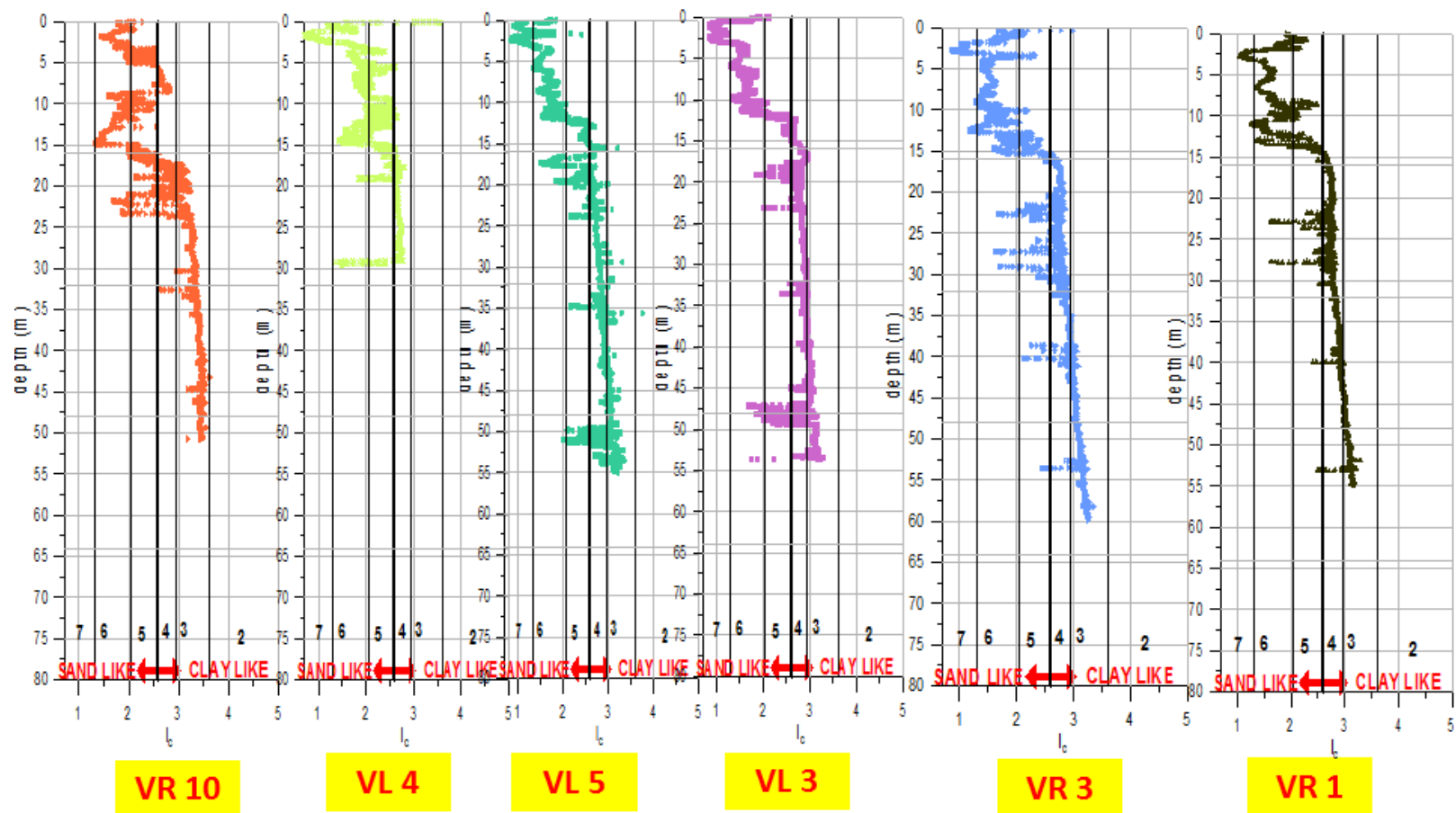


Figure A1.12. CPTu tests near cross-section C-3. Estimation of Soil Index Behaviour ( $I_c$ )

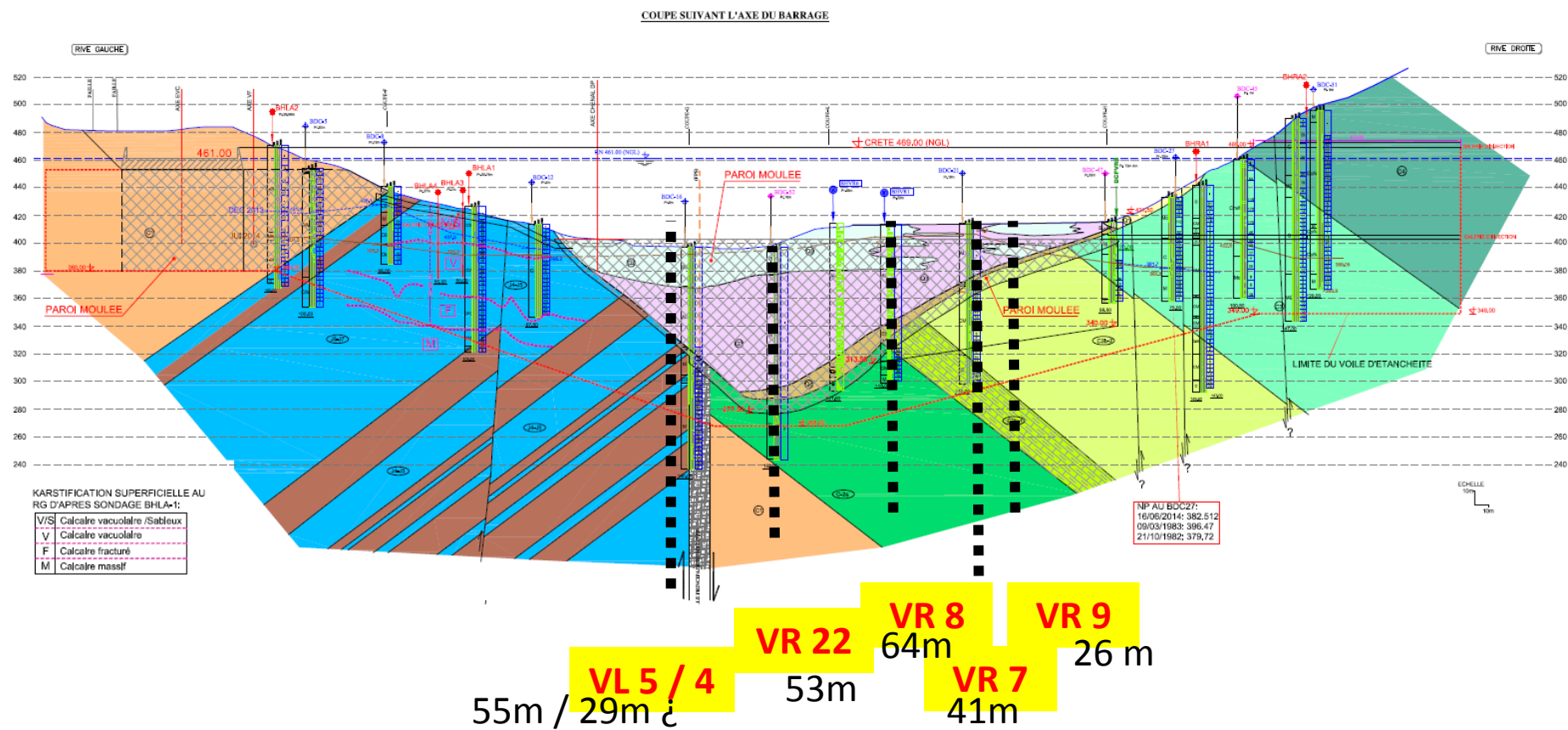


Figure A1.13. CPTu tests near longitudinal section A (dam axis)

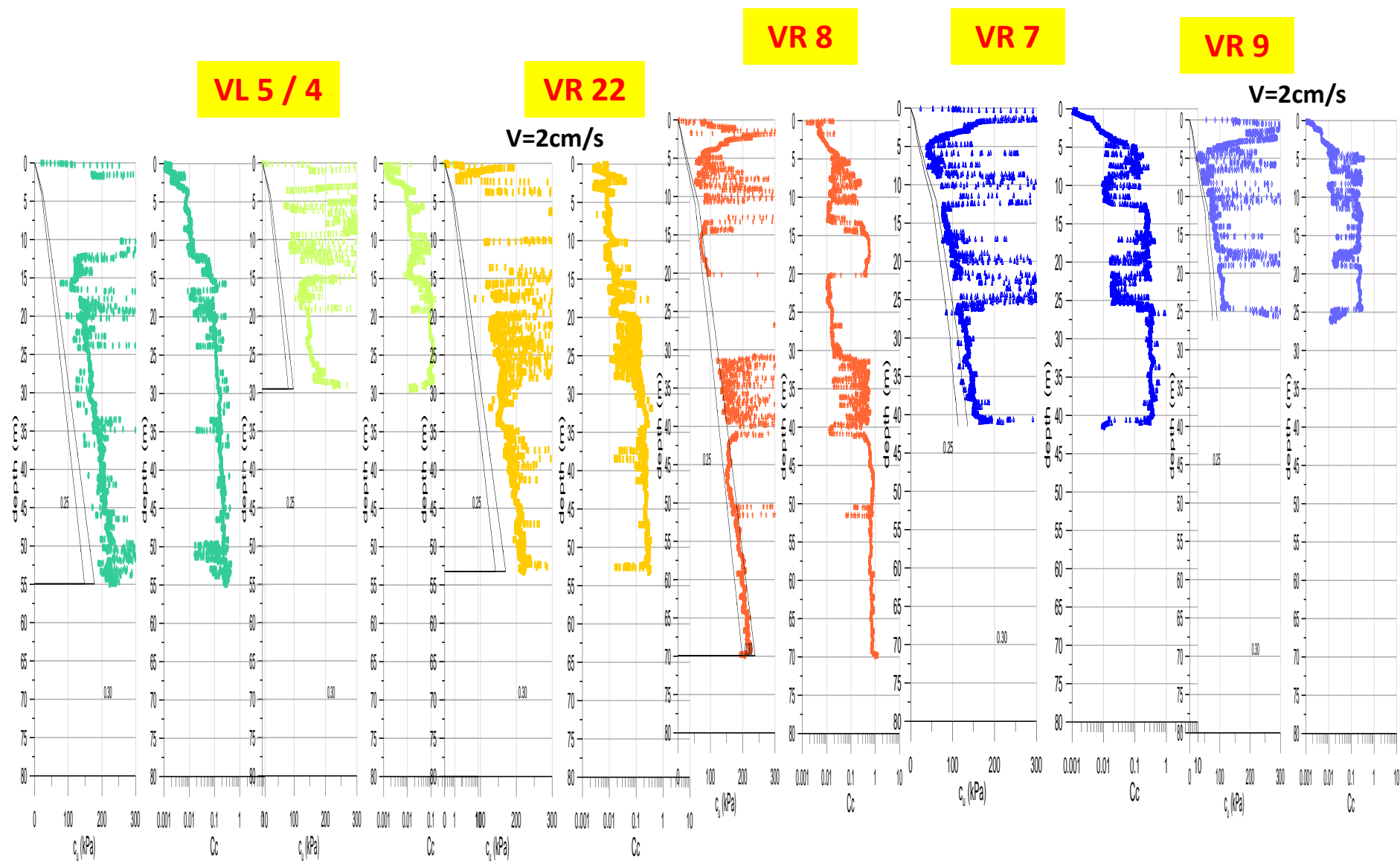


Figure A1.14. CPTu tests near longitudinal section A (dam axis). Estimation of undrained shear strength,  $c_u$ , and compression index,  $C_c$ .



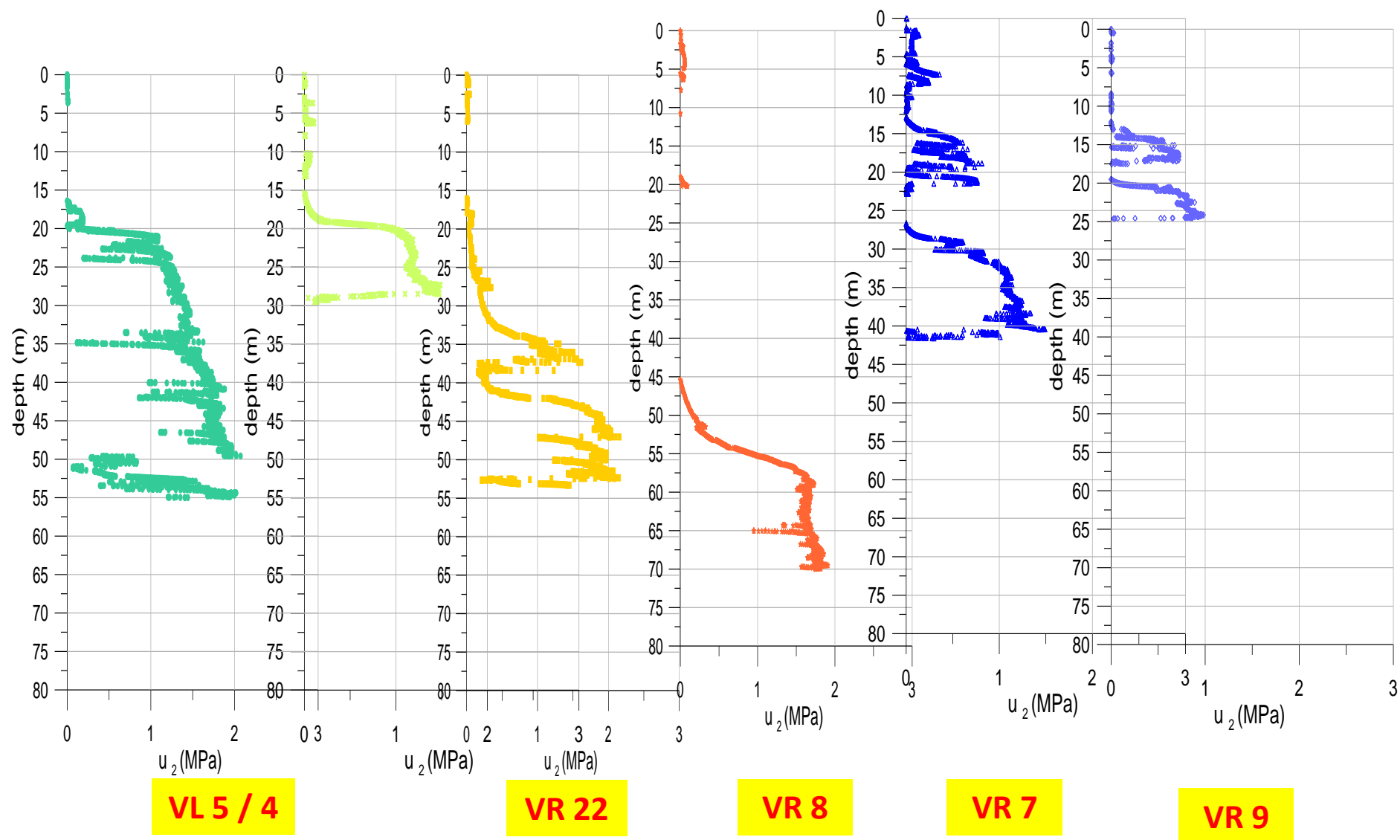


Figure A1.15. CPTu tests near longitudinal section A (dam axis). Measurement of pore pressure

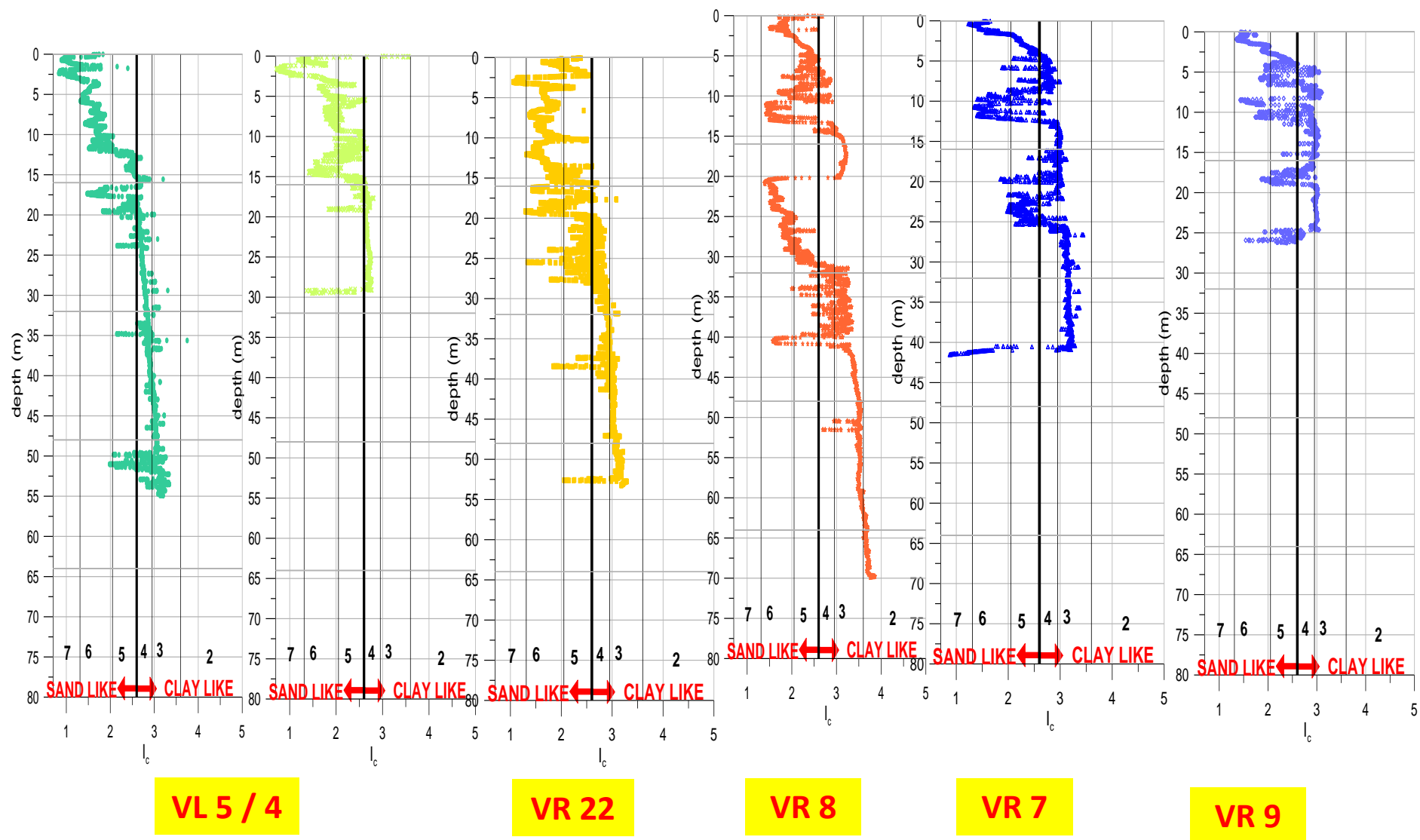


Figure A1.16. CPTu tests near longitudinal section A (dam axis). Estimation of Soil Index Behaviour ( $I_c$ )

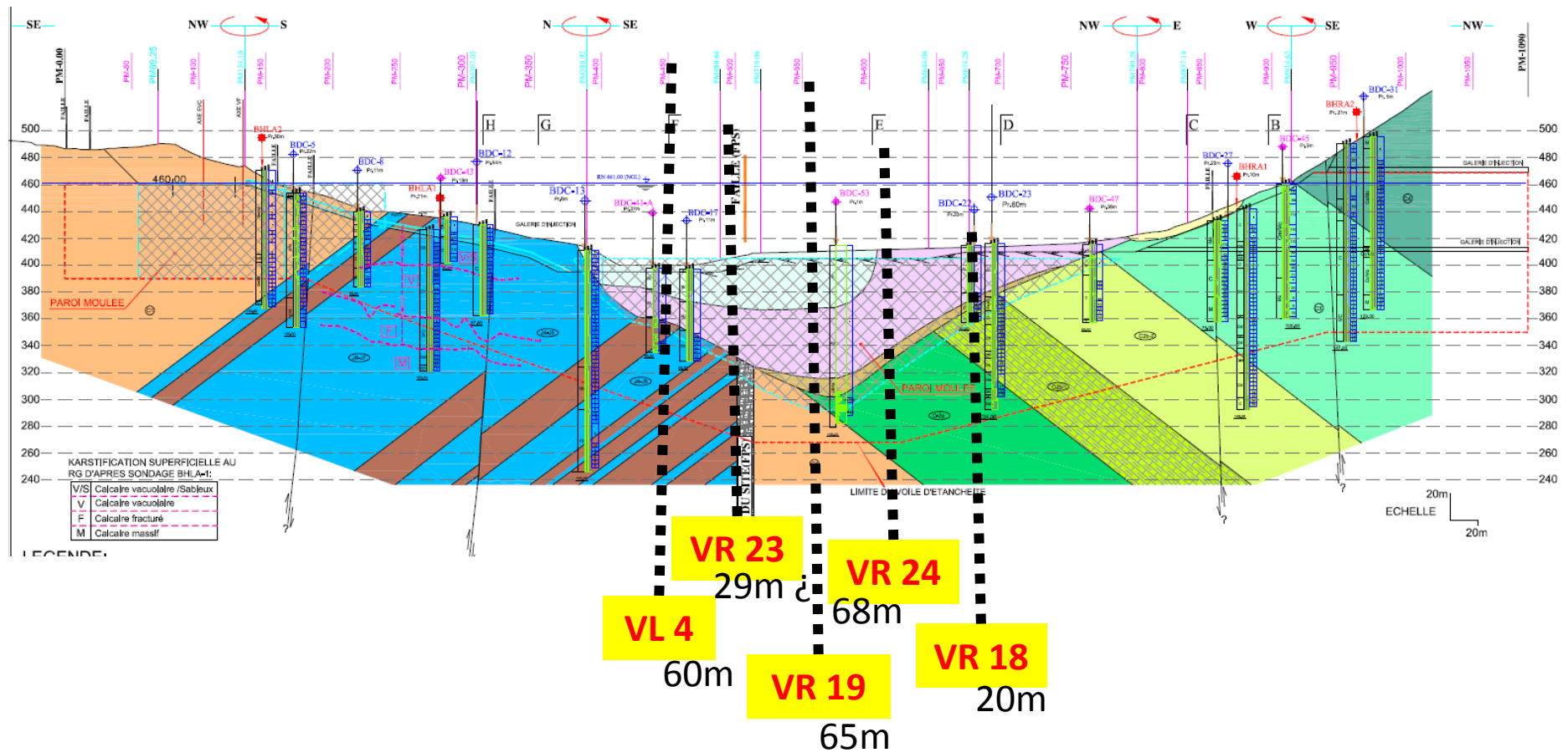


Figure A1.17. CPTu tests near longitudinal section C (cut-off wall)

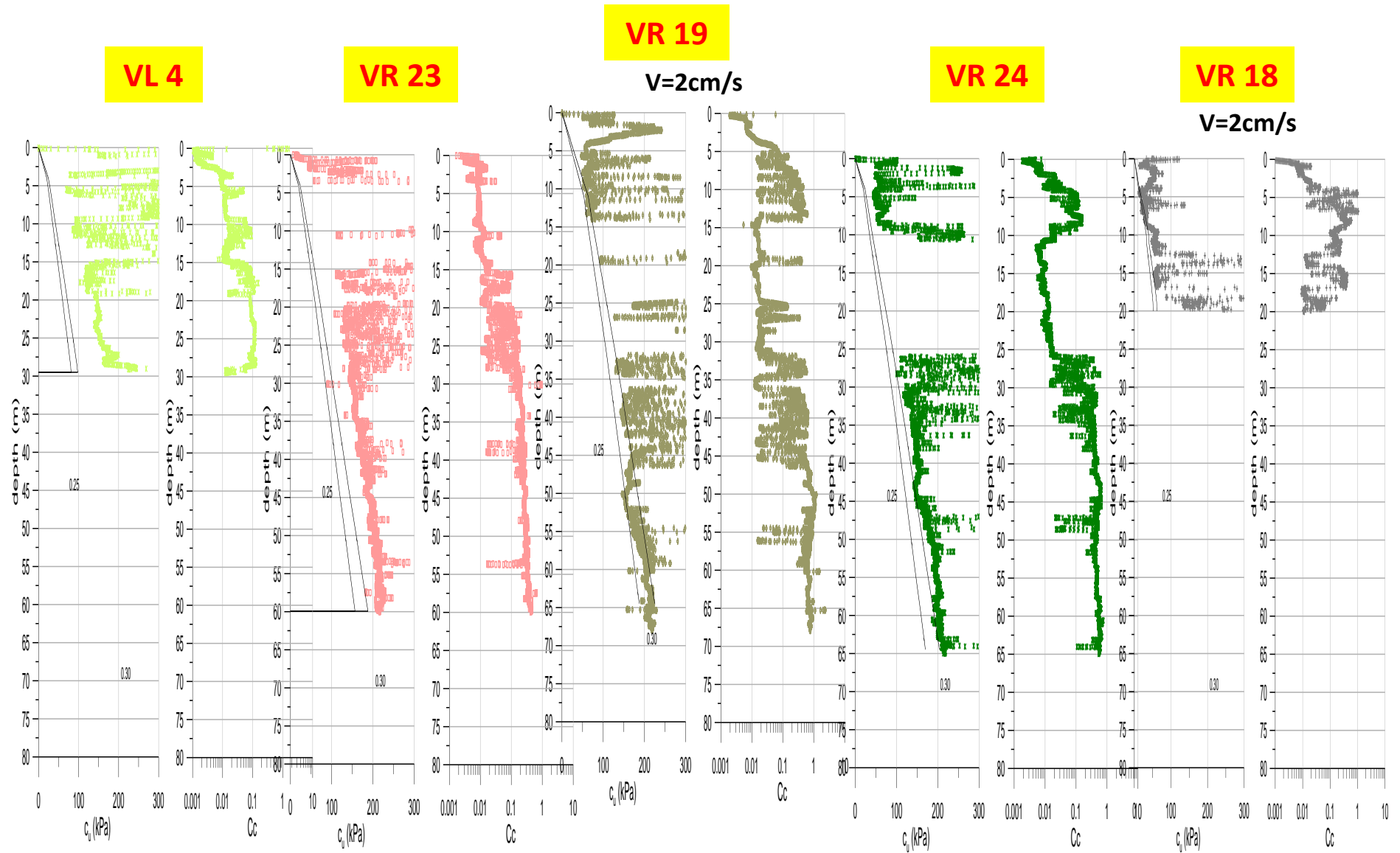


Figure A1.18. CPTu tests near longitudinal section C (cut-off wall). Estimation of undrained shear strength,  $c_u$ , and compression index,  $C_c$ .

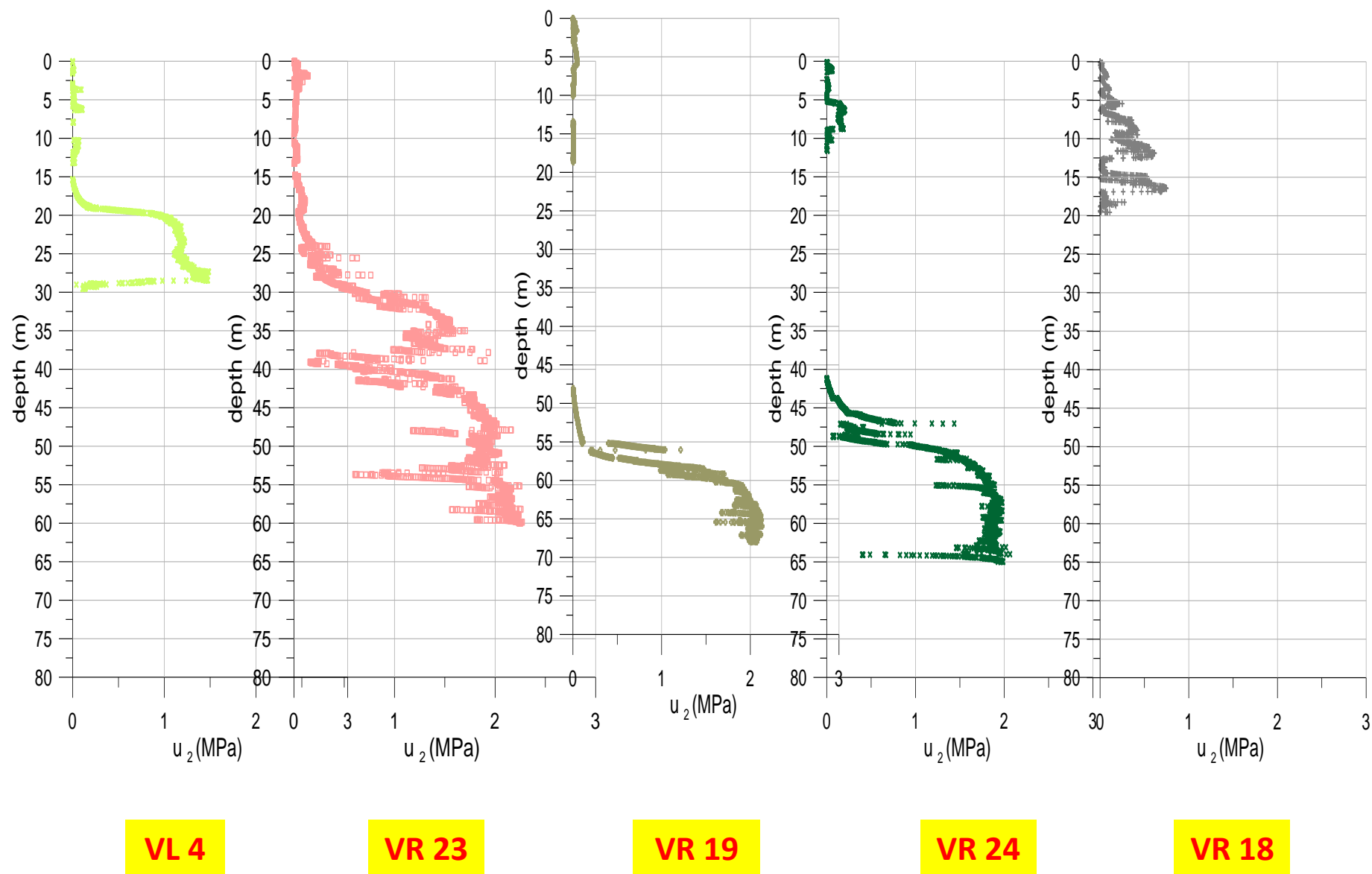


Figure A1.19. CPTu tests near longitudinal section C (cut-off wall). Measurement of pore pressure

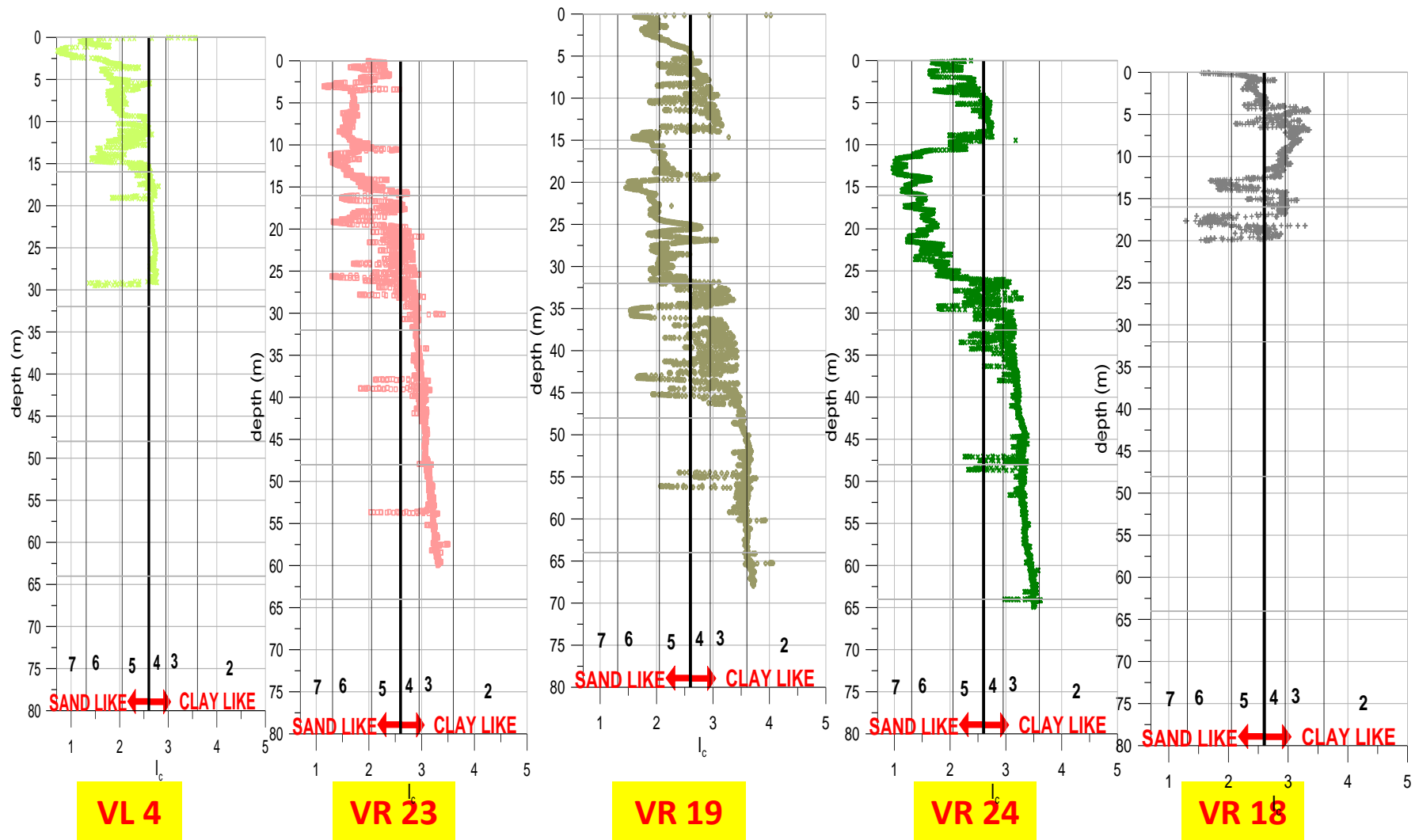


Figure A1.20. CPTu tests near longitudinal section C (cut-off wall). Estimation of Soil Index Behaviour ( $I_c$ )